

THE UNIVERSITY OF CHICAGO

CAPITALIZING ON SECURITY, PERFORMANCE, AND ENERGY TRADEOFFS IN
FULL DRIVE ENCRYPTION SCHEMES FOR FUN AND PROFIT

A DISSERTATION SUBMITTED TO
THE FACULTY OF THE DIVISION OF THE PHYSICAL SCIENCES
IN CANDIDACY FOR THE DEGREE OF
DOCTOR OF PHILOSOPHY

DEPARTMENT OF COMPUTER SCIENCE

BY
BERNARD DICKENS III

CHICAGO, ILLINOIS

AUGUST 2020

Copyright © 2020 by Bernard Dickens III
All Rights Reserved

To my kiddos (whom at the time of writing do not yet exist): I find the courage to peer over the edge of human knowledge and reach down into that abyss of the unknown with the hope that you may one day benefit from my struggles. I can't wait to meet you!

TABLE OF CONTENTS

LIST OF FIGURES	vi
LIST OF TABLES	vii
ACKNOWLEDGMENTS	viii
ABSTRACT	x
1 INTRODUCTION	1
1.1 Thesis Statement	1
1.2 Contributions	1
1.2.1 StrongBox	1
1.2.2 SwitchCrypt	2
1.2.3 HASCHK	2
2 BACKGROUND AND RELATED WORK	3
3 STRONGBOX: USING STREAM CIPHERS FOR HIGH PERFORMANCE FULL DRIVE ENCRYPTION	10
3.1 Motivation	10
3.1.1 Performance Potential	12
3.1.2 Append-mostly Filesystems	13
3.1.3 Threat Model	13
3.2 System Design	15
3.2.1 Backing Store Function and Layout	17
3.2.2 Rekeying Procedure	23
3.2.3 Defending Against Rollback Attacks	23
3.2.4 Recovering from Inconsistent State	24
3.3 Implementation	25
3.3.1 Deriving Subkeys	26
3.3.2 A Secure, Persistent, Monotonic Counter	26
3.3.3 LFS Garbage Collection	28
3.3.4 Overhead	28
3.4 Evaluation	29
3.4.1 Experimental Setup	29
3.4.2 Experimental Methodology	29
3.4.3 StrongBox Read Performance	31
3.4.4 StrongBox Write Performance	32
3.4.5 On Replacing dm-crypt and Ext4	33
3.4.6 Performance in StrongBox: ChaCha20 vs AES	34
3.4.7 Overhead with a Full Drive	35
3.4.8 Threat Analysis	36

4	SWITCHCRYPT: NAVIGATING TRADEOFFS IN STREAM CIPHER BASED FULL DRIVE ENCRYPTION	41
4.1	Motivation	41
4.1.1	Example: Filesystem Reacts to “Battery Saver”	44
4.1.2	Key Challenges	47
4.2	System Design	48
4.2.1	SwitchCrypt Overview	48
4.2.2	Quantifying Cipher Security Properties	50
4.2.3	Generic Stream Cipher Interface	53
4.2.4	Cipher Switching Strategies	55
4.2.5	Putting It All Together	61
4.3	Implementation	62
4.3.1	Implementing Cipher Switching	63
4.4	Evaluation	65
4.4.1	Switching Strategies Under Various Workloads	67
4.4.2	Reaching Between Static Configuration Points	68
4.4.3	Cipher Switching Overhead	70
4.4.4	Revisiting Our Threat Model	71
4.5	Case Studies	71
4.5.1	Balancing Security Goals with a Hard Energy Cap	72
4.5.2	Variable Security Regions	74
4.5.3	Responding to End-of-Life Slowdown in SSDs	75
5	HASCHK: TRADING OFF BUILD PROCESS COMPLEXITY FOR RESOURCE SECURITY	77
5.1	Motivation	77
5.1.1	Resource Integrity SCAs	82
5.1.2	Real World Motivations	83
5.2	Protocol Design	86
5.2.1	Participants	86
5.2.2	Protocol Overview	87
5.3	Implementation	91
5.3.1	URNs, BDs, and Fallthrough in Google Chrome	93
5.4	Evaluation	94
5.4.1	Security Goals and Threat Model	94
5.4.2	Security and Performance	95
5.4.3	Scalability and Deployment	97
5.4.4	Limitations	98
6	CONCLUSION	100
6.1	Future Work	101
A	CODE AVAILABILITY	103

BIBLIOGRAPHY	104
------------------------	-----

LIST OF FIGURES

3.1	AES-XTS and ChaCha20+Poly1305 Comparison.	12
3.2	Overview of the StrongBox construction.	15
3.3	Layout of StrongBox's backing storage.	17
3.4	Test of the F2FS LFS mounted atop both dm-crypt and StrongBox; median latency of different sized whole file read and write operations normalized to unencrypted access. By harmonic mean, StrongBox is $1.72\times$ faster than dm-crypt for sequential reads and $1.27\times$ faster for sequential writes.	37
3.5	Comparison of four filesystems running on top of StrongBox performance is normalized to the same file system running on dm-crypt. Points below the line signify StrongBox outperforming dm-crypt. Points above the line signify dm-crypt outperforming StrongBox.	38
3.6	Comparison of Ext4 on dm-crypt and F2FS on StrongBox. Results are normalized to unencrypted Ext4 performance. Unencrypted F2FS results are shown for reference. Points below the line are outperforming unencrypted Ext4. Points above the line are underperforming compared to unencrypted Ext4.	39
3.7	Comparison of AES in XTS and CTR modes versus ChaCha20 in StrongBox; median latency of different sized whole file sequential read and write operations normalized to ChaCha20 (default cipher in StrongBox). Points below the line signify AES outperforming ChaCha20. Points above the line signify ChaCha20 outperforming AES.	40
3.8	Comparison of F2FS baseline, atop dm-crypt, and atop StrongBox. All configurations are initialized with a near-full backing store; median latency of different sized whole file read and write operations normalized to dm-crypt. Points below the line are outperforming dm-crypt. Points above the line are underperforming compared to dm-crypt.	40
4.1	Overview of the SwitchCrypt construction.	49
4.2	Layout of SwitchCrypt's drive layout.	50
4.3	Median sequential and random write and then read performance baseline.	67
4.4	Median sequential and random write and then read back performance comparison of Forward switching to baseline. Each cluster of 3 dots between configurations represents the 7:3, 5:5, and 3:7 primary-vs-secondary I/O ratios described in the text.	68
4.5	Median sequential and random write and then read back performance comparison of Mirrored and Selective switching strategies to baseline.	70
4.6	Median sequential write total energy use with respect to time with respect to time.	73
4.7	Median sequential read and write performance comparison of 4KB, 5MB I/O with 7-to-3 ratio, ChaCha8 vs Freestyle Strong (respectively).	75
4.8	Median sequential and random 40MB read and write performance comparison: baseline versus simulated faulty block device.	76
5.1	A high level overview of the (generic) automated checksum verification process beginning when a user downloads a resource.	87

LIST OF TABLES

3.1	File System Overwrite Behavior	13
3.2	Attacks on StrongBox and their results	36
4.1	Our framework for classifying stream ciphers according to three ideal features: relative round count, ciphertext randomization, and ciphertext expansion.	51
4.2	A summary comparison between the three cipher switching strategies.	58
4.3	Attacks on SwitchCrypt and their results	72
5.1	The generic software engineering supply chain.	83
A.1	Provides URLs for the products yielded and/or used by this research. The first four URIs refer to repositories on GitHub.	103

ACKNOWLEDGMENTS

I would first and foremost like to thank my advisor, Dr. Henry (Hank) Hoffmann. Without your compassion, patience, conscientiousness, and cosmic wealth of knowledge and experience, none of this work would have been possible. Thank you for everything you’ve done for my students and me. You are truly a rare ally.

I’d like to thank my committee members Dr. Ariel J. Feldman (Applied Crypto), Dr. Haryadi S. Gunawi (File Systems), and Dr. David Cash (Theoretical Crypto) for all their hours of hard work and tireless dedication even in the middle of a pandemic. I learned so much studying under you. Hopefully I spelled everyone’s names correctly this time!

I’d also like to acknowledge my former students Richard Anthony Alvarez and Trevor James Medina for their huge contributions to HASCHK and to my sanity. Equally important are Abraham Valle (a fullstack flexer!), Mark Alvarez (elite politico), Malik Swanson (one of my greatest friends), Michael Desiderio (we have the most interesting conversations), along with former students Tyrese Cook, Rakim Jazz Verner (aka Green Arrow), Ephriam, Matthew, Malcolm, Byron, Leroy, and all the others! I love you guys.

I’d be remiss if I did not acknowledge the pivotal role played by my lovely hyper-intelligent mother (I had to get it from somewhere, haha!) Michelle Davis who, throughout my childhood, *always* had money for Computer Science workbooks (but somehow not McDonalds!); as well as my unstoppable father Bernard Dickens II for always taking the extra effort to be there for me and demonstrating how to be relentless in the pursuit of my dreams. Thank you also go out to: my inspiring siblings Davis and Milan; Zara for the infinity life lessons—you were my rock, my reality hook; Jeff Holmes of the old Chicago Broadway Armory for showing an eight-year-old me just how fun and powerful ~~hacking~~ computers can be; Von Steuben high school Computer Science teachers Stirling Crow and Andres Hernandez for teaching me web design and gifting me the wisdom to “use my CS powers for good;” my coach Audra Anderson and the BDPA for teaching me humility and how fulfilling it is to

be an engaging teacher and effective helper; Dr. Rahmelle Thompson of the Morehouse College Hopps Scholars program for revealing my trajectory to me; Dr. Adrienne Raglin of the Department of Defense Army Research Laboratory for putting up with me (twice!) and teaching me what real research looks like; neighborhood matriarch Martha Alvarez for looking out for me during my last few years in Chicago; my decade-long friend and confidant Joshua Moore for never being afraid to challenge my thoughts and keeping me on my toes with his rare wit; the University of Chicago and all its faculty and staff for fostering a culture of socially conscious elite intellectual pursuit; President Barack H. Obama and Senator Elizabeth Warren for demonstrating black excellence and how to persist nevertheless; and all my mentors, former students, and true friends over the years for their unwavering support throughout this process. Know I would not have made it without every last one of you.

I must give special thanks to my UChicago family: Connor and Saeid, our interactions were usually brief, but you both blazed the trail for me in particular. I was so nervous (my default state!) but hearing you both talk about your experiences post-M.S.-defense really helped me calm down and focus. Thank you for all your wisdom. Anne, thanks for listening to my boring talk! Your feedback during the group meeting really helped hone my presentation. Ivana and Will, thank you for reaching out! I'm just a hopeless recluse. Kavon, our conversations were fun. Huazhe would greet me on those rare occasions I entered the office. Thank you for the warm welcomes! Nikita, Yi, Santriaji, Yuli, Tejas, Ahsan, it was my pleasure to get to know you all.

This material is based upon work supported by the National Science Foundation under Grant No. CNS-1526304. So thank you too United States discretionary spending budget authorized by Congress.

ABSTRACT

The security of data at rest—widely understood as FDE or Full Drive Encryption—is an important concern among several in modern computer systems. These concerns exist in contention over a set of finite resources. For instance: a device that is battery-constrained must remain within its energy budget which may change over time, e.g. when a device enters “battery-saver mode”; regardless, this device must meet certain performance guarantees or the user experience will suffer; above all, the data on the device must be secure from adversaries; and the device has a finite amount of drive space available. At any given moment we trade battery life for performance, performance for security, security for drive space, and so on. Unfortunately, designing a FDE system that can navigate such treacherous tradeoffs efficiently, effectively, and with respect to performance and security guarantees is entirely non-trivial. This dissertation explores this space of tradeoffs and how we might optimize for one concern without violating another given kernel and/or user space in-context invariants that might shift over time.

Full drive encryption is especially important for mobile devices because they contain large quantities of sensitive data yet are easily lost or stolen. As this research demonstrates, the standard approach to FDE—the AES block cipher in XTS mode—is 3-5x slower than unencrypted storage. Authenticated encryption based on stream ciphers is already used as a faster alternative to AES in other contexts, such as HTTPS, but the conventional wisdom is that stream ciphers are unsuitable for FDE. Used naively in drive encryption, stream ciphers are vulnerable to attacks, and mitigating these attacks with on-drive metadata is generally believed to ruin performance.

We address the difficulty of using stream ciphers for FDE with StrongBox, a stream cipher based FDE layer that is a drop-in replacement for dm-crypt, the standard Linux FDE module based on AES-XTS. StrongBox introduces a system design and on-drive data structures that exploit certain properties of filesystems to avoid costly rekeying penalties and

a counter stored in trusted hardware to protect against attacks. We implement StrongBox and SwitchCrypt on an ARM big.LITTLE mobile processor and test its performance under multiple popular production filesystems.

We push the envelope further with SwitchCrypt, a software mechanism that allows us to move beyond merely making stream ciphers available for FDE. SwitchCrypt enables practical navigation of the tradeoff space made by balancing competing security and latency requirements via *cipher switching* in space or time. Our key insight in achieving low-overhead switching is to leverage the overwrite-averse, append-mostly behavior of underlying solid-state storage to trade throughput for reduced energy use and/or certain security properties. Similar to StrongBox, we implement SwitchCrypt on an ARM big.LITTLE mobile processor and test its performance under the popular F2FS LFS. We provide empirical results demonstrating the conditions under which different switching strategies are optimal through the exploration of three cases studies.

Finally, with HASCHK, we consider the same stream cipher based cryptographic primitives in an alternative domain: data *in motion* rather than at rest. Specifically: securing data downloads over the internet. Such downloads come with many risks, including the chance that the resource has been corrupted, or that an attacker has replaced your desired resource with a compromised version. The de facto standard for addressing this risk is the use of *checksums* coupled with a secure transport layer; users download a resource, compute its checksum, and compare that with an authoritative checksum. Problems with this approach include (1) *user apathy*—for most users, calculating and verifying the checksum is too tedious; and (2) *co-hosting*—an attacker who compromises a resource can trivially compromise a checksum hosted on the same system. The co-hosting problem remains despite advancements in tools that automate checksum verification and generation. In this dissertation we propose *HASCHK*, a resource verification protocol expanding on de facto checksum-based integrity protections to defeat co-hosting while automating the tedious parts of checksum

verification to secure “data in motion” over the internet.

StrongBox, SwitchCrypt, and HASCHK together demonstrate that security is indeed a paramount concern and valid dimension with which to tradeoff alongside other tier-one concerns. We show that these tradeoffs are possible without compromising data security or requiring egregious performance sacrifices, all while staying within a shifting energy budget.

CHAPTER 1

INTRODUCTION

1.1 Thesis Statement

With this research into filesystem, device driver, and hardware Flash Translation Layer (FTL) based Full Disk Encryption (FDE) schemes for “data at rest”, we primarily consider: (1) the established wisdom in the crypto community that stream ciphers are unsuitable for FDE and (2) exploring the tradeoff space made between total energy use, filesystem performance, and reasonable security guarantees when comparing specific cipher configurations. In the first case, we develop and implement a secure approach to FDE based on stream ciphers, the proliferation of secure hardware, and the characteristics of Log-Structured Filesystems (LFS). In the second case, we implement a dozen stream ciphers—each exposing several knobs—and demonstrate navigating our tradeoff space via runtime cipher switching while maintaining reasonable security guarantees. We then present a formal analysis of our system’s security guarantees. Finally, we consider data authenticity schemes using some of the same cryptographic primitives but in the context of “data in motion” through the development and implementation of a resource verification protocol expanding on de facto checksum-based integrity protections to defeat co-hosting while automating the tedious parts of checksum verification.

1.2 Contributions

1.2.1 *StrongBox*

StrongBox is a novel scheme for securing data at rest and is a drop-in replacement for AES-XTS-backed FDE such as dm-crypt [60]. StrongBox uses a fast stream cipher for confidentiality and performance with integrity preserving Message Authentication Codes [66]

and a secure, persistent hardware counter to ensure integrity and counter the weaknesses inherent in stream cipher based FDE. With StrongBox’s, we present a system design enabling the first confidential, high-performance drive encryption scheme based on stream ciphers.

1.2.2 *SwitchCrypt*

SwitchCrypt is software mechanism that navigates the tradeoff space made by balancing competing security and latency requirements via *cipher switching* in space or time and represents a vastly improved FDE approach based on StrongBox. SwitchCrypt addresses the reality that optimizing for performance often conflicts with other key concerns like energy usage and desired security properties. SwitchCrypt leverages the behavior of underlying solid-state storage to trade between throughput, energy use, and desirable security properties of various ciphers. This is accomplished dynamically and at run time.

1.2.3 *HASCHK*

HASCHK is a resource verification protocol expanding on de facto checksum-based integrity protections to defeat co-hosting while automating the tedious parts of checksum verification. HASCHK mitigates the authenticity risks of data in motion; in this instance: downloading resources over the internet. We find our approach is more effective than existing mitigation methods, significantly raises the bar for the attacker, and is deployable at scale.

CHAPTER 2

BACKGROUND AND RELATED WORK

Some of the most popular cryptosystems offering a confidentiality guarantee for data at rest employ a symmetric encryption scheme known as a Tweakable Enciphering Scheme (TES) [17, 86]. There have been numerous TES-based constructions securing data at rest [17, 42, 105], including the well known XEX-based XTS operating mode of AES [98] explored earlier in this work. Almost all TES constructions and the storage management systems that implement them use one or more block ciphers as their primary primitive [17, 90].

Our StrongBox implementation borrows from the design of these systems. One in particular is *dm-crypt*, a Linux framework employing a *LinuxDeviceMapper* to provide a virtual block interface for physical block devices. Dm-crypt provides an implementation of the AES-XTS algorithm among others and is used widely in the Linux ecosystem [6, 60]. The algorithms provided by dm-crypt all employ block ciphers [60]. Instead of a block cipher, however, StrongBox uses a stream cipher to provide the same confidentiality guarantee and consistent or better I/O performance. Further unlike dm-crypt and other similar virtualization frameworks, StrongBox’s ciphering operations do not require sector level tweaks, depending on the implementation. With StrongBox, several physical blocks consisting of one or more sectors are considered as discrete logical units, *i.e.*, nuggets and flakes.

Substituting a block cipher for a stream cipher forms the core of several contributions to the state-of-the-art [17, 90]. Chakraborty et al. proposed STES—a stream cipher based low cost scheme for securing stored data [17]. STES is a novel TES which can be implemented compactly with low overall power consumption. It combines a stream cipher and a universal hash function via XOR and is targeting low cost FPGAs to provide confidentiality of data on USBs and SD cards. Our StrongBox, on the other hand, is not a TES and does not directly implement a TES. StrongBox combines a stream cipher with nonce “tweak” and nugget data via XOR and is targeting any configuration employing a well-behaved Log-structured

Filesystem (LFS) at some level to provide confidentiality of data.

Offering a transparent cryptographic layer at the block device level has been proposed numerous times [47]. Production implementations include storage management systems like dm-crypt. Specifically, Hein et al. proposed the Secure Block Device (SBD) [47]—an ARM TrustZone secure world transparent filesystem encryption layer optimized for ANDIX OS and implemented and evaluated using the Linux Network Block Device (NBD) driver. StrongBox is also implemented and evaluated using the NBD, but is not limited to one specific operating system. Further unlike StrongBox, SBD is not explicitly designed for use outside of the ARM TrustZone secure world. Contrarily, StrongBox was designed to be used on any system that provides a subset of functionality provided by a Trusted Platform Module (TPM) and/or Trusted Execution Environment (TEE). Specifically, StrongBox requires the availability of a dedicated hardware protected secure monotonic counter to prevent rollback attacks and ensure the freshness of StrongBox. The primary design goal of StrongBox is to achieve provide higher performance than the industry standard AES-XTS algorithm utilizing a stream cipher.

StrongBox’s design is only possible because of the availability of hardware support for security, which has been a major thrust of research efforts [33, 48, 58, 100, 104, 112], and is now available in almost all commercial mobile processors [40, 53, 79, 97]. Our implementation makes use of the replay protected memory block on eMMC devices [31, 79], but it could be reimplemented using any hardware that supports persistent, monotonic counters.

The combination of trusted hardware and monotonic counters enables new security mechanisms. For example, van Dijk et al. use this combination allow clients to securely store data on an untrusted server [29]. Like StrongBox, their approach relies on trusted hardware (TPM specifically [40]), logs, and monotonic counters. The van Dijk et al. approach, however, uses existing secure storage and is not concerned with storage speed. StrongBox uses

these same mechanisms along with novel metadata layout and system design to solve a different problem: providing higher performance than AES-XTS based approaches.

Achieving on-drive data integrity protection through the use of checksums has been used by filesystems and many other storage management systems. Examples include ZFS [75] and others [47]. As we explore later with HASCHK, checksums also form the backbone of authenticity protections for objects downloaded over the internet. For our implementation of StrongBox, we used the Merkle Tree library offered by SBD to manage our in-memory checksum verification. A proper implementation of StrongBox need not use the SDB SHA-256 Merkle Tree library. It was chosen for convenience.

Further, trading off security for energy, performance, and other concerns is not a new research area [38, 41, 57, 64, 109–111]. Goodman et al. introduced selectively decreasing the security of some data to save energy [38]. However, their approach is designed for communication and only considered iteration/round count, thus it did not anticipate the need for SwitchCrypt’s generic interface, switching strategies, or quantification framework. Wolter and Reinecke study approaches to quantifying security in several contexts [109]. This study anticipates the value of dynamically switching ciphers but proposes no mechanisms to enable this in FDE. Similarly, companies like LastPass and Google have explored performance-security tradeoffs. Google’s Adiantum uses a reduced-round version of ChaCha in exchange for performance [22]. While not an FDE solution, LastPass has dealt with scaling the number of iterations of PBKDF#2, trading performance for security during login sessions [106].

Finally, we examine prior approaches to guaranteeing resource integrity over the internet. We then highlight some drawbacks to these approaches and how HASCHK differs.

Anti-malware software, heuristics, and blacklists. Anti-malware software is a heuristic-based program designed for the specific purpose of detecting and removing various kinds of malware. However, updates to anti-malware definitions often lag behind or occur in re-

sponse to the release of crippling malware. For example, during the 2017 compromise of the HandBrake distribution mirror, users who first ran the compromised HandBrake image through *VirusTotal*—a web service that will run a resource through several dozen popular anti-malware products—received a report claiming no infections were detected despite the presence of the Proton malware [44]. In the 2012 compromise of SourceForge’s CDN, the malicious changes to the phpmyAdmin image do not appear as malware to anti-malware software [77].

Similarly, all modern browsers employ heuristic and blacklist-based detection and prevention schemes in an attempt to protect users from malicious content on the internet. The warnings generated by browser-based heuristics and blacklists are also reactive rather than proactive; hence, they are generally ineffective at detecting active or novel attacks on the integrity of the resources downloaded over the internet.

On the other hand, HASCHK relies on no heuristics or blacklists and is not anti-malware software. HASCHK is a protocol for automating checksum verification of resources. This ensures download integrity—that a user is receiving the expected resource a provider is advertising—not that the expected resource is not malware.

Link Fingerprints and Subresource Integrity. The Link Fingerprints (LF) draft describes an early HTML hyperlinks and URI based resource integrity verification scheme that “provides a backward-compatible technique for resource providers to ensure that the resource originally referenced is the same as the resource retrieved by an end user.” [63]. The World Wide Web Consortium’s (W3C) Subresource Integrity (SRI) describes a similar HTML-based scheme designed exclusively with CDNs and web assets in mind.

Like HASCHK, both LF and SRI employ cryptographic digests to ensure no changes of any kind have been made to a resource [3]. Unlike HASCHK, LF and SRI apply *only to resources referenced by script and link HTML elements*; HASCHK, on the other hand, can

ensure the integrity of *any arbitrary resource downloaded over the internet*, even outside of HTML web pages and browser software. Further, the checksums contained in the HTML source must be accurate for SRI to work. If the system *behind* the CDN is compromised, the attacker can alter the HTML and inject a malicious checksum or even strip checksums from the HTML entirely. With HASCHK, however, an attacker would additionally have to compromise the separate backend system that advertises the provider’s resources, thus raising the bar.

Content-MD5 Header. The Content-MD5 header field is a deprecated email and HTTP header that delivers a checksum similar to those used by Subresource Integrity. It was removed from the HTTP/1.1 specification because of the inconsistent implementation of partial response handling between vendors [34]. Further, the header could be easily stripped off or modified by proxies and other intermediaries [70]. HASCHK exhibits none of these weaknesses.

Deterministic Build Systems and Binary Transparency. A deterministic build system is one that, when given the same source, will deterministically output the same binary on every run. For example, many packages in Debian [83] and Arch Linux can be rebuilt from source to yield an identical byte for byte result [82], allowing for verification of the *Integration* and perhaps *Development* supply chain phases (see Table 5.1). Further, using a merkle tree [65] or similar construction, an additional chain of trust can be established that allows for public verification of the *Deployment*, *Maintenance*, and *Retirement* supply chain phases. Companies such as Mozilla refer to the latter as “Binary Transparency.”

Like HASCHK, binary transparency establishes a public verification scheme that allows third party consumers access to a listing of source updates advertised by a provider [91]. Consumers can leverage deterministic build systems and Binary Transparency together to

ensure their software is the same software deployed to every other system. Unlike HASCHK, binary transparency only allows a user to verify the integrity of *source updates to binaries*; our protocol allows a user to verify the integrity of *any arbitrary resource* while specifically addressing co-hosting.

Stickler and Cherubini et al. Stickler [56] by Levy et al. is an automated JavaScript-based stand-in for SRI for protecting the integrity of web application files hosted on CDNs. Stickler does not require any modifications to the client (*i.e.*, a frontend), instead delivering a bootloader to load and verify resources signed before the fact. However, as it was designed to stand-in for SRI, Stickler inherits some of SRI’s limitations. Specifically: Stickler was not designed to protect arbitrary resource downloads and, if the publisher’s server is compromised, Stickler’s bootloader can be stripped out of the initial HTTP response altogether. Something like this is not possible with HASCHK.

The automated checksum verification approach described by Cherubini et al. [18], also based on SRI, is similarly vulnerable to (and relies upon) co-hosting. Cherubini’s browser extension works by both looking for embedded checksums in download links (SRI) and extracting hexadecimal strings that look like checksums directly from the HTML source. An attacker, after compromising the resource file, need only modify the provider’s HTML file to inject a corrupted “integrity” attribute containing a checksum matching that corrupted resource, causing Cherubini’s extension to misreport the dangerous download as safe [18]. Additionally, Cherubini’s extension: (1) does not alert users when corresponding authoritative checksums are not found, which means an attacker can simply strip all checksums from the server response to pass off compromised resources to users; (2) considers a download “safe” so long as *any checksum found on the page matches it*, which means an attacker can just inject the compromised checksum somewhere in the HTML source alongside the legitimate checksum to similarly pass off compromised resources to users; (3) does not support

direct downloads, *i.e.*, when a user enters a resource's URI into the browser manually rather than click a hyperlink. None of this is a problem for HASCHK.

CHAPTER 3

STRONGBOX: USING STREAM CIPHERS FOR HIGH PERFORMANCE FULL DRIVE ENCRYPTION

3.1 Motivation

Full drive encryption (FDE)¹ is an essential technique for protecting the privacy of data at rest. For mobile devices, maintaining data privacy is especially important as these devices contain sensitive personal and financial data yet are easily lost or stolen. The current standard for securing data at rest is to use the AES cipher in XTS mode [78, 98]. Unfortunately, employing AES-XTS increases read/write latency by 3–5× compared to unencrypted storage.

It is well known that authenticated encryption using *stream* ciphers—such as ChaCha20 [11]—is faster than using AES (see Fig. 3.1). Indeed, Google made the case for stream ciphers over AES, switching HTTPS connections on Chrome for Android to use a stream cipher for better performance [101]. Stream ciphers are not used for FDE, however, for two reasons: (1) confidentiality and (2) performance. First, when applied naively to stored data, stream ciphers are trivially vulnerable to attacks—including *many-time pad* and *rollback attacks*—that reveal the plaintext by overwriting a secure storage location with the same key. Second, it has been assumed that adding the meta-data required to resist these attacks would ruin the stream cipher’s performance advantage. Thus, the conventional wisdom is that FDE necessarily incurs the overhead of AES-XTS or a similar primitive.

We argue that two technological shifts in mobile device hardware overturn this conventional wisdom, enabling confidential, high-performance storage with stream ciphers. First, these devices commonly employ solid-state storage with Flash Translation Layers (FTL), which operate similarly to Log-structured File Systems (LFS) [54, 55, 88]. Second, mobile

1. The common term is full *disk* encryption, but this work targets SSDs, so we use *drive*.

devices now support trusted hardware, such as Trusted Execution Environments (TEE) [59, 97] and secure storage areas [31]. FTLs and LFSes are used to limit sector/cell overwrites, hence extending the life of the drive. Most writes simply appended to a log, reducing the occurrence of overwrites and the chance for attacks. The presence of secure hardware means that drive encryption modules have access to persistent, monotonically increasing counters that can be used to prevent rollback attacks when overwrites do occur.

Given these trends, we propose StrongBox, a new method for securing data at rest. StrongBox is a drop-in replacement for AES-XTS-backed FDE such as dm-crypt [60]; *i.e.*, it requires no interface changes. The primary challenge is that even with a FTL or LFS running above an SSD, filesystem blocks will occasionally be overwritten; *e.g.*, by segment cleaning or *garbage collection*. StrongBox overcomes this challenge by using a fast stream cipher for confidentiality and performance with integrity preserving Message Authentication Codes [66] or “MAC tags” and a secure, persistent hardware counter to ensure integrity and prevent attacks. *StrongBox’s main contribution is a system design enabling the first confidential, high- performance drive encryption scheme based on a stream cipher.*

We demonstrate StrongBox’s effectiveness on a mobile ARM big.LITTLE system—a Samsung Exynos Octa 5—running Ubuntu Trusty 14.04 LTS, kernel 3.10.58. We use ChaCha20 [11] as our stream cipher, Poly1305 [10] as our MAC algorithm, and the eMMC Replay Protected Memory Block partition to store a secure counter [31]. As StrongBox requires no change to any existing interfaces, we benchmark it on two of the most popular LFSes: NILFS [54] and F2FS [55]. We compare the performance of these LFSes on top of AES-XTS (via dm-crypt) and StrongBox. Additionally, we compare the performance of AES-XTS encrypted Ext4 filesystems with StrongBox and F2FS. Our results show:

- *Improved read performance:* StrongBox provides decreased read latencies across all tested filesystems in the majority of benchmarks when compared to dm-crypt; *e.g.*, under F2FS, StrongBox provides as much as a $2.36\times$ ($1.72\times$ average) speedup over

AES-XTS.

- *Equivalent write performance:* despite having to maintain more metadata than FDE schemes based on AES-XTS, StrongBox achieves near parity or provides an improvement in observed write latencies in the majority of benchmarks; *e.g.*, under F2FS, StrongBox provides an average $1.27\times$ speedup over AES-XTS.

StrongBox achieves these performance gains while providing a stronger integrity guarantee than AES-XTS. Whereas XTS mode only hopes to randomize plaintext when the ciphertext is altered [98], StrongBox provides the security of standard authenticated encryption. In addition, StrongBox’s implementation is available open-source.²

3.1.1 Performance Potential

We demonstrate the potential performance win from switching to a stream cipher by comparing AES-XTS to ChaCha20+ Poly1305. We use an Exynos Octa processor with an ARM big.LITTLE architecture—the same processor used in the Samsung Galaxy line of phones. We encrypt and then decrypt 250MB of randomly generated bits 3 times and take the median time for each of encryption and decryption. Fig. 3.1 shows the distinct advantage of the stream cipher over AES—a consistent $2.7\times$ reduction in run time.

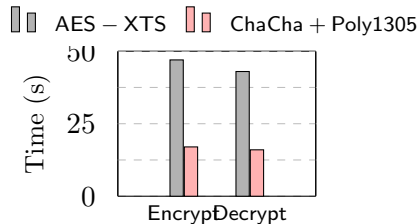


Figure 3.1: AES-XTS and ChaCha20+Poly1305 Comparison.

2. <https://github.com/Xunnamius/strongbox-switchcrypt>

3.1.2 Append-mostly Filesystems

Of course, stream ciphers are not designed to encrypt data at rest. If we naively implement block device encryption with a stream cipher, overwriting the same memory location with the same key would trivially allow an attacker to recover the secret key. Thus we believe stream ciphers are best suited for encrypting block devices backing Log-structured File Systems (LFSes), as these filesystems are designed to append data to the end of a log rather than overwrite data. In practice, some overwrites occur; *e.g.*, in metadata, but they are small in number during normal execution.

To demonstrate this fact, we write 800MB of random data directly to the backing store using four different file systems: Ext4, LogFS, NILFS, and F2FS. We count the number of total writes to the underlying block device and the number of times data is overwritten for each file system.

Table 3.1: File System Overwrite Behavior

File System	Total Write Ops	Overwrites
ext4	16,756	10,787
LogFS	4,244	32
NILFS	4,199	24
F2FS	2,107	2

Table 3.1 shows the data for this experiment. Ext4 has the highest number of writes, but many of those are small writes for book-keeping purposes. Ext4 also has the largest number of overwrites. Almost 65% of the writes are to a previously written location in the backing store. In contrast, all three Log-structured file systems have very few overwrites.

3.1.3 Threat Model

A stream cipher can be more than twice as fast as AES-XTS while providing the same confidentiality guarantee. The problem is that a stream cipher is not secure if the same key is used to overwrite the same storage location. Fortunately, FTLs and LFSes rarely overwrite

the same location.

We cannot, however, ignore the fact that overwrites do occur. While Table 3.1 shows overwrites are rare during normal operation, we know they will occur when garbage collecting the LFS. Thus, we will need some metadata to track writes and ensure that data is handled securely if overwrites occur. Therefore, we recognize three key challenges to replacing AES with a stream cipher for FDE:

- Tracking writes to the block device to ensure that the same location is never overwritten with the same key.
- Ensuring that the metadata that tracks writes is secure and is not subject to leaks or rollback attacks.
- Accomplishing the above efficiently so that we maintain the performance advantage of the stream cipher.

The key to StrongBox is using a secure, persistent counter supported in modern mobile hardware; *e.g.*, for limiting password attempts. This counter can track writes, and thus *versions* of the encrypted data. If an attacker tried to *roll back* the file system to overwrite the same location with the same key, our StrongBox detects that the local version number is out of sync with the global version number stored in the secure counter. In that case, StrongBox refuses to initialize and the attack fails. The use of the hardware-supported secure counter significantly raises the bar when it comes to rollback attacks, requiring a costly and non-discrete physical attack on the hardware itself to be effective. The actual structure of the metadata required to track writes and maintain integrity is significantly more complicated than simply implementing a counter and is the subject of the next section.

An additional challenge is that of crash recovery. StrongBox relies on the overlying filesystem to manage data recovery in the event of a crash that leaves user data in an inconsistent state. StrongBox handles metadata recovery after a crash by giving the root

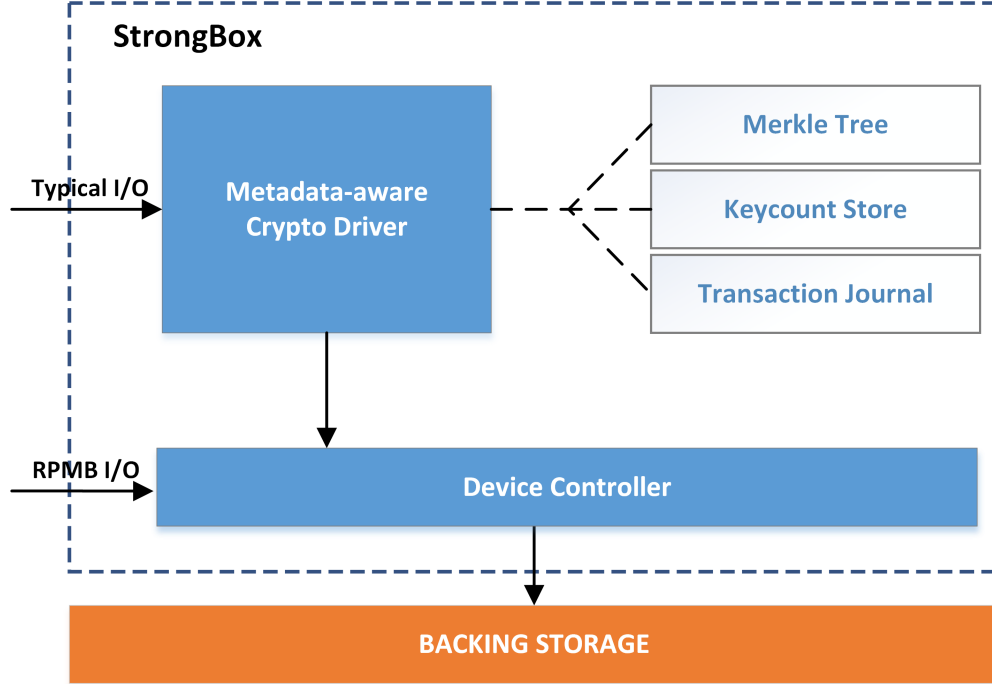


Figure 3.2: Overview of the StrongBox construction.

user the option to accept the current metadata state as the new consistent state, *i.e.*, “force mounting”. This allows the root user to mount the filesystem and access data after an unexpected shutdown. An attacker might try to take advantage of this feature by modifying the backing store, forcing an inconsistent state, and hoping the root user will ignore it and force mount the system anyway. StrongBox defends against this attack by preventing force mounts when metadata state is wildly inconsistent with the global version counter. Otherwise, the root user is warned if they attempt a force mount. Thus, attacking StrongBox by forcing a crash can only be successful if the attacker also has root permission, in which case security is already compromised. Crash recovery is also detailed in the next section.

3.2 System Design

StrongBox acts as a translation layer sitting between the drive and the operating system. It provides confidentiality and integrity guarantees while minimizing performance loss due to

metadata management overhead. StrongBox accomplishes this by leveraging the speed of stream ciphers over the AES block cipher and taking advantage of the append-mostly nature of Log-structured Filesystems (LFS) and modern Flash Translation Layers (FTL) [20].

Hence, there are several locations where StrongBox could be implemented in the system stack. StrongBox could be integrated into an LFS kernel module itself—*e.g.*, F2FS—specifically leveraging the flexibility of the Virtual Filesystem Switch (VFS). StrongBox could be implemented as an actual block device, or virtual block device layered atop a physical block device; the latter is where we chose to implement our prototype. StrongBox could even be implemented within the SSD drive controller’s FTL, which handles scatter gather, garbage collection, wear-leveling, etc.

Fig. 3.2 illustrates StrongBox’s design. StrongBox’s metadata is encapsulated in four components: an in-memory *Merkle Tree* and two drive-backed byte arrays—the *Keycount Store* and the *Transaction Journal*—and a persistent monotonic counter we implement with the *Replay Protected Memory Block* or RPMB. All four are integrated into the *Cryptographic Driver*, which handles data encryption, verification, and decryption during interactions with the underlying backing store. These interactions take place while fulfilling high-level I/O requests received from the LFS. The *Device Controller* handles low-level I/O between StrongBox and the backing store.

The rest of this section describes the components referenced in Fig. 3.2. Specifically: we first describe the backing store and StrongBox’s layout for data and metadata. This is followed by an exploration of the cryptographic driver and how it interacts with that metadata, the role of the device controller, an overview of rekeying in the backing store, and further considerations to ensure confidentiality in the case of rollbacks and related attacks.

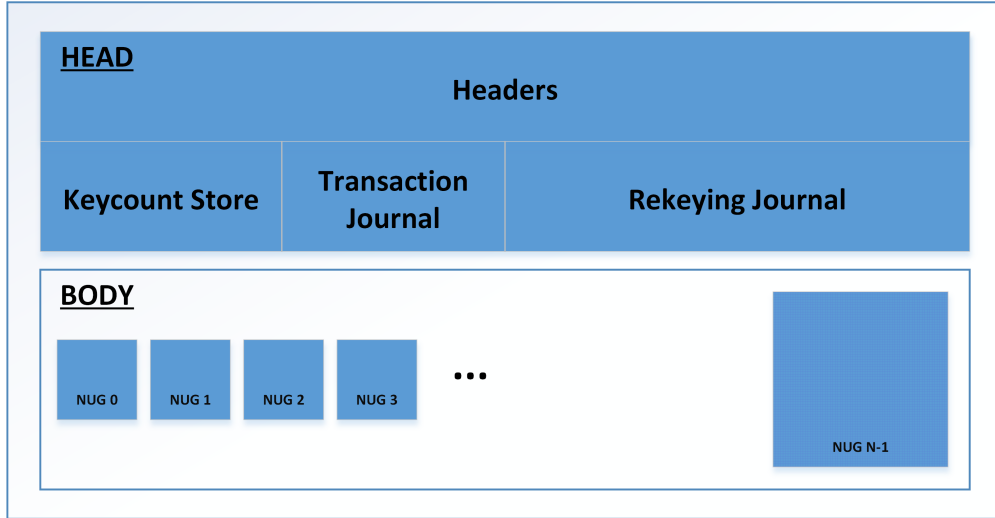


Figure 3.3: Layout of StrongBox's backing storage.

3.2.1 Backing Store Function and Layout

The backing store is the storage media on which StrongBox operates. Fig. 3.3 illustrates StrongBox's layout on this store.

In the *body* section of the backing store layout, end-user data is partitioned into a series of same-size *logical blocks*. These are distinct from the concept of *physical drive blocks*, which are collections of one or more drive sectors. To make this distinction clear, we refer to these wider logical blocks as *nuggets*, marked *NUG* in the Body section of Fig. 3.3. Hence, a nugget consists of one or more physical drive blocks, depending on its configured size. Each nugget is subdivided into a constant number of sub-blocks we refer to as *flakes*.

The reason for these nugget/flake divisions are two-fold:

1. To track, detect, and handle overwrites and
2. To limit the maximum length of any plaintexts operated on by the cryptographic driver, decreasing the overhead incurred per I/O operation and per overwrite.

Considering the first item, we are required to keep track of writes so that we may detect when an overwrite occurs. Flakes are key to this tracking. When a request comes in to

write to one or more flakes in a nugget, StrongBox marks the affected flakes as “flagged”. Here, “flagged” implies that another write to some portion of that flake would constitute an overwrite. If a new request comes in to write to one or more of those same flakes another time, StrongBox triggers a “rekeying” procedure over the entire nugget to safely overwrite the old data in those flakes. This rekeying procedure is necessarily time consuming, ballooning the overhead of overwrites translated by StrongBox.

Considering the second item, nugget size here governs the granularity of rekeying while flake size governs granularity when identifying overwrites. A larger nugget size will increase the penalty incurred with rekeying (you are re-encrypting a larger number of bytes) while a smaller nugget size will increase the quantity of nuggets needing to be rekeyed when an overwrite is detected as well as increase the amount of metadata stored on drive and in memory. On the other hand, a larger flake size will increase the number of times an incoming write is seen as an overwrite, with a non-optimal nugget-sized flake requiring a rekeying on *every write*. A smaller flake size will increase the amount of metadata stored on drive and in memory.

The size and structure of that metadata is described in greater detail throughout the rest of this section.

The *head* section of the backing store layout contains the metadata written to drive during StrongBox’s initialization. These headers govern StrongBox’s operation and are, in order:

1. VERSION, 4 bytes; specifies the StrongBox version originally used to initialize the backing store
2. SALT, 16 bytes; the salt used in part to derive the global master secret
3. MTRH, 32 bytes; the hash of the Merkle Tree root
4. TPMGLOBALVER, 8 bytes; the monotonic global version count, parity in hardware-supported secure storage

5. VERIFICATION, 32 bytes; used to determine if the key derived from a password is correct
6. NUMNUGGETS, 4 bytes; the number of nuggets contained by the backing store
7. FLAKESPERNUGGET, 4 bytes; the number of flakes/nugget
8. FLAKESIZE, 4 bytes; the size of each flake, in bytes
9. INITIALIZED, 1 byte; used to determine if the backing store has been properly initialized
10. REKEYING, 4 bytes; the index of the nugget in need of rekeying if there is a pending rekeying procedure

After the headers, two byte arrays are stored in the Head section: one of N 8-byte integer *keycounts* and one of $N \lceil P/8 \rceil$ -byte *transaction journal entries*, where N is the number of nuggets and P is the number of flakes per nugget.

Finally, the *Rekeying Journal* is stored at the end of the Head section. The rekeying journal is where nuggets and their associated metadata are transiently written, enabling StrongBox to resume rekeying in the event that it is interrupted during the rekeying procedure.

Metadata-aware Cryptographic Driver

The cryptographic driver coordinates StrongBox’s disparate components. Its primary function is to map incoming reads and writes to their proper destinations in the backing store, applying our chosen stream cipher and message authentication code to encrypt, verify, and decrypt data on the fly with consideration for metadata management.

When a read request is received, it is first partitioned into affected nuggets; *e.g.*, a read that spans two nuggets is partitioned in half. For each nugget affected, we calculate which flakes are touched by the request. We then verify the contents of those flakes. If all the flakes

Algorithm 1 StrongBox handling an incoming read request.

Require: The read request is over a contiguous segment of the backing store

Require: $\ell, \ell' \leftarrow$ read requested length

Require: $\aleph \leftarrow$ master secret

Require: $n_{index} \leftarrow$ first nugget index to be read

```
1:  $data \leftarrow empty$ 
2: while  $\ell \neq 0$  do
3:    $k_{n_{index}} \leftarrow GenKeynugget(n_{index}, \aleph)$ 
4:   Fetch nugget keycount  $n_{kc}$  from Keycount Store.
5:   Calculate indices touched by request:  $f_{first}, f_{last}$ 
6:    $n_{flakedat} \leftarrow ReadFlakes(f_{first}, \dots, f_{last})$ 
7:   for  $f_{current} = f_{first}$  to  $f_{last}$  do
8:      $k_{f_{current}} \leftarrow GenKeyflake(k_{n_{index}}, f_{current}, n_{kc})$ 
9:      $tag_{f_{current}} \leftarrow GenMac(k_{f_{current}}, n_{flakedat}[f_{current}])$ 
10:    Verify  $tag_{f_{current}}$  in Merkle Tree.
     $\triangleright$  (*) denotes requested subset of nugget data
11:    $data \leftarrow data + Decrypt(*n_{flakedat}, k_{n_{index}}, n_{kc})$ 
12:    $\ell \leftarrow \ell - \|*n_{flakedat}\|$ 
13:    $n_{index} \leftarrow n_{index} + 1$ 
14: return  $data$   $\triangleright$  Fulfill the read request
Ensure:  $\|data\| \leq \ell'$ 
Ensure:  $\ell = 0$ 
```

are valid, whatever subset of data that was requested by the user is decrypted and returned.

Algorithm 1 details StrongBox’s read operation.

Like reads, when a write request is received, the request is first partitioned with respect to affected nuggets. For each affected nugget, we calculate which flakes are touched by the request and then check if any of those flakes are marked as flagged in the transaction journal. If one or more of them have been marked flagged, we trigger rekeying for this specific nugget (see: Algorithm 3) and end there. Otherwise, we mark these touched flakes as flagged in the transaction journal. We then iterate over these touched flakes. For the first and last flakes touched by the write request, we execute an internal read request (see: Algorithm 1) to both obtain the flake data and verify that data with the Merkle Tree. We then overwrite every touched flake with the data from the requested operation, update the Merkle Tree to reflect this change, encrypt and write out the new flake data, and commit all corresponding metadata. Algorithm 2 details StrongBox’s write operation.

Algorithm 2 StrongBox handling an incoming write request.

Require: The write request is to a contiguous segment of the backing store

Require: $\ell, \ell' \leftarrow$ write requested length

Require: $\aleph \leftarrow$ master secret

Require: $data \leftarrow$ cleartext data to be written

Require: $n_{index} \leftarrow$ first nugget index to be affected

```
1: Increment secure counter: by 2 if we recovered from a crash, else 1
2: while  $\ell \neq 0$  do
3:   Calculate indices touched by request:  $f_{first}, f_{last}$ 
4:   if Transaction Journal entries for  $f_{first}, \dots, f_{last} \neq 0$  then
5:     Trigger rekeying procedure (see: Algorithm 3).
6:     continue
7:   Set Transaction Journal entries for  $f_{first}, \dots, f_{last}$  to 1
8:    $k_{n_{index}} \leftarrow GenKey_{nugget}(n_{index}, \aleph)$ 
9:   Fetch nugget keycount  $n_{kc}$  from Keycount Store.
10:  for  $f_{current} = f_{first}$  to  $f_{last}$  do
11:     $n_{flakedat} \leftarrow empty$ 
12:    if  $f_{current} == f_{first} || f_{current} == f_{last}$  then
13:       $n_{flakedat} \leftarrow CryptedRead(FSIZE, \aleph, n_{index}@f_{offset})$ 
14:       $n_{flakedat} \leftarrow Encrypt(n_{flakedat}, k_{n_{index}}, n_{kc})$ 
15:       $k_{f_{current}} \leftarrow GenKey_{flake}(k_{n_{index}}, f_{current}, n_{kc})$ 
16:       $tag_{f_{current}} \leftarrow GenMac(k_{f_{current}}, n_{flakedat})$ 
17:      Update new  $tag_{f_{current}}$  in Merkle Tree.
18:       $WriteFlake(f_{current}, n_{flakedat})$ 
19:  $\triangleright (*)$  denotes requested subset of nugget data if applicable
20:    $\ell \leftarrow \ell - || * n_{flakedat} ||$ 
21:    $n_{index} \leftarrow n_{index} + 1$ 
22: Update and commit metadata and headers
Ensure:  $\ell = 0$ 
```

Transaction Journal

An overwrite breaks the security guarantee offered by any stream cipher. To prevent this failure, StrongBox tracks incoming write requests to prevent overwrites. This tracking is done with the transaction journal, featured in Fig. 3.2.

The transaction journal consists of N $\lceil P/8 \rceil$ -byte bit vectors where N is the number of nuggets and P is the number of flakes per nugget. A bit vector v contains at least P bits $v = \{b_0, b_1, b_2, \dots, b_{P-1}, \dots\}$, with extra bits ignored. Each vector is associated with a nugget and each bit with a flake belonging to that nugget. When an incoming write request occurs, the corresponding bit vector is updated (set to 1) to reflect the new flagged state of those flakes.

The transaction journal is referenced during each write request, where it is updated to reflect the state of the nugget and checked to ensure the operation does not constitute an overwrite. If the operation *does* constitute an overwrite, StrongBox triggers a rekeying procedure for the entire nugget before safely completing the request.

Merkle Tree

Tracking writes with the transaction journal may stymie a passive attacker by preventing explicit overwrites, but a sufficiently motivated active attacker could resort to all manner of cut-and-paste tactics with nuggets, flakes, and even blocks and sectors. If, for example, an attacker purposefully zeroed-out the transaction journal entry pertaining to a specific nugget in some out-of-band manner—such as when StrongBox is shut down and then later re-initialized with the same backing store—StrongBox would consider any successive incoming writes as if the nugget were in a completely clean state, even though it actually is not. This attack would force StrongBox to make compromising overwrites. To prevent such attacks, we must ensure that the backing store is always in a valid state. More concretely: we must provide an integrity guarantee on top of a confidentiality guarantee.

StrongBox uses our chosen Message Authentication Code (MAC) generating algorithm and each flake’s unique key to generate a per-flake MAC tag (“MACed”). The purpose of this tag is to authenticate flake data and confirm that it has not been tampered with. Each tag is then appended to the Merkle Tree along with StrongBox’s metadata.

The transaction journal entries are handled specially in that the bit vectors are MACed and the result is appended to the Merkle Tree. This is done to save space.

The Merkle Tree then ties the integrity of any single flake to the integrity of the system as a whole such that if the former fails, *i.e.*, there is a MAC tag mismatch for any particular flake, the latter immediately and obviously fails.

Keycount Store

To prevent a many-time pad attack, each nugget is assigned its own form of nonce we refer to as a *keycount*. The keycount store in Fig. 3.2 represents a byte-array containing N 8-byte integer keycounts indexed to each nugget. Along with acting as the per-nugget nonce consumed by the stream cipher, the keycount is used to derive the per-flake unique subkeys used in MAC tag generation.

3.2.2 Rekeying Procedure

When a write request would constitute an overwrite, StrongBox will trigger a rekeying process instead of executing the write normally. This rekeying process allows the write to proceed without causing a catastrophic confidentiality violation.

When rekeying begins, the nugget in question is loaded into memory and decrypted. The target data is written into its proper offset in this decrypted nugget. The nugget is then encrypted, this time with a different nonce ($keycount + 1$), and written to the backing store, replacing the outdated nugget data. See: Algorithm 3.

3.2.3 Defending Against Rollback Attacks

To prevent StrongBox from making overwrites, the status of each flake is tracked and overwrites trigger a rekeying procedure. Tracking flake status alone is not enough, however. An attacker could take a snapshot of the backing store in its current state and then easily rollback to a previously valid state. At this point, the attacker could have StrongBox make writes that it does not recognize as overwrites.

With AES-XTS, the threat posed by rolling the backing store to a previously valid state is outside of its threat model. Despite this, data confidentiality guaranteed by AES-XTS holds in the event of a rollback, even if integrity is violated.

StrongBox uses a monotonic global version counter to detect rollbacks. When a rollback

Algorithm 3 StrongBox rekeying process.

Require: The original write applied to a contiguous backing store segment

Require: $\ell \leftarrow$ write requested length

Require: $\aleph \leftarrow$ master secret

Require: $data \leftarrow$ cleartext data to be written

Require: $n_{index} \leftarrow$ nugget rekeying target

▷ Read in and decrypt the entire nugget

- 1: $n_{nuggetdat} \leftarrow \text{CryptedRead}(NSIZE, \aleph, n_{index})$
- 2: Calculate indices touched by request: f_{first}, f_{last}
- 3: Write $data$ into $n_{nuggetdat}$ at proper offset with length ℓ
- 4: Set Transaction Journal entries for $f_{first}, \dots, f_{last}$ to 1
- 5: $k_{n_{index}} \leftarrow \text{GenKeynugget}(n_{index}, \aleph)$
- 6: Fetch nugget keycount n_{kc} from Keycount Store. Increment it by one.
- 7: $n_{nuggetdat} \leftarrow \text{Encrypt}(n_{nuggetdat}, k_{n_{index}}, n_{kc})$
- 8: Commit $n_{nuggetdat}$ to the backing store

▷ Iterate over all flakes in the nugget

- 9: **for all** flakes $f_{current}$ **in** n_{index} **do**
 - 10: $k_{f_{current}} \leftarrow \text{GenKeyflake}(k_{n_{index}}, f_{current}, n_{kc})$
 - 11: Copy $f_{current}$ data from $n_{nuggetdat} \rightarrow n_{flakedat}$
 - 12: $tag_{f_{current}} \leftarrow \text{GenMac}(k_{f_{current}}, n_{flakedat})$
 - 13: Update new $tag_{f_{current}}$ in Merkle Tree.
 - 14: Update and commit metadata and headers
-

is detected, StrongBox will refuse to initialize unless forced, using root permission. Whenever a write request is completed, this global version counter is committed to the backing store, committed to secure hardware, and updated in the in-memory Merkle Tree.

3.2.4 Recovering from Inconsistent State

If StrongBox is interrupted during operation, the backing store—consisting of user data and StrongBox metadata—will be left in an inconsistent state. StrongBox relies on the overlying filesystem *e.g.*, F2FS to manage user-data recovery, which is what these filesystems are designed to do and do well. We detail how StrongBox handles its own inconsistent metadata.

Let c be the value of the on-chip monotonic global version counter and d be the value of the on-drive global version counter header (TPMGLOBALVER). Consider the following:

- $c == d$ and *MTRH is consistent*: StrongBox is operating normally and will mount without issue.

- $c < d$ or $c == d$ but *MTRH is inconsistent*: Since the global version counter is updated before any write, this case cannot be reached unless the backing store was manipulated by an attacker. So, StrongBox will refuse to initialize and cannot be force mounted.
- $c > d + 1$: Since the global version counter is updated once per write, this case cannot be reached unless the backing store was rolled back or otherwise manipulated by an attacker. In this case, the root user is warned and StrongBox will refuse to initialize and cannot be force mounted unless the MTRH is consistent. We allow the root user to force mount here if the root user initiated the rollback themselves, such as when recovering from a drive backup.
- $c == d + 1$: In this case, StrongBox likely crashed during a write, perhaps during an attempted rekeying. If the rekeying journal is empty or the system cannot complete the rekeying and/or bring the MTRH into a consistent state, the root user is warned and allowed to force mount. Otherwise, StrongBox will not initialize.

For subsequent rekeying efforts in the latter two cases, rather than incrementing the corresponding keystore counters by 1 during rekeying, they will be incremented by 2. This is done to prevent potential reuse of any derived nugget keys that might have been in use right before StrongBox crashed.

When StrongBox can detect tampering, it will not initialize. When StrongBox cannot distinguish between tampering and crash, it offers the root user a choice to force mount. Thus, an attacker could force a crash and use root access to force mount. We assume, however, that if an attacker has root access to a device, its security is already compromised.

3.3 Implementation

Our implementation of StrongBox is comprised of 5000 lines of C code. StrongBox uses OpenSSL version 1.0.2 and LibSodium version 1.0.12 for its ChaCha20, Argon2, Blake2, and

AES-XTS implementations, likewise implemented in C. The SHA-256 Merkle Tree implementation is borrowed from the Secure Block Device library [47]. StrongBox’s implementation is available as open-source.³

To reduce the complexity of the experimental setup, establish a fair baseline, and allow StrongBox to run in user space, we use a BUSE [2] virtual block device. BUSE is a thin (200 LOC) wrapper around the standard Linux Network Block Device (NBD), which allows a machine to serve requests for reads and writes to virtual block devices exposed via domain socket. We built StrongBox on top of BUSE/NBD because a simple block device in user space allows for quick experimentation and rapid prototyping. It is not required for a proper implementation.

3.3.1 Deriving Subkeys

The cryptographic driver requires a shared master secret. The derivation of this master secret is implementation specific and has no impact on performance as it is completed during StrongBox’s initialization. Our implementation uses the Argon2 KDF to derive a master secret from a given password with an acceptable time-memory trade-off.

To assign each nugget its own unique keystream, that nugget requires a unique key and associated nonce. We derive these nugget subkeys from the master secret during StrongBox’s initialization. To guarantee the backing store’s integrity, each flake is tagged with a MAC. We use Poly1305, accepting a 32-byte one-time key and a plaintext of arbitrary length to generate tags. These one-time flake subkeys are derived from their respective nugget subkeys.

3.3.2 A Secure, Persistent, Monotonic Counter

Our target platform uses an embedded Multi-Media Card (eMMC) as a backing store. In addition to boot and user data partitions, the eMMC standard includes a secure storage

3. <https://github.com/Xunnamius/strongbox-switchcrypt>

partition called a Replay Protected Memory Block (RPMB) [31]. The RPMB partition's size is configurable to be at most 16MB (32MB on some Samsung devices) [79]. All read and write commands issued to the RPMB must be authenticated by a key burned into write-once storage (typically eFUSE) during some one-time, secure initialization process.

To implement rollback protection on top of the RPMB, the key for authenticating RPMB commands can be contained in TEE sealed storage or derived from the TPM. For this implementation, StrongBox requires interaction with TPM/TEE secure storage only at mount time, where the authentication key can be retrieved and cached for the duration of StrongBox's lifetime. With the cached key on hand, our implementation makes traditional IOCTL calls to read and write global version counter data to the RPMB eMMC partition, enforcing the invariant that it only increase monotonically.

Our design is not dependent on the eMMC standard, however. Trusted hardware mechanisms other than the eMMC RPMB partition, including TPMs, support secure, persistent storage and/or monotonic counters directly. These can be adapted for use with StrongBox just as well.

There are two practical concerns we must address while implementing the secure counter: wear and performance overhead. Wear is a concern because the counter is implemented in non-volatile storage. The RPMB implements all the same wear protection mechanisms that are used to store user-data [31]. Additionally, StrongBox writes to the global version counter once per write to user-data. Given that the eMMC implements the same wear protection for the RPMB and user data, and that the ratio of writes to these areas is 1:1, we expect StrongBox places no additional wear burden on the hardware. Further, with the JEDEC spec suggesting RPMB implementations use more durable and faster single-level NAND flash cells rather than cheaper and slower multi-level NAND flash cells [31, 79], the RPMB partition will likely outlive and outperform the user-data portion of the eMMC.

In terms of performance overhead, updating the global version counter requires making

one 64-bit authenticated write per user-data write. As user-data writes are almost always substantially larger, we see no significant overhead from the using the RPMB to store the secure counter.

3.3.3 LFS Garbage Collection

An LFS attempts to write to a drive sequentially in an append-only fashion, as if writing to a log. This requires large amounts of contiguous space, called *segments*. Since any backing store is necessarily finite, an LFS can only append so much data before it runs out of space. When this occurs, the LFS triggers a *segment cleaning algorithm* to erase outdated data and compress the remainder of the log into as few segments as possible [55, 88]. This procedure is known more broadly as *garbage collection* [55].

In the context of StrongBox, garbage collection could potentially incur high overhead. The procedure itself would, with its every write, require a rekeying of any affected nuggets. Worse, every proceeding write would appear to StrongBox as if it were an overwrite, since there is no way for StrongBox to know that the LFS triggered garbage collection internally.

In practice, modern production LFSes are optimized to perform garbage collection as few times as possible [55]. Further, they often perform garbage collection in a background thread that triggers when the filesystem is idle and only perform expensive on-demand garbage collection when the backing store is nearing capacity [54, 55]. We leave garbage collection turned on for all of our tests and see no substantial performance degradation from this process because it is scheduled not to interfere with user I/O.

3.3.4 Overhead

StrongBox stores metadata on the drive it is encrypting (see Fig. 3.3). This metadata should be small compared to the user data. Our implementation uses 4KB flakes, 256 flakes/nugget, and 1024 nuggets per GB of user data. Given the flake and nugget overhead,

this configuration requires just over 40KB of metadata per 1 GB of user data. There is an additional, single static header that requires just over 200 bytes. *Thus StrongBox’s overhead in terms of storage is less than one hundredth of a percent.*

3.4 Evaluation

3.4.1 Experimental Setup

We implement a prototype of StrongBox on a Hardkernel Odroid XU3 ARM big.LITTLE system (Samsung Exynos5422 A15 and A7 quad core CPUs, 2Gbyte LPDDR3 RAM at 933 MHz, eMMC5.0 HS400 backing store) running Ubuntu Trusty 14.04 LTS, kernel version 3.10.58. The maximum theoretical memory bandwidth for this model is 14.9GB/s. Observed maximum memory bandwidth is 4.5GB/s.

3.4.2 Experimental Methodology

In this section we seek to answer three questions:

1. What is StrongBox’s overhead when compared to dm-crypt AES-XTS?
2. How does StrongBox under an LFS (*i.e.*, F2FS) configuration compare to the popular dm-crypt under Ext4 configuration?
3. Where does StrongBox derive its performance gains? Implementation? Choice of cipher?

To evaluate StrongBox’s performance, we measure the latency (seconds/milliseconds per operation) of both sequential and random read and write I/O operations across four different standard Linux filesystems: NILFS2, F2FS, Ext4 in ordered journaling mode, and Ext4 in full journaling mode. The I/O operations are performed using file sizes between 4KB and

40MB. These files were populated with random data. The experiments are performed using a 1GB standard Linux ramdisk (tmpfs) as the ultimate backing store.

For sequential F2FS specifically, we include latency measurements dealing with a file size $2.5\times$ the size of available DRAM, *i.e.*, 5GB, supported by a distinct tmpfs backing store swapped into memory.

Ext4’s default is ordered journaling mode (`data=ordered`), where metadata is committed to the filesystem’s journal while the actual data is written through to the main filesystem. Given a crash, the filesystem uses the journal to avoid damage and recover to a consistent state. Full journaling mode (`data=journal`) journals both metadata and the filesystem’s actual data—essentially a double write-back for each write operation. Given a crash, the journal can replay entire I/O events so that both the filesystem and its data can be recovered. We include both modes of Ext4 to further explore the impact of frequent overwrites against StrongBox.

The experiment consists of reading and writing each file in its entirety 30 times sequentially, and then reading and writing random portions of each file 30 times. In both cases, the same amount of data is read and written per file. The median latency is taken per result set. We chose 30 read/write operations (10 read/write operations repeated three times each) to handle potential variation. The Linux page cache is dropped before every read operation, each file is opened in synchronous I/O mode via `O_SYNC`, and we rely on non-buffered `read()/write()` system calls. A high-level I/O size of 128KB was used for all read and write calls that hit the filesystems; however, the I/O requests being made at the block device layer varied between 4KB and 128KB depending on the filesystem under test.

The experiment is repeated on each filesystem in three different configurations:

1. *unencrypted*: Filesystem mounted atop a BUSE virtual block device set up to immediately pass through any incoming I/O requests straight to the backing store. We use this as the baseline measurement of the filesystem’s performance without any encryption.

2. *StrongBox*: Filesystem mounted atop a BUSE virtual block device provided by our StrongBox implementation to perform full drive encryption.
3. *dm-crypt*: Filesystem mounted atop a Device Mapper [80] higher-level virtual block device provided by dm-crypt to perform full drive encryption, which itself is mounted atop a BUSE virtual block device with pass through behavior identical to the device used in the baseline configuration. dm-crypt was configured to use AES-XTS as its full drive encryption algorithm. All other parameters were left at their default values.

Fig. 3.4 compares StrongBox to dm-crypt under the F2FS filesystem. The gamut of result sets over different filesystems can be seen in Fig. 3.5. Fig. 3.6 compares Ext4 with dm-crypt to F2FS with StrongBox.

3.4.3 *StrongBox Read Performance*

Fig. 3.4 shows the performance of StrongBox in comparison to dm-crypt, both mounted with the F2FS filesystem. We see StrongBox improves on the performance of dm-crypt’s AES-XTS implementation across sequential and random read operations on all file sizes. Specifically, $2.36\times$ (53.05m/22.48m) for sequential 5GB, $2.07\times$ (2.09s/1.00s) for sequential 40MB, $2.08\times$ (267.34ms/128.22ms) for sequential 5MB, $1.85\times$ (28.30ms/15.33ms) for sequential 512KB, and $1.03\times$ (0.95ms/0.86ms) for sequential 4KB.

Fig. 3.5 provides an expanded performance profile for StrongBox, testing a gamut of filesystems broken down by workload file size. For sequential reads across all filesystems and file sizes, StrongBox outperforms dm-crypt. This is true even on the non-LFS Ext4 filesystems. Specifically, we see read performance improvements over dm-crypt AES-XTS for 40MB sequential reads of $2.02\times$ (2.15s/1.06s) for NILFS, $2.07\times$ (2.09s/1.00s) for F2FS, $2.09\times$ (2.11s/1.01s) for Ext4 in ordered journaling mode, and $2.06\times$ (2.11s/1.02s) for Ext4 in full journaling mode. For smaller file sizes, the performance improvement is less pronounced. For 4KB reads we see $1.28\times$ (1.62ms/1.26ms) for NILFS, $1.03\times$ (0.88ms/0.86ms) for F2FS,

$1.04\times$ (0.95ms/0.92ms) for Ext4 in ordered journaling mode, and $1.07\times$ (0.97ms/0.91ms) for Ext4 in full journaling mode. When it comes to random reads, we see virtually identical results save for 4KB reads, where dm-crypt proved slightly more performant under the NILFS LFS at $1.12\times$ (1.73ms/1.54ms). This behavior is not observed with the more modern F2FS.

3.4.4 StrongBox Write Performance

Fig. 3.4 shows the performance of StrongBox in comparison to dm-crypt under the modern F2FS LFS broken down by workload file size. Similar to read performance under the F2FS, we see StrongBox improves on the performance of dm-crypt’s AES-XTS implementation across sequential and random write operations on all file sizes. Hence, StrongBox under F2FS is holistically faster than dm-crypt under F2FS. Specifically, $1.55\times$ (1.80h/1.16h) for sequential 5GB, $1.33\times$ (3.19s/2.39s) for sequential 40MB, $1.21\times$ (412.51ms/341.56ms) for sequential 5MB, $1.15\times$ (65.23ms/56.63ms) for sequential 512KB, and $1.19\times$ (30.30ms/25.46ms) for sequential 4KB.

Fig. 3.5 provides an expanded performance profile for StrongBox, testing a gamut of filesystems broken down by workload file size. Unlike read performance, write performance under certain filesystems is more of a mixed bag. For 40MB sequential writes, StrongBox outperforms dm-crypt’s AES-XTS implementation by $1.33\times$ (3.19s/2.39s) for F2FS and $1.18\times$ (4.39s/3.74s) for NILFS. When it comes to Ext4, StrongBox’s write performance drops precipitously with a $3.6\times$ *slowdown* for both ordered journaling and full journaling modes (respectively: 12.64s/3.51s, 24.89s/6.88s). For non-LFS 4KB writes, the performance degradation is even more pronounced with a $8.09\times$ (118.48ms/14.65ms) slowdown for ordered journaling and $14.5\times$ (143.15ms/9.87ms) slowdown for full journaling.

This slowdown occurs in Ext4 because, while writes in StrongBox from non-LFS filesystems have a metadata overhead that is comparable to that of forward writes in an LFS filesystem, Ext4 is not an append-only or append-mostly filesystem. This means that, at

any time, Ext4 will initiate one or more overwrites anywhere on the drive (see Table 3.1). As described in Section 3.2, overwrites once detected trigger the rekeying process, which is a relatively expensive operation. Multiple overwrites compound this expense further. This makes Ext4 and other filesystems that do not exhibit at least append-mostly behavior unsuitable for use with StrongBox. We include it in our result set regardless to illustrate the drastic performance impact of frequent overwrites on StrongBox.

For both sequential and random 4KB writes among the LFSes, the performance improvement over dm-crypt’s AES-XTS implementation for LFSes deflates. For the more modern F2FS atop StrongBox, there is a $1.19\times$ (30.30ms/25.46ms) improvement. For the older NILFS filesystem atop StrongBox, there is a $2.38\times$ (27.19ms/11.44ms) slowdown. This is where we begin to see the overhead associated with tracking writes and detecting overwrites potentially becoming problematic, though the overhead is negligible depending on choice of LFS and workload characteristics.

These results show that StrongBox is sensitive to the behavior of the LFS that is mounted atop it, and that any practical use of StrongBox would require an extra profiling step to determine which LFS works best with a specific workload. With the correct selection of LFS, such as F2FS for workloads dominated by small write operations, potential slowdowns when compared to mounting that same filesystem over dm-crypt’s AES-XTS can be effectively mitigated.

3.4.5 *On Replacing dm-crypt and Ext4*

Fig. 3.6 describes the performance benefit of using StrongBox with F2FS over the popular dm-crypt with Ext4 in ordered journaling mode combination for both sequential and random read and write operations of various sizes. Other than 4KB and 512KB write operations, which are instances where baseline F2FS without StrongBox is simply slower than baseline Ext4 without dm-crypt, StrongBox with F2FS outperforms dm-crypt’s AES-XTS

implementation with Ext4.

These results show that configurations taking advantage of the popular combination of dm-crypt, AES-XTS, and Ext4 could see a significant improvement in read performance without a degradation in write performance except in cases where small ($\leq 512KB$) writes dominate the workload.

Note, however, that several implicit assumptions exist in our design. For one, we presume there is ample memory at hand to house the Merkle Tree and all other data abstractions used by StrongBox. Efficient memory use was not a goal of our implementation of StrongBox. In an implementation aiming to be production ready, much more memory efficient data structures would be utilized.

It is also for this reason that populating the Merkle Tree necessitates a rather lengthy mounting process. In our tests, a 1GB backing store on the odroid system can take as long as 15 seconds to mount.

3.4.6 Performance in StrongBox: ChaCha20 vs AES

Fig. 3.5 and Fig. 3.4 give strong evidence for our general performance improvement over dm-crypt not being an artifact of filesystem choice. Excluding Ext4 as a non-LFS filesystem under which to run StrongBox, our tests show that StrongBox outperforms dm-crypt under an LFS filesystem in the vast majority of outcomes.

We then test to see if our general performance improvement can be attributed to the use of a stream cipher over a block cipher. dm-crypt implements AES in XTS mode to provide full drive encryption functionality. Fig. 3.7 describes the relationship between ChaCha20, the cipher of choice for our implementation of StrongBox, and the AES cipher. Swapping out ChaCha20 for AES-CTR resulted in slowdowns of up to $1.33\times$ for reads and $1.15\times$ for writes across all configurations, as described in Fig. 3.7.

Finally, we test to see if our general performance improvement can be attributed to our

implementation of StrongBox rather than our choice of stream cipher. We test this by implementing AES in XTS mode on top of StrongBox using OpenSSL EVP (see: Fig. 3.7). StrongBox using OpenSSL AES-XTS experiences slowdowns of up to $1.33\times$ for reads and $1.6\times$ for writes compared to StrongBox using ChaCha20 (sequential, 40MB). Interestingly, while significantly less performant, this slowdown is not entirely egregious, and suggests that perhaps there are parts of the dm-crypt code base that would benefit from further optimization; however, it is possible that necessary choices to harden StrongBox for a production environment could slow it down as well.

Considering hardware support for dedicated AES instructions, Fig. 3.7 shows StrongBox with AES-CTR outperforms AES-XTS. Therefore, StrongBox should still outperform dmccrypt where AES hardware support is available.

3.4.7 Overhead with a Full Drive

During I/O operations under an appropriate choice of LFS, we have shown that full drive encryption provided by StrongBox outperforms full drive encryption provided by dm-crypt. However, this is not necessarily the case when the backing store becomes full and the LFS is forced to cope with an inability to write forward as efficiently.

In the case of the F2FS LFS, upon approaching capacity and being unable to perform garbage collection effectively, it resorts to writing blocks out to where ever it can find free space in the backing store [55]. It does this instead of trying to maintain an append-only guarantee. This method of executing writes is similar to how a typical non-LFS filesystem operates. When this happens, the F2FS aggressively causes overwrites in StrongBox, which has a drastic impact on performance.

Fig. 3.8 shows the impact of these (sequential) overwrites. Read operation performance remains faster on a full StrongBox backing store compared to dm-crypt. This is not the case with writes. Compared to StrongBox under non-full conditions, 40MB sequential writes were

Table 3.2: Attacks on StrongBox and their results

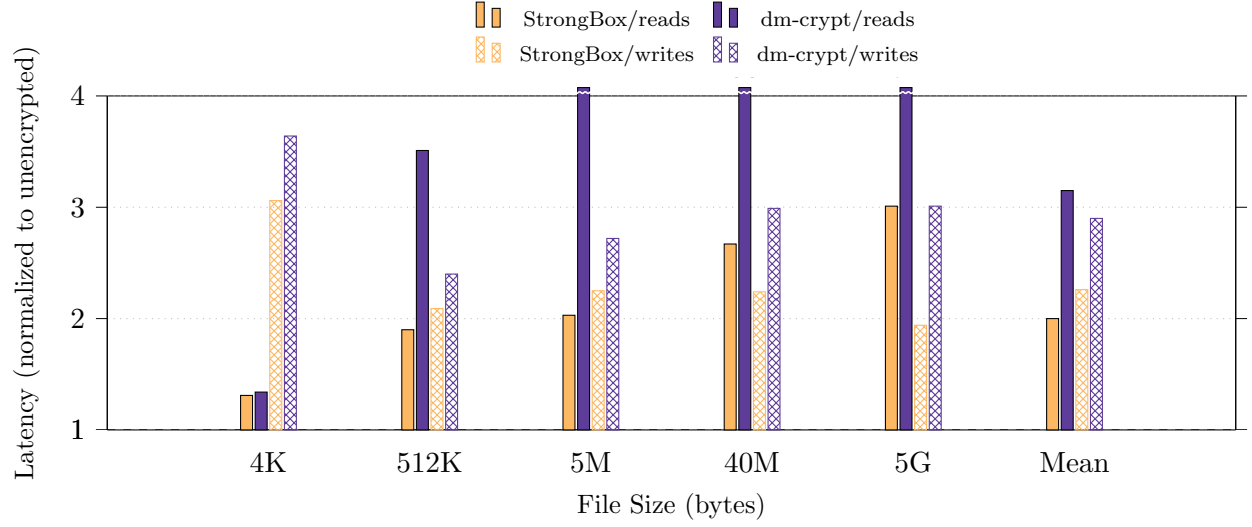
Attack	Result	Explanation
Nugget user data in backing store is mutated out-of-band online	StrongBox Immediately fails with exception on successive IO request	The MTRH is inconsistent
Header metadata in backing store is mutated out-of-band online, making the MTRH inconsistent	StrongBox Immediately fails with exception on successive IO request	The MTRH is inconsistent
Backing store is rolled back to a previously consistent state while online	StrongBox Immediately fails with exception on successive IO request	TPMGLOBALVER and RPMB secure counter out of sync
Backing store is rolled back to a previously consistent state while offline, RPMB secure counter wildly out of sync	StrongBox refuses to mount; allows for force mount with root access	TPMGLOBALVER and RPMB secure counter out of sync
MTRH made inconsistent by mutating backing store out-of-band while offline, RPMB secure counter in sync	StrongBox refuses to mount	TPMGLOBALVER and RPMB secure counter are in sync, yet illegal data manipulation occurred

slowed by $2.8\times$ as StrongBox approached maximum capacity.

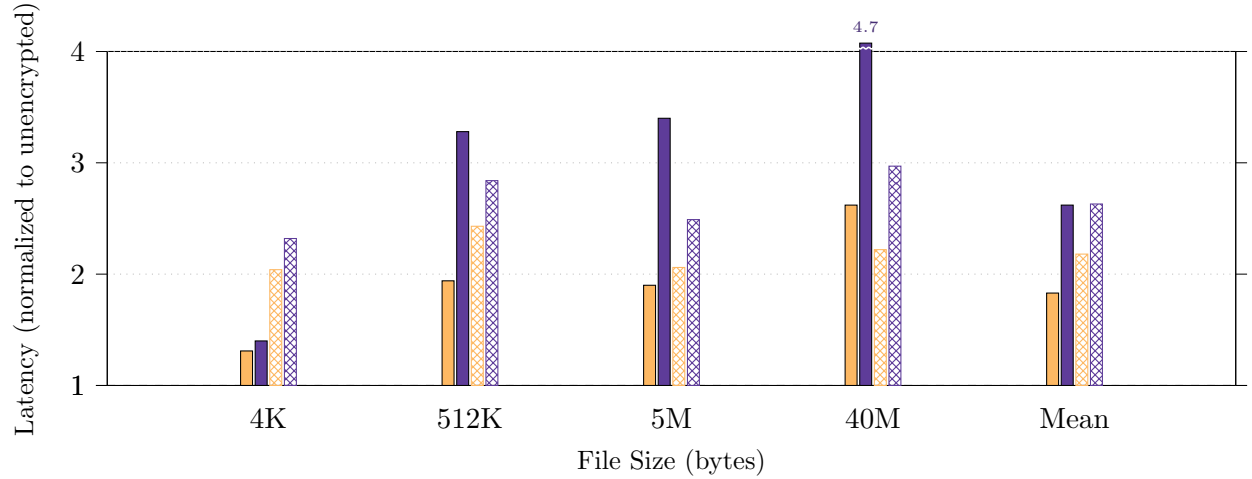
3.4.8 Threat Analysis

Table 3.2 lists possible attacks and their results. It can be inferred from these results and StrongBox’s design that StrongBox addresses its threat model and maintains confidentiality and integrity guarantees.

StrongBox vs dm-crypt AES-XTS: F2FS Test



(a) Sequential I/O expanded F2FS result set.



(b) Random I/O expanded F2FS result set.

Figure 3.4: Test of the F2FS LFS mounted atop both dm-crypt and StrongBox; median latency of different sized whole file read and write operations normalized to unencrypted access. By harmonic mean, StrongBox is $1.72\times$ faster than dm-crypt for sequential reads and $1.27\times$ faster for sequential writes.

StrongBox Four Filesystems Test

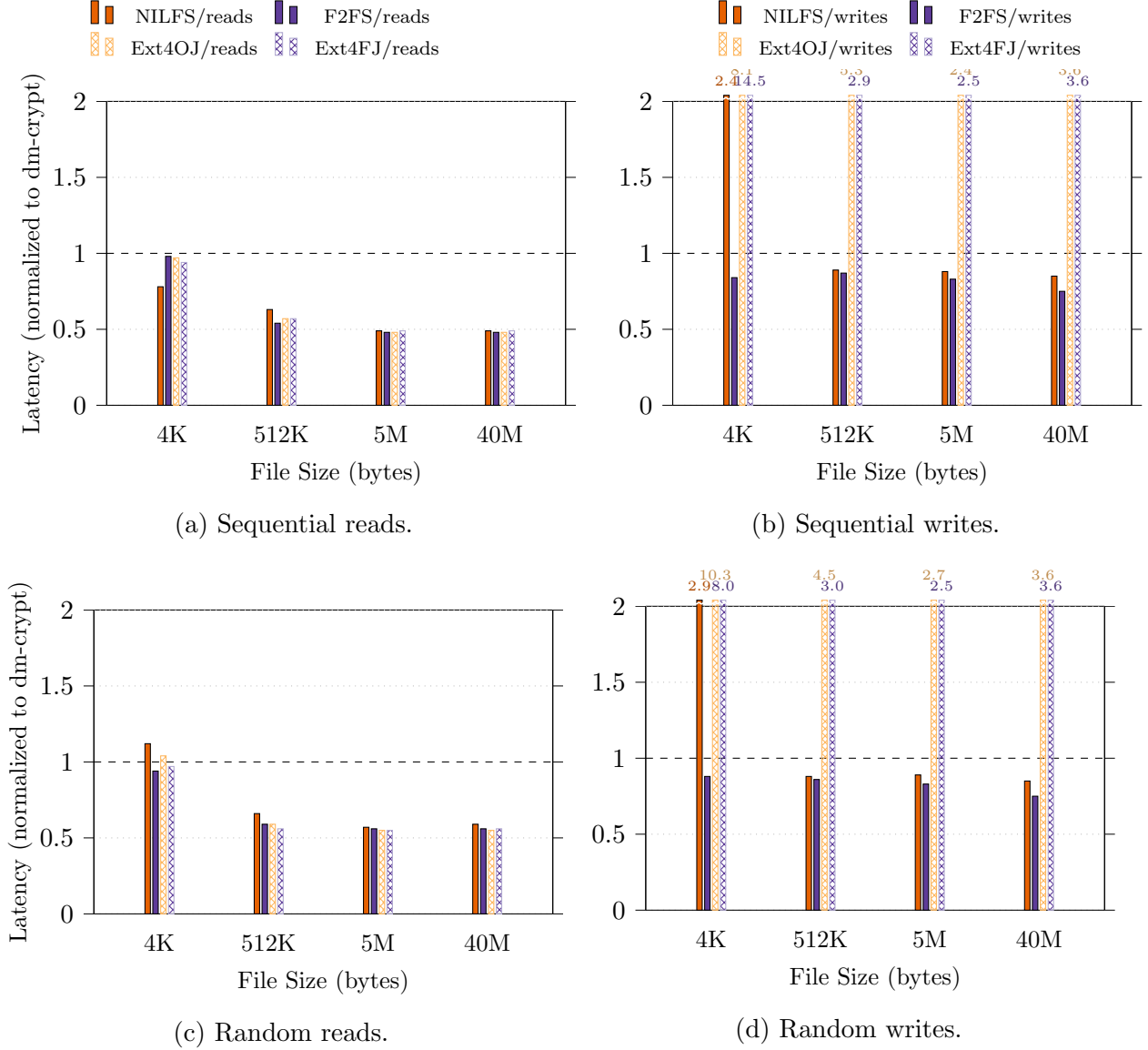
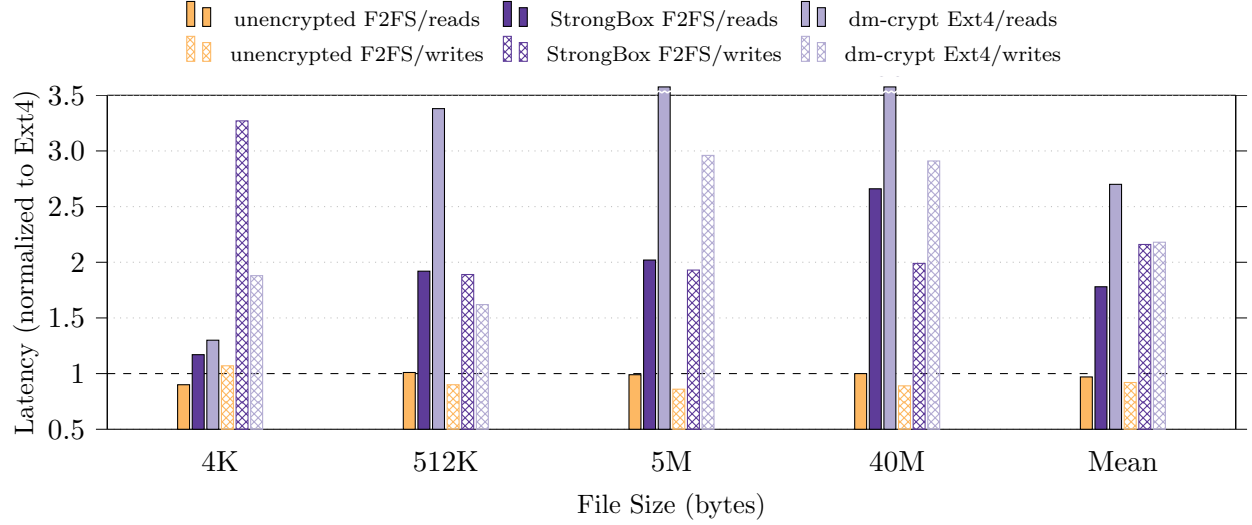
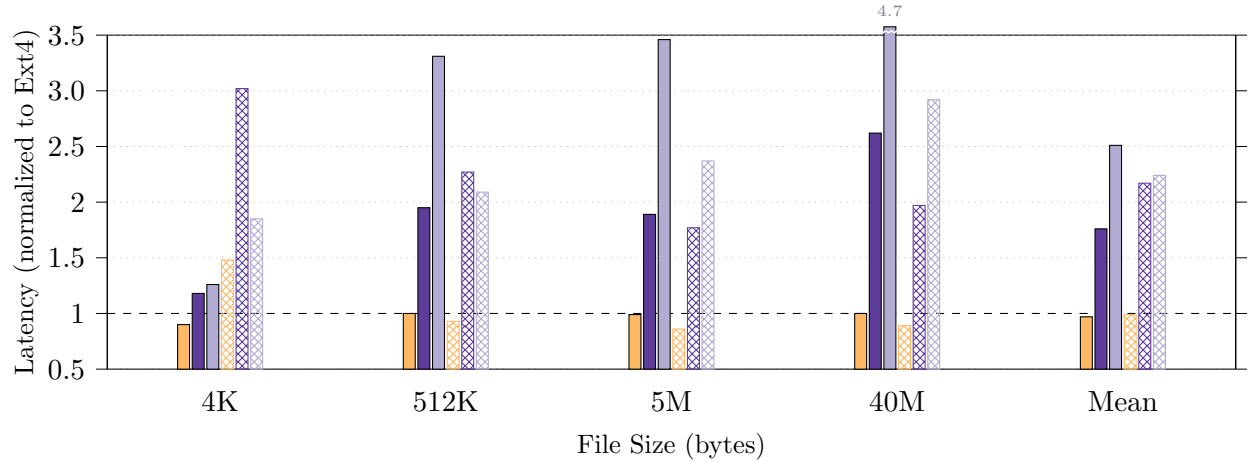


Figure 3.5: Comparison of four filesystems running on top of StrongBox performance is normalized to the same file system running on dm-crypt. Points below the line signify StrongBox outperforming dm-crypt. Points above the line signify dm-crypt outperforming StrongBox.

StrongBox F2FS vs dm-crypt AES-XTS Ext4-OJ



(a) Sequential I/O F2FS vs Ext4 result set.



(b) Random I/O F2FS vs Ext4 result set.

Figure 3.6: Comparison of Ext4 on dm-crypt and F2FS on StrongBox. Results are normalized to unencrypted Ext4 performance. Unencrypted F2FS results are shown for reference. Points below the line are outperforming unencrypted Ext4. Points above the line are underperforming compared to unencrypted Ext4.

ChaCha20 vs AES: StrongBox F2FS Sequential Test

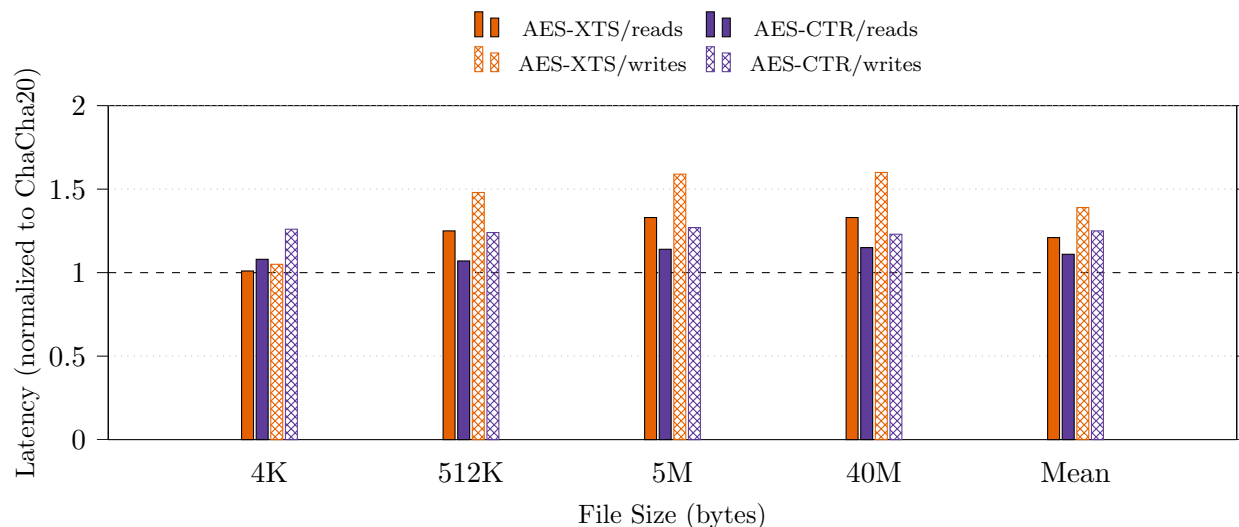


Figure 3.7: Comparison of AES in XTS and CTR modes versus ChaCha20 in StrongBox; median latency of different sized whole file sequential read and write operations normalized to ChaCha20 (default cipher in StrongBox). Points below the line signify AES outperforming ChaCha20. Points above the line signify ChaCha20 outperforming AES.

Near-Full Drive F2FS Test

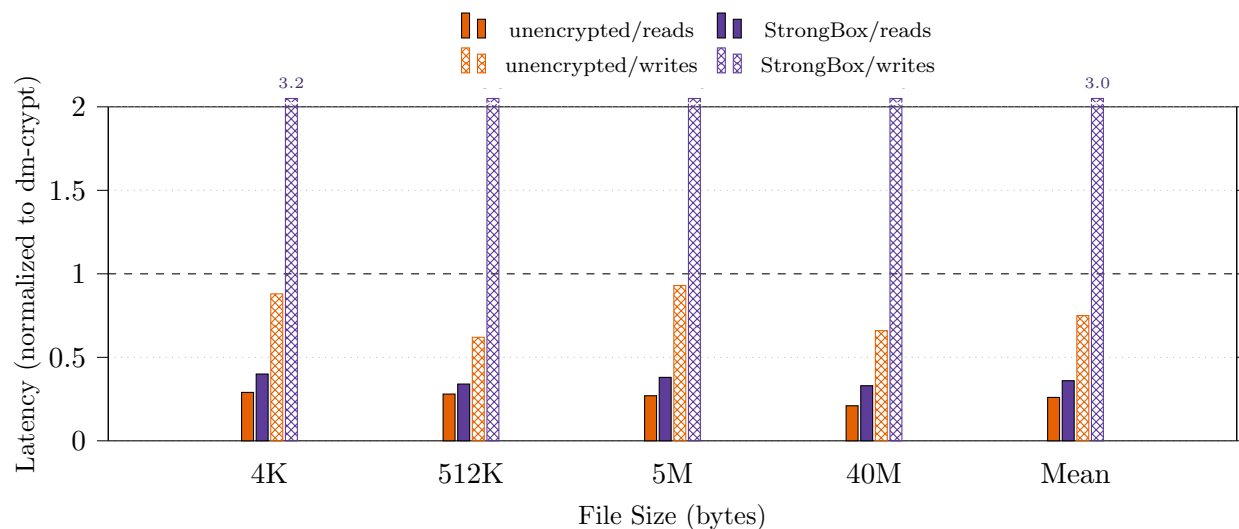


Figure 3.8: Comparison of F2FS baseline, atop dm-crypt, and atop StrongBox. All configurations are initialized with a near-full backing store; median latency of different sized whole file read and write operations normalized to dm-crypt. Points below the line are outperforming dm-crypt. Points above the line are underperforming compared to dm-crypt.

CHAPTER 4

SWITCHCRYPT: NAVIGATING TRADEOFFS IN STREAM CIPHER BASED FULL DRIVE ENCRYPTION

4.1 Motivation

The state of the art for securing data at rest, such as the contents of a laptop’s SSD, is Full Drive Encryption (FDE). Traditional FDE employs a single cryptographic cipher to encrypt, decrypt, and authenticate drive contents on the fly. Unfortunately, encryption introduces overhead that drastically impacts system performance and total energy consumption. Hence, modern storage systems must carefully balance these competing concerns. On the one hand, stronger security guarantees come with increased latency and threaten to balloon energy consumption. On the other, capping total energy consumption requires tolerating increased latency or weaker security guarantees.

FDE implementations such as dm-crypt [6, 60] for Linux and BitLocker for Windows balance these concerns with respect to some generic “common case” workload, but this approach often fails to deliver an optimal outcome for specific workloads. Google’s Android OS is a good example. Android supported FDE with the release of Android 3.0, yet it was not enabled by default until Android 6.0 [23]. Two years prior, Google attempted to roll out FDE by default on Android 5.0 but had to backtrack. In a statement to Engadget, Google blamed “performance issues on some partner devices’ ... for the backtracking” [92]. At the same time, AnandTech reported a “62.9% drop in random read performance, a 50.5% drop in random write performance, and a staggering 80.7% drop in sequential read performance” versus Android 5.0 unencrypted storage for various workloads [49].

FDE’s impact on drive performance and energy efficiency depends on a multitude of choices. Paramount among them is the choice of cipher, as different ciphers expose different performance and energy efficiency characteristics. In this way, cipher choice can be viewed

as a key *configuration parameter* for FDE systems. The benefits of choosing one cipher over another might include: 1) improved performance (*i.e.*, overall reduction in FDE overhead), 2) reduced energy use, 3) more useful security guarantees, and 4) the ability to encrypt devices that would otherwise be too slow or energy-inefficient to support FDE.

However, the standard cipher choice for FDE is the slow AES *block cipher* (AES-XTS) [73, 78, 98]. With StrongBox, we introduced a method for using ciphers other than AES-XTS for FDE; specifically, the high performance ChaCha20 *stream cipher* [11, 26]. More recent work—such as Google’s HBSH (hash, block cipher, stream cipher, hash) and Adiantum [22]—brings stream cipher based FDE to devices that do not or cannot support hardware accelerated AES. Hence, it has been demonstrated that using stream ciphers for FDE is both desirable in a variety of contexts and feasible at industry scale.

With this research, we explore the rich configuration space of stream ciphers beyond the narrow scope of previous work. Each cipher comes with a variety of performance, energy efficiency, and security properties in the FDE context. These ciphers include ChaCha variants with different round counts (e.g., ChaCha8 and ChaCha12) [11], ciphers with stronger security guarantees versus more robust adversaries (e.g., Freestyle [7]), and other ciphers like SalsaX [12], AES in counter mode (AES-CTR) [102], Rabbit [15], Sosemanuk [8], etc. Given this variety, the cipher configuration providing the least latency overhead is almost always different than the configuration providing the most desirable security properties, and both may differ from the configuration using the least energy or preserving the most free space on the encrypted drive.

Further, while cipher choice might be configured statically at compile or boot time with respect to some common case in traditional FDE, such configurations cannot dynamically adapt to changes that arise while the system is running. Examples include changes in resource availability, runtime environment, desired security properties, and respecting changing OS energy budgets.

Hence, any static common-case FDE configuration will sacrifice one concern for another, even when it is not optimal to do so for a given workload. But what if a system could dynamically transition into a more desirable configuration given runtime changes?

Our Contributions

To realize the goal of dynamically adjusting storage tradeoffs at runtime, we:

- Define a scheme to *quantify* the usefulness of each cipher based on key security properties relevant to FDE in context. Using this scheme, we define a tradeoff space of cipher configurations over competing concerns: total energy use, desirable security properties, read and write performance (latency), total writable space on the drive, and how quickly the contents of the drive can converge to a single encryption configuration.
- Introduce a novel design substantively expanding prior FDE work by wholly *decoupling* cipher implementations from the encryption process.
- Develop the idea of cipher switching using *switching strategies* to “re-cipher” storage units dynamically, allowing us to tradeoff different performance and security properties of various configurations at runtime.

Unifying these contributions, we present SwitchCrypt: a software system that navigates the tradeoff space made by balancing competing security and latency requirements via cipher switching in space and time. We implement SwitchCrypt and three switching strategies—*Forward*, *Selective*, and *Mirrored*—to dynamically transition the system between configurations using our generic cipher interface. We then study the utility of cipher switching through three case studies where latency, energy, and desired security properties change over time.

In one study, where we require the filesystem to react to a shrinking energy budget by switching ciphers, we find that SwitchCrypt achieves up to a 3.3x total energy use reduction compared to prior static approaches that only use the Freestyle stream cipher without

switching. In another case, where we allow the user to manually switch between ChaCha20 and Freestyle stream ciphers dynamically, we achieve a 3.1x to 4.8x reduction to read latency and 1.6x to 2.8x reduction to write latency compared to prior static approaches.

We make the SwitchCrypt source publicly available open source¹.

4.1.1 Example: Filesystem Reacts to “Battery Saver”

Suppose we have an ARM-based ultra-low-voltage netbook provided to us by our employer. As this is an enterprise device, our employer requires that 1) our drive is fully encrypted at all times and 2) our encrypted data is constantly backed up to an offsite system. The industry standard in full drive encryption is AES-XTS, so we initialize our drive with it. Given these requirements, three primary concerns present themselves.

First, it is well known that FDE using AES-XTS adds significant latency and power overhead to I/O operations, especially on mobile and battery-constrained devices [23, 49, 92]. To keep our drive encrypted at all times with AES-XTS means we must accept this hit to performance and battery life. Worse, if our device does not support hardware accelerated AES, performance can be degraded even further; I/O latency can be as high as 3–5x [26]. Hardware accelerated AES is hardly ubiquitous, and the existence of myriad devices that do not support it cannot simply be ignored, hence Google’s investment in Adiantum—an FDE solution for “the next billion users” of low-cost devices without support for hardware accelerated AES [22].

Second, AES-XTS is designed to mitigate threats to drive data “at rest,” which assumes an attacker cannot access snapshots of our encrypted data nor manipulate our data without those manipulations being immediately obvious to us. With access to multiple snapshots of a drive’s AES-XTS-encrypted contents, an attacker can passively glean information about the plaintext over time by contrasting those snapshots, leading to confidentiality violations in

1. <https://github.com/Xunnamius/strongbox-switchcrypt>

some situations [86, 98]. Similarly, an attacker that can manipulate encrypted bits without drawing our attention will corrupt any eventual plaintext, violating data integrity and, in the worst case, influencing the behavior of software. Unfortunately, in real life, data rarely remains “at rest” in these ways. In our example, our employer requires we back up the contents of our drive to some offsite backup service; this service will receive periodic snapshots of the encrypted state of our drive, violating our “at rest” invariant. These backups occur at a layer above the drive controller, meaning any encryption happening at the FTL or below is irrelevant.

Third, our system is battery constrained, placing a cap on our energy budget that can change at any moment as we transition from line power to battery power and back. Our system should respond to these changing requirements without violating any other concerns.

To alleviate the performance concern, we can choose a stream cipher like ChaCha20 rather than the AES-XTS block cipher. Using StrongBox, an encryption driver built for ChaCha20-based FDE, we can achieve on average a 1.7x speedup and a commensurate reduction in energy use [26].

When it comes to the security concern, StrongBox solves both the snapshot and integrity problems by 1) never writing data encrypted with the same key to the same location and 2) tracking drive state using a Merkle tree and monotonic counter supported by trusted hardware to prevent rollbacks. This ensures data manipulations cannot occur and guarantees confidentiality even when snapshots are compared regardless of the stream cipher used. Unfortunately, restoring from a backup necessitates a forced rollback of drive state, potentially opening us back up to confidentiality-violating snapshot comparison attacks [26].

To truly address the security concern requires a cipher with an additional security property: *ciphertext randomization*. Without ciphertext randomization, an attacker can map plaintexts to their ciphertext counterparts during snapshot comparison, especially if they can predict what might be written to certain drive regions. However, with ciphertext ran-

domization, a cipher will output a different “random” ciphertext even when given the same key, nonce, and plaintext; this means, even after a forced rollback of system state and/or legitimate restoration from a backup, comparing future writes is no longer violates confidentiality because each snapshot will always consist of different ciphertext regardless of the plaintext being encrypted or the state of the drive. Using Freestyle [7], a ChaCha20-based stream cipher that supports ciphertext randomization, we can guarantee data confidentiality in this way. So, we switch from StrongBox to an encryption driver that supports Freestyle.

Unfortunately, like AES-XTS, Freestyle has significant overhead compared to the original ChaCha20. In exchange for stronger security properties, Freestyle is up to 1.6x slower than ChaCha20, uses more energy, has a higher initialization cost, and expands the ciphertext which reduces total writeable drive space [7].

Further complicating matters is our final concern: a constrained energy budget. Our example system is battery constrained. Even if we accepted trading off performance, drive space, and energy for security in some situations, in other situations we might prioritize reducing total energy use. For example, when we trigger “battery saver” mode, we expect our device to conserve as much energy as possible. It would be ideal if our device could pause backups and the encryption driver could switch from the ciphertext-randomizing Freestyle configuration back to our high performance energy-efficient ChaCha20 configuration when conserving energy is a top priority, and then switch back to the Freestyle configuration when we connect to a charger and backups are eventually resumed.

In this dissertation we present SwitchCrypt, a device mapper that can trade off between these two configurations and others without compromising security or performance or requiring the device be restarted. With prior work, the user must select a static operating point in the energy-security-latency space at initialization time and hope it is optimal across all workloads and cases. If they choose the Freestyle configuration, their device will be slower and battery hungry even when they are not backing up. If they choose the more performant

ChaCha20 configuration, they risk confidentiality-violating snapshot comparison attacks. SwitchCrypt solves this problem by encrypting data with the high performance ChaCha20 when the battery is low and switching to Freestyle when plugged in and syncing with the backup service resumes.

4.1.2 Key Challenges

To trade off between different cipher configurations, we must address three key challenges. First, we must determine what cipher configurations are most desirable in which contexts and why. This requires we *quantify* the desirable properties of these configurations. Second, we must have some way to encrypt independent storage units with any one of these configurations. This requires we *decouple* cipher implementations from the encryption process used in prior work. Third, we need to determine when to re-encrypt those units, which configuration to use, and where to store the output, all with minimal overhead. This requires we implement efficient cipher *switching strategies*.

Quantifying the properties traded off between configurations. To obtain a space of configurations that we might reason about, it is necessary to compare certain properties of stream ciphers useful in the FDE context. However, different ciphers have a wide range of security properties, performance profiles, and output characteristics, including those that randomize their outputs and those with non-length-preserving outputs—*i.e.*, the cipher outputs more data than it takes in. To address this, we propose a framework for quantitative cipher comparison in the FDE context; we use this framework to define our configurations.

Decoupling ciphers from the encryption process. To flexibly switch between configurations in SwitchCrypt requires a generic cipher interface. This is challenging given the variety of inputs required by various stream ciphers, the existence of non-length-preserving ciphers, and other differences. We achieve the required generality by defining independent storage units called *nuggets*; we borrow this terminology from prior work (see [26]) to easily

differentiate our logical blocks (nuggets) from physical drive and other storage blocks. And since they are independent, we can use our interface to select any configuration to encrypt or decrypt any nugget at any point.

Implementing efficient switching strategies. Finally, to determine when to switch a nugget’s cipher and to where we commit the output, we implement a series of high-level policies we call *cipher switching strategies*. These strategies leverage our generic cipher interface and flexible drive layout to selectively “re-cipher” groups of nuggets, whereby the key and the cipher used to encrypt/decrypt a nugget are switched at runtime. These strategies allow SwitchCrypt to move from one configuration point to another or even settle on optimal configurations wholly unachievable with prior work. The challenge here is to accomplish this while minimizing overhead.

4.2 System Design

4.2.1 SwitchCrypt Overview

SwitchCrypt consists of a *Generic Stream Cipher Interface* and *Cryptographic Driver* and sits between a Log-structured File System (LFS) on the OS, and the underlying drive (backing storage) and device controller (e.g. Flash Translation Layer). This is illustrated in Fig. 4.1, which provides an overview of the SwitchCrypt system design.

The drive itself is divided into a *HEAD* section and *BODY* section upon initialization, illustrated in Fig. 4.2. The HEAD consists of metadata headers written during initialization [26] along with the *Keycount Store*, *Transaction Journal*, *Rekeying Journal*, and *Per-Nugget Metadata*, each drive-backed. These components are used by the *Cryptographic Driver* together with the *Cipher Switching Strategy* implementations to enable efficient per-unit cipher switching.

The BODY consists of a series independent same-size logical units called *nuggets*. A

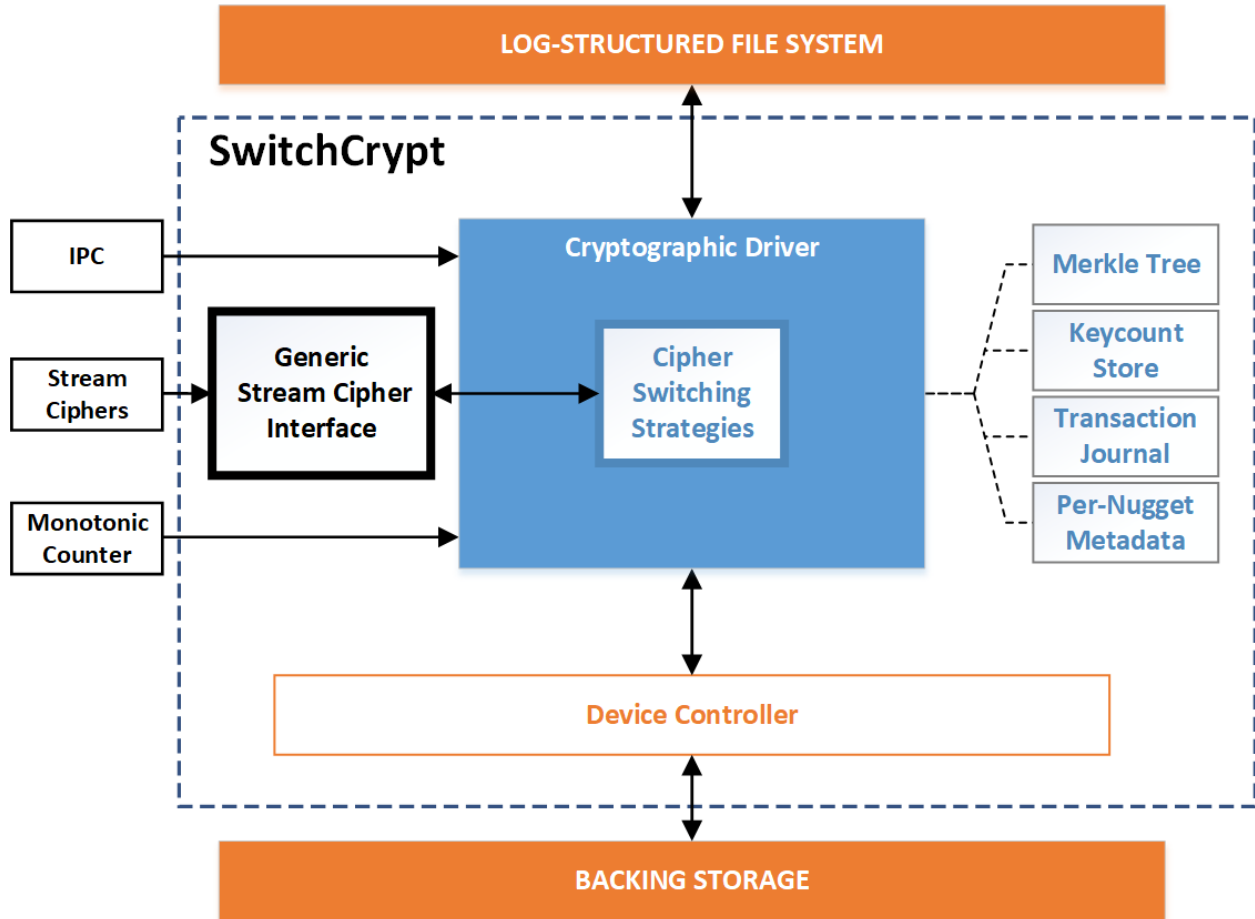


Figure 4.1: Overview of the SwitchCrypt construction.

nugget consists of one or more contiguous physical drive blocks. Each nugget is coupled with metadata in the HEAD indicating which cipher was used to encrypt the nugget along with any additional ciphertext output; the latter allows us to treat any non-length-preserving ciphers as if they were length-preserving. SwitchCrypt uses the Keycount Store and Transaction Journal components along with our nugget layout to 1) track, detect, and handle overwrites, 2) limit the maximum length of any plaintext input to ciphers, thus amortizing the overhead incurred during encryption, and 3) independently and efficiently switch the cipher used to encrypt individual nuggets.

StrongBox demonstrated how to make nugget-based drive organization secure using a single stream cipher, ChaCha20, to handle overwrites, prevent rollback attacks, and limit

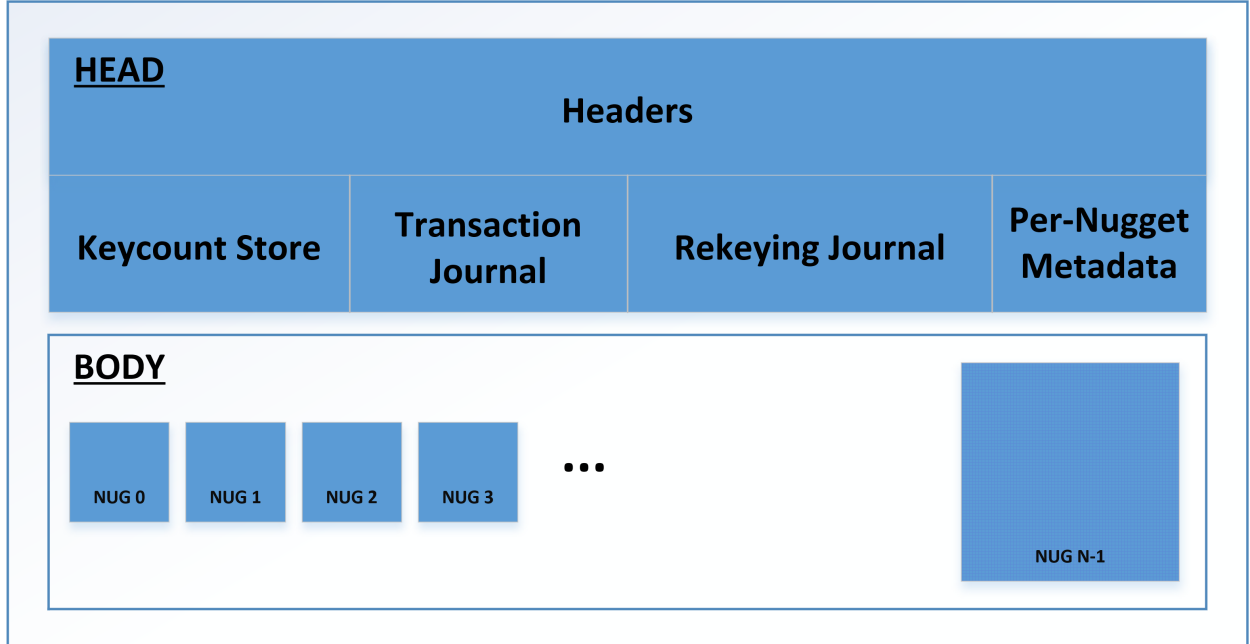


Figure 4.2: Layout of SwitchCrypt’s drive layout.

plaintext length [26]. However, StrongBox’s was not designed envisioning the utility in trading off between concerns at the filesystem or device-mapper level, dynamic cipher switching, or protecting against attacks on data “in motion;” the remainder of this section details the novel components that enable this functionality. Specifically: how we quantify the properties traded off between configurations (§4.2.2), the Generic Stream Cipher Interface and Per-Nugget Metadata components (§4.2.3) which decouple cipher implementations from the encryption process, and our Cipher Switching Strategy implementations (§4.2.4) used to efficiently encrypt nuggets with different ciphers.

4.2.2 *Quantifying Cipher Security Properties*

To reason about when to trade off between the ciphers evaluated in this work, we must have a way to compare ciphers’ utility in the context of SwitchCrypt FDE. However, different ciphers have a wide range of security properties, performance profiles, and output characteristics. To address this need, we propose a novel evaluation framework (see: Table 4.1). Our

framework classifies stream ciphers according to three quantitative features: relative round count, ciphertext randomization, and ciphertext expansion. Taken together, these features reveal a rich tradeoff space of cipher configurations optimizing for different combinations of concerns.

Cipher	Rounds	Randomization	Expansion
ChaCha8	0	0	1
ChaCha12	0.5	0	1
ChaCha20	1	0	1
Salsa8	0	0	1
Salsa12	0.5	0	1
Salsa20	1	0	1
HC128	0	0	1
HC256	1	0	1
Freestyle (F)	0	2	0
Freestyle (B)	0.5	2.5	0
Freestyle (S)	1	3	0

Table 4.1: Our framework for classifying stream ciphers according to three ideal features: relative round count, ciphertext randomization, and ciphertext expansion.

Relative Rounds (Rounds)

The ciphers we examine in this work are all constructed around the notion of *rounds*, where a higher number of rounds (and possibly longer key) is positively correlated with a higher resistance to brute force given no fatal related-key or other attacks [62]. Hence, this feature represents how many rounds a cipher executes relative to other implementations of the same algorithm. For instance: ChaCha8 is a reduced-round version of ChaCha12, which is a reduced-round version of ChaCha20, all using the ChaCha algorithm [11, 62].

We limit our analysis to groups of three implementations, each using a different number of rounds. In the case of HC-128 and HC-256, we limit our analysis to a group of two implementations. Scores range from 0 (least number of rounds considered) to 1 (greatest number of rounds considered).

Ciphertext Randomization (Randomization)

A cipher with ciphertext randomization generates different ciphertexts non-deterministically given the same key, nonce, and plaintext. This makes it much more difficult to execute chosen-ciphertext attacks (CCA), key re-installation attacks, XOR-based cryptanalysis and other comparison attacks, and other confidentiality-violating schemes where the ciphertext is in full control of the adversary [7]. This property is useful in cases where we cannot prevent the same key, nonce, and plaintext from being reused, such as with data “in motion” (see the motivational example in Section 4.1). Ciphers without this property—such as ChaCha20 on which prior work is based—are trivially broken when key-nonce-plaintext 3-tuples are reused. In StrongBox, this is referred to as an “overwrite condition” or simply “overwrite” [26].

Though there are many ways to achieve ciphertext randomization, the ciphers included in our analysis implement it using a random number of rounds for each block of the message where the exact number of rounds are unknown to the receiver a priori [7]. In determining the minimum and maximum number of rounds used per block in this non-deterministic mode of operation, we can customize the computational burden an attacker must bear by choosing lower or higher minimums and maximums. Hence, this is not a binary feature; scores range from 0 (no ciphertext randomization) to 1 (lowest minimum and maximum rounds per block) to 3 (highest minimum and maximum rounds per block).

Ciphertext Expansion (Expansion)

A cipher that exhibits ciphertext expansion is non-length-preserving: it outputs more or less ciphertext than was originally input as plaintext. This can cause major problems in the FDE context. For instance, cryptosystems that rely on AES-XTS (e.g. Linux’s dm-crypt, Microsoft’s BitLocker, Apple’s FileVault) or ChaCha (e.g. StrongBox, Google’s Adiantum) have storage layouts that hold length-preserving output as an invariant, making ciphers that do not exhibit this property incompatible with their implementations; yet, ciphertext

expansion is often (but not always) a necessary side-effect of ciphertext randomization.

The ciphers included in our analysis that exhibit ciphertext expansion have an overhead of around 1.56% per plaintext message block [7]. Even a single byte of additional ciphertext vs plaintext would make a cipher inappropriate for use with prior work. Hence, this is a binary feature in that a cipher either outputs ciphertext of the same length as its plaintext input or it does not. A cipher scores either a 0 if it *is not* length-preserving in this way or a 1 if the ciphertext is always the same length as the plaintext.

4.2.3 *Generic Stream Cipher Interface*

One of the goals of SwitchCrypt is that we might use any stream cipher regardless of its implementation details. Yet this is entirely non-trivial. There are many cipher implementations that we might use with SwitchCrypt, each with unique input requirements and output considerations. For instance, Salsa and Chacha implementations require a certain IV and key size and handle plaintext input through successive invocations of a single state update function [35]. Using OpenSSL’s AES implementation in CTR mode requires manually tracking the counter state and individual ciphertext blocks are retrieved through corresponding function invocations. Freestyle’s reference implementation requires we calculate the extra space necessary per nugget (due to ciphertext expansion) along with configuration-dependent minimum and maximum rounds-per-block, hash interval, and pepper bits [7]. HC-128 and other ciphers have similarly disparate requirements.

Unlike prior work, SwitchCrypt must be able to encrypt and decrypt arbitrary nuggets *with any of these ciphers* at any moment with low overhead and without tight coupling to any specific implementation detail. Hence, there is a need for an interface that completely decouples cipher implementations from the encryption/decryption process. Our novel cipher interface allows any stream cipher to be integrated into SwitchCrypt without modifications to third-party code, enabling normally incompatible ciphers to encrypt and decrypt arbitrary

nuggets. The ability for disparate cipher implementations to co-exist forms the foundation for SwitchCrypt’s ability to switch the system between different cipher configurations in our tradeoff space efficiently and effectively.

To facilitate this, the Generic Stream Cipher Interface presents the cryptographic driver with a single unified encryption/decryption model. SwitchCrypt receives I/O requests from the operating system at the block device level like any other device-mapper. These requests come in the form of either reads or writes. When a read request is received, the OS hands SwitchCrypt an offset and a length and expects a response with plaintext of that specific length starting at that specific offset taken from the beginning of storage (i.e. the BODY section; see Fig. 4.2). When a write request is received, the OS hands SwitchCrypt an offset, a length, and a buffer of plaintext and expects that plaintext to be encrypted and committed to storage such that the plaintext is later retrievable given that same offset and length in a future read request. These requests can either be handled together by a single function or handled individually as distinct read and write operations, each with different tradeoffs.

1. `xor_interface`

`xor_interface` executes independently of SwitchCrypt internals and treats encryption and decryption as the same operation. Implementations receive an integer offset F , an integer length L , a key buffer K corresponding to the current nugget, and an empty L -length XOR buffer. SwitchCrypt expects the XOR buffer to be populated with L bytes of keystream output from some stream cipher seeked to offset F with respect to key K . The length of the key buffer will always be exactly what the cipher implementation expects, alleviating the burden of key management; similarly, the XOR buffer will be XOR-ed with the appropriate portion of nugget contents automatically, alleviating the burden of drive access and other tedious calculations.

2. `read_interface` and `write_interface`

Unlike `xor_interface`, encryption and decryption are distinct concerns at this abstraction level.

`read_interface` handles decryption during reads.

`write_interface` handles encryption during writes. Implementations receive full access to SwitchCrypt internals, giving wrapper code complete control over the encryption and decryption process and allowing implementers to bypass parts of the nugget-based drive layout abstraction (i.e. BODY) if necessary. This comes at the cost of 1) significantly increased code complexity, as the implementer must perform certain I/O manually, distinguish between independent nuggets on the drive, determine what to encrypt or decrypt at what offset and when, when to commit which metadata and where and 2) potential performance implications, since SwitchCrypt must account for not having absolute control over its internal data structures during function invocation. For a cipher like Freestyle, configurations with lower minimum and maximum rounds per block may see a performance improvement here, while configurations with higher minimum and maximum rounds per block may see reduced performance.

4.2.4 Cipher Switching Strategies

The Generic Stream Cipher Interface allows many differently ciphered nuggets to co-exist on the same drive. However, at any moment, there is only a single *active cipher configuration* (henceforth *active configuration*). The active configuration is used to encrypt nugget contents. When a cipher switch is triggered, a different configuration becomes the active configuration. At this point, SwitchCrypt must determine *when* to re-cipher a nugget and *where* to store the output on the drive. “Re-ciphering” here means using an inactive configuration to decrypt a nugget’s contents and using the active configuration to re-cipher it. Depending on the use case, it may make the most sense to re-cipher a nugget immediately, or eventually, or to maintain several areas of differently-ciphered nuggets concurrently.

A naive approach would switch every nugget in BODY to the active configuration immediately, but the latency and energy cost would be unacceptable. Hence, a more strategic approach is necessary. We satisfy this need with our *cipher switching strategies*. These novel strategies allow for nuggets to be re-ciphered in a variety of cases with minimal impact on performance and battery life and without compromising security. This is thanks to the nugget-based drive layout, which limits the churn of cipher switching operations to relatively small regions of ciphertext on the drive.

Determining *when* to target a nugget for re-ciphering we call *temporal switching*, for which we propose the *Forward* switching strategy. Determining *where*—in which storage region and across which nuggets—to output ciphertext we call *spatial switching*, for which we propose the *Mirrored* and *Selective* switching strategies.

Forward Switching Strategy. When a nugget is encountered during I/O that was encrypted using something other than the active configuration, the Forward strategy dictates that this nugget be re-ciphered immediately. If a particular nugget encrypted with an inactive configuration is never encountered during I/O, it is never re-ciphered and remains on the drive in its original state. In this way, the Forward strategy represents a form of temporal cipher switching.

Rather than re-cipher the entire drive every time the active configuration changes, this strategy limits the performance impact of cipher switching to individual nuggets. The expense of re-ciphering is paid only once, after which the nugget is accessed normally during I/O until the active configuration is switched again.

There are several forms the Forward strategy might take. The default and most intuitive is *0-forward*, in which SwitchCrypt immediately transitions individual nuggets encountered during I/O to the active configuration if they are not using it. Over time, if various I/O operations end up touching every nugget in the drive, the encrypted contents of every nugget

will become decryptable with the currently active configuration.

The Forward strategy might also take the form of *N-forward*, where SwitchCrypt attempts to take advantage of spatial sequential locality to transition whole sets of nuggets into the active configuration. We can trivially expand the forward strategy to encompass the entire drive by selecting N equal to the total number of nuggets managed by SwitchCrypt. This would have the overhead of re-ciphering large swaths of the drive upon every I/O operation where a nugget encrypted with the inactive configuration is encountered. Of course, this has the same dire implications for performance as simply re-initializing the entire system or encrypted container with the new cipher.

Selective Switching Strategy. When SwitchCrypt is initialized with the Selective strategy, the drive is partitioned into C regions where C represents the total number of available ciphers in the system; each regions' nuggets are encrypted by each of the C ciphers respectively. For instance, were SwitchCrypt initialized using two ciphers ($C = 2$), the drive would be partitioned in half; all nuggets in the first region would be encrypted with the first cipher while all nuggets in the second would be encrypted with the other.

When using this strategy, the active cipher determines which partition we “select” for I/O operations. Hence, unlike the Forward strategy, which schedules individual nuggets to be re-ciphered at some point in time after the active configuration is switched, the Selective strategy allows the wider system to indicate *where* on the drive a read or write operation should occur. In this way, the Selective strategy represents a form of spatial cipher switching where different regions of the drive can store differently-ciphered nuggets independently and concurrently. A user could take advantage of this to, for instance, set up regions with different security properties and performance characteristics, managing them as distinct virtual drives or transparently reading/writing bytes to different security regions on the same drive.

Strategy	Convergence	Waste	Performance
Forward	Slower	None	Faster reads and writes unless switching
Mirrored	Nearly instant	High	Faster reads; slower writes
Selective	Slower	High	Faster reads and writes

Table 4.2: A summary comparison between the three cipher switching strategies.

Mirrored Switching Strategy. Similar to the Selective strategy, when SwitchCrypt is initialized with the Mirrored strategy, the drive is partitioned into C regions where C represents the total number of available ciphers in the system; each regions’ nuggets are encrypted by each of the C ciphers respectively.

However, unlike the Selective strategy, all write operations that hit one region are mirrored into the other regions immediately, so all regions of the drive will always be in a consistent state and always share the same data. The active configuration determines *where* a read operation should occur. In this way, the Mirrored strategy represents a form of spatial cipher switching because we are switching which configuration we are using to read in data. A user could take advantage of this along with SSD TRIM or deletion operations provided by the filesystem to delete other regions, thus quickly and securely converging the drive to a single configuration without losing any data or suffering the egregious performance or battery penalty that comes with re-ciphering every nugget.

Comparing Cipher Switching Strategies

Table 4.2 summarizes the higher level tradeoffs between the three cipher switching strategies.

Convergence. Depending on the use case, the ability to quickly converge the entire drive to a single cipher configuration without losing data is very useful (see: Section 4.5).

The Forward strategy is slow to converge compared to Mirrored since, in the worse case, every nugget on the drive will require re-ciphering. The Selective strategy is similarly slow to converge since entire regions of nuggets must be moved and re-ciphered to prevent data loss; those regions could be destroyed without moving data around using TRIM or similar SSD functionality too, which would be very fast, but unlike Mirrored some data would be lost forever.

Waste. Unlike the other two strategies, using the Forward strategy does not reduce the total usable space on the drive by the end-user, ciphertext expansion notwithstanding. We refer to this as “waste”. The Forward strategy is not wasteful in this way because it allows differently-ciphered nuggets to co-exist contiguously on the drive without special partitions. Since the Mirrored and Selective strategies require partitioning the drive into some number of regions—where the writeable size reported back to the OS is some function of region size—there is a necessary reduction in usable space.

Performance. The Selective and Mirrored strategies can read data from the drive with low overhead, reaching performance parity with prior work, because they never have to deal with on-demand re-ciphering. This is because switching ciphers using these two strategies amounts to offsetting the read index so that it lands in the proper BODY partition on the drive, which has little overhead. The Forward strategy also reads with low overhead except in the case where a nugget was not encrypted with the active configuration. This triggers re-ciphering on-demand, which can be costly if the workload constantly touches unique nuggets and is small enough that cost is not amortized.

The Selective strategy also writes with low overhead because, like with reads, an index offset is the only requirement. The Mirrored strategy, on the other hand, can be up to two times slower for writes (when $C = 2$) compared to baseline. Each additional region ($C > 2$) compounds the write penalty depending on the workload. This is because each write is mirrored across *all* regions. As with reads, the Forward strategy writes with low overhead

except in the case where a nugget was not encrypted with the active configuration. This triggers re-ciphering on-demand, which can be costly if the workload touches unique nuggets and is small enough that cost is not amortized.

With these tradeoffs in mind: Mirrored is ideal when the drive must converge quickly, write performance is not a primary concern, and drive space is abundant; Selective is ideal when different data should be encrypted differently and drive space is abundant; and Forward is ideal when some subset of nuggets should be encrypted differently without wasting drive space. See Section 4.5 for specific scenarios that demonstrate these differences in practice.

Threat Model for Cipher Switching Strategies

The primary concern facing any FDE solution is that of confidentiality. An adversary should not be able to reveal any information about encrypted plaintext without the proper key. As with prior work, encryption is achieved via a binary additive approach: cipher output (keystream) is combined with plaintext nugget contents using XOR, with metadata to track writes and ensure that pad reuse never occurs during overwrites and that the system can recover from crashes into a secure state. Another concern is data integrity: an adversary should not be able to tamper with ciphertext and it go unnoticed. Nugget integrity is tracked by an in-memory Merkle tree. See the threat model addressed by Dickens et al. [26] for further details.

Switching strategies add an additional security concern not addressed by prior work: even if we initiate a “cipher switch,” there may still be data on the drive that was encrypted with an inactive configuration. Is this a problem? For the Forward strategy, this implies data may at any time be encrypted using the “least desirable cipher”. For the Mirrored and Selective strategies, the drive is partitioned into regions where nuggets are guaranteed to be encrypted with each cipher, including the “least desirable cipher”. However, in terms of

confidentiality, the confidentiality guarantee of SwitchCrypt can be reduced to the individual confidentiality guarantees of the available ciphers used to encrypt nuggets.

4.2.5 Putting It All Together

We revisit the motivating example from Section 4.1, where we are using Freestyle to ensure secure backups. Initially, I/O requests come down from the LFS and are received by the cryptographic driver, which divides the request based on which nuggets it touches. For each nugget, the per-nugget metadata is consulted to determine with which cipher the nugget is encrypted. If it is encrypted with the active cipher configuration (Freestyle), which must be true if we have not initiated a cipher switch, the write is handled similarly to prior work: encrypted data is read in from the drive, the merkle tree and monotonic counter are consulted to ensure the integrity of encrypted data, the transaction journal is consulted during write operations so that overwrites are handled and pad reuse violations are avoided, and then the keycount store is consulted to derive the nugget’s unique encryption key from some master secret. Finally, using the Generic Stream Cipher Interface, we call out to the Freestyle, allowing SwitchCrypt to encrypts/decrypts the nugget’s contents and commit any updates back to storage. All the while, the drive’s Freestyle-encrypted contents are being uploaded up to our enterprise backup service every so often.

When the device enters “battery saver” mode, drive backups are paused, the energy monitoring software downclocks the CPU, and the OS signals to SwitchCrypt that a more energy-efficient cipher (ChaCha20) should be used until we return to a non-curtailed energy budget. SwitchCrypt sets ChaCha20 as the active cipher configuration. Now, when the cryptographic driver divides I/O requests into each affected nugget, the per-nugget metadata shows SwitchCrypt that each nugget is encrypted using a cipher that is not the active configuration. This triggers the re-ciphering code path. Since we are using the Forward switching strategy in this example, nugget data is immediately decrypted by calling out

to the inactive configuration through the Generic Stream Cipher Interface, after which the nugget is re-ciphered by calling out to the active configuration. Finally, the cryptographic driver manages encrypting/decrypting data and updating the merkle tree and monotonic counter, transaction journal, and keycount store as the I/O operation and related metadata is committed to the drive afterwards.

Now, thanks to SwitchCrypt, the system can adapt to changing requirements beyond the capability of prior work. See Section 4.5 for specifics.

4.3 Implementation

Our SwitchCrypt implementation consists of 9,491 lines of C code; our test suite consists of 6,077 lines of C code. All together, our solution is comprised of 15,568 lines of C code. Our implementation is also publicly available open-source¹.

SwitchCrypt uses OpenSSL version 1.1.0h and LibSodium version 1.0.12 for its AES-XTS and AES-CTR implementations. Open source ARM NEON optimized implementations of ChaCha are provided by Floodyberry [35]. The Freestyle cipher reference implementation is from the original Freestyle paper [7]. The eSTREAM Profile 1 cipher implementations are from the open source libstream cryptographic library [61] by Lucas Clemente Vella. The Merkle Tree implementation is from the Secure Block Device [47].

We implement SwitchCrypt on top of the BUSE [2] virtual block device, using it as our mock device controller. BUSE is a thin (200 LoC) wrapper around the standard Linux Network Block Device (NBD). BUSE allows an operating system to transact block I/O requests to and from virtual block devices exposed via domain socket.

For experimental purposes, our implementation makes the choice of ciphers binary: either the system wants SwitchCrypt to access the backing store using the active cipher or the inactive cipher. However, there is no technical limitation preventing various different nuggets encrypted with three, four, or more unique ciphers.

We use POSIX message queues to indicate intent to switch. A production-ready implementation would be greatly simplified by adding an “intent” parameter to the POSIX *read()* and *write()* system calls, allowing SwitchCrypt to more exactly map individual I/O operations to specific areas of the backing store when spatially switching. We simulate this with IPC. This is especially important when considering the selective switching strategy; a production-ready implementation supporting selective switching would need to differentiate between metadata operations belonging to the filesystem (should be mirrored across all regions) and actual end-user data (should be selectively read from and written to nuggets in specific regions).

Further, to operate securely, SwitchCrypt must be seeded with random data initially rather than have the backing store consist of all zeroes. This is a one-time cost paid during initialization and has no tangible effect on performance. SSDs that support TRIM or similar quick secure deletion operations can accomplish this with minimal wear.

Finally, as the Freestyle cipher is highly configurable, we implement it in three different configurations: a “fast” mode with parameters

`FreestyleFast`($R_{min}=8$, $R_{max}=20$, $H_I=4$, $I_C=8$), a “balanced” mode with parameters `FreestyleBalanced`($R_{min}=12$, $R_{max}=28$, $H_I=2$, $I_C=10$), and a “strong” mode with parameters `FreestyleStrong`($R_{min}=20$, $R_{max}=36$, $H_I=1$, $I_C=12$).

Thanks to Freestyle’s output randomization (see Section 4.2), we can skip the overhead of tracking, detecting, and handling overwrites when nuggets are using it, offsetting the 1.6x to 3.2x performance loss of using Freestyle versus ChaCha20 [7].

4.3.1 Implementing Cipher Switching

A naive implementation is trivial (*e.g.*, execute the chosen strategy on every I/O operation), this navigation must occur with acceptable overhead by preserving performance wherever possible. Our cryptographic driver provides such a mechanism, tying together cipher switch-

ing strategies.

In the cases of Mirrored and Selective switching, we use offset to determine in which area of the backing store receives I/O.

In the case of Forward switching, it is tempting to implement it such that a nugget is completely re-ciphered during I/O every time its metadata indicates that it was previously encrypted using a non-active cipher. However, such a naive implementation can have disastrous effects on performance.

First, a nugget is considered *pristine* if it has not had any data written into it yet. SwitchCrypt determines if a nugget is pristine by checking the state of the transaction journal for that nugget. All nuggets start out pristine with metadata indicating that they are to be encrypted and decrypted by the initially active cipher. This is true *even if the nugget has not been written to yet*. This means, on read and write operations after a different cipher becomes the active cipher configuration using a naively implemented forward switching strategy, every write operation will trigger a re-keying, which carries significant overhead.

Our solution was to divide forward switching into *soft re-ciphering* and *hard re-ciphering*. During soft re-ciphering, only the nugget’s metadata is changed to indicate that the nugget can be encrypted and decrypted with the newly active cipher configuration but *without actually re-ciphering the nugget data itself*. This keeps the nugget in its pristine condition, preserving SwitchCrypt’s ability to write data into it without triggering a costly re-keying operation every time. On the other hand, during hard re-cipher, the nugget’s metadata is changed to match the active cipher configuration *and* the nugget data is encrypted using the new cipher.

When using forward switching other than 0-forward, *i.e.*, N-forward where $N > 0$, only read operations are allowed to trigger hard re-ciphering for nuggets other than the currently active nugget. This is still not enough to preserve our performance advantage, however, as I/O operations can span multiple nuggets, and attempting to take advantage of spatial

locality after interacting with every nugget is counterproductive. Hence, only the last nugget touched by a read operation will trigger the more aggressive N-forward behavior if $N > 0$. These considerations have the effect of 1) preserving our performance advantage and 2) allowing more aggressive N-forward behavior (where $N > 0$) to take advantage of spatial locality during read-heavy workloads to result in a further performance advantage (see: Section 4.4).

4.4 Evaluation

We implement SwitchCrypt and our experiments on a Hardkernel Odroid XU3 ARM big.LITTLE system with Samsung Exynos 5422 A15/A7 heterogeneous multi-processing quad core CPUs at maximum clock speed, 2 gigabyte LPDDR3 RAM at 933 MHz, and an eMMC5.0 HS400 backing store running Ubuntu Trusty 14.04.6 LTS, kernel version 3.10.106. Energy monitoring was provided by the Odroid’s integrated INA-231 power sensors polled every ≈ 260 milliseconds (not including noise/overhead).

We evaluate SwitchCrypt using a Linux RAM disk (tmpfs). The maximum theoretical memory bandwidth for this Odroid model is 14.9GB/s. Our observed maximum memory bandwidth is 4.5GB/s. Using a RAM disk focuses the evaluation on the performance differences due to different ciphers.

In each experiment below, we evaluate SwitchCrypt on two high level workloads: sequential and random I/O. In both workloads, a number of bytes are written and then read (either 4KB, 512KB, 5MB, 40MB) 10 times. Each workload is repeated three times for a total of 240 tests per cipher (720 runs per cipher pair/ratios, explained below); 30 results per byte size, 120 results per workload. Results are accumulated and the median is taken for each byte size.

When evaluating switching strategies, a finer breakdown in workloads is made using a pre-selected pair of ciphers we call the *primary cipher configuration* and *secondary cipher*

configuration. SwitchCrypt is initialized at the primary configuration. Once we trigger a cipher switch, SwitchCrypt moves towards the secondary configuration via switching strategy.

The cipher switch is triggered according to a certain *ratio* of I/O operations. For example: given 10 40MB read-write operations, we may write and then read back 40MB 3 times using the primary cipher, initiate a cipher switch, and then write and then read back (write-read) 40MB 7 times. This would be a 3:7 ratio. It follows that there are three ratios we use to evaluate SwitchCrypt’s performance in this regard: 7:3, 5:5, and 3:7. Respectively, that is 7 file write-read operation in the primary cipher for every 3 file write-read operations in the secondary cipher (7:3), 7 file write-read operation in the primary cipher for every other file write-read operation in the secondary cipher (5:5), and 3 file write-read operations in the primary cipher for every 7 file write-read operation in the secondary cipher (3:7).

To reason about the desirability of cipher configurations, we define the *security vector*, $R+R$, as a vector consisting of a configuration’s relative rounds (Rounds) quantification and its ciphertext randomization (Randomization) quantification defined in Section 4.2. We define the norm over this vector as the sum of its components. Hence, we consider a cipher configuration “stronger” if it has higher ciphertext randomization and uses more rounds, i.e. has a higher normed $R+R$.

All experiments are performed with basic Linux I/O commands, bypassing system caching.

In this section we answer the following questions:

1. What shape does the cipher configuration tradeoff space take under our workloads?
(§4.4.1)
2. Can SwitchCrypt achieve dynamic security/energy tradeoffs by reaching configuration points not accessible with prior work? (§4.4.2)
3. What is the performance and storage overhead of each cipher switching strategy?
(§4.4.3)

4.4.1 Switching Strategies Under Various Workloads

Baseline Cipher I/O Performance

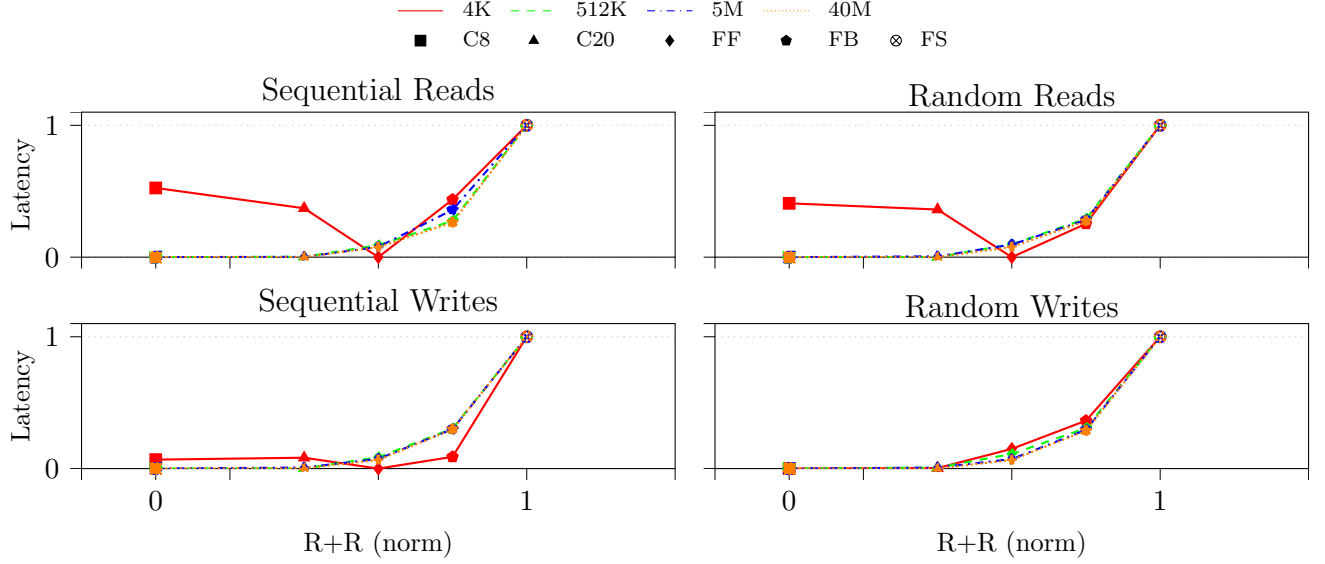


Figure 4.3: Median sequential and random write and then read performance baseline.

Fig. 4.3 shows the normalized relative round count and ciphertext randomization (normed R+R vector) versus median normalized latency tradeoff between different stream cipher configurations for our sequential and random I/O workloads. Trends for median hold when looking at tail latencies as well. Each line represents one workload: 4KB, 512KB, 5MB, and 40MB respectively (see legend). Each symbol represents one of our ciphers: ChaCha8, ChaCha20, Freestyle Fast, Freestyle Balanced, and Freestyle Strong. Of the ciphers we tested, those with higher round counts and higher ciphertext randomization scores resulted in higher overall latency and increased energy use for I/O operations. The relationship between these concerns is not always linear, however, which exposes a rich tradeoff space.

Besides the 4KB workload, the shape of each workload follows a similar trend, hence we will focus on 40MB and 4KB workloads going forward. Due to the overhead of metadata management and the fast completion time of the 4KB workloads (*i.e.*, little time for amortization of overhead), ChaCha8 and ChaCha20 take longer to complete than Freestyle Fast.

This advantage is not enough to make Freestyle Balanced or Secure workloads complete faster than the ChaCha variants, however.

Though ChaCha8 is faster than ChaCha20, there is some variability in our timing setup when capturing extremely fast events occurring close together in time. This is why ChaCha8 sometimes appears with higher latency than ChaCha20 for normalized 4KB workloads. ChaCha8 is not slower than ChaCha20.

4.4.2 Reaching Between Static Configuration Points

Forward Switching I/O Ratio Performance

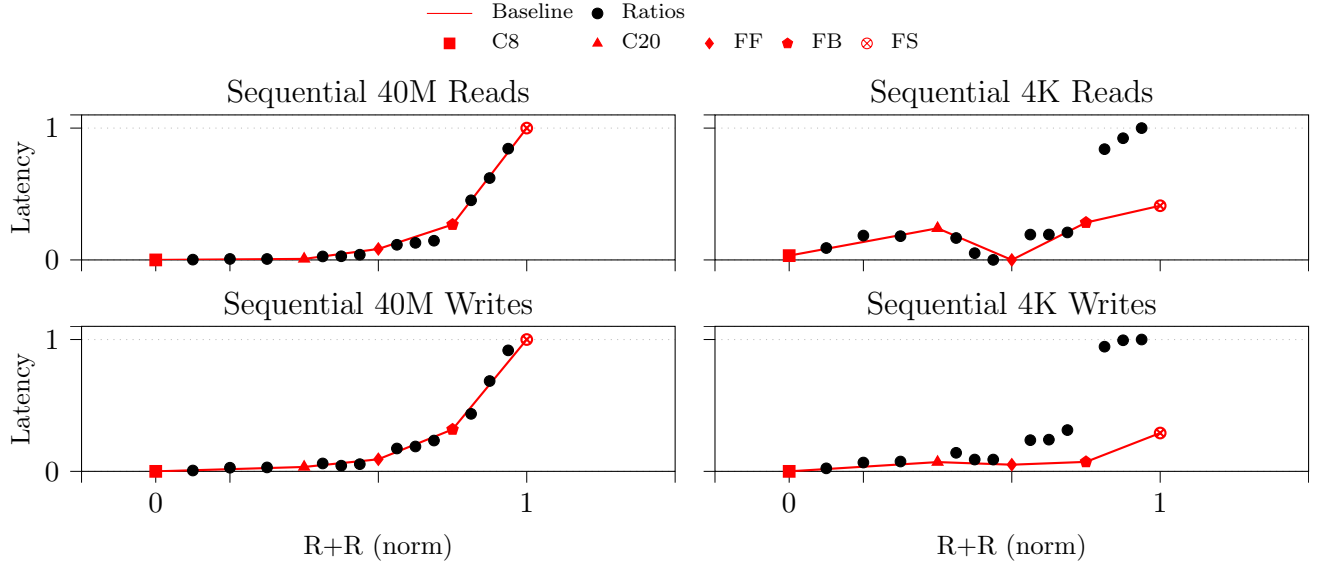


Figure 4.4: Median sequential and random write and then read back performance comparison of Forward switching to baseline. Each cluster of 3 dots between configurations represents the 7:3, 5:5, and 3:7 primary-vs-secondary I/O ratios described in the text.

Fig. 4.4 shows the normalized relative round count and ciphertext randomization (normed $R+R$ vector) versus median normalized latency tradeoff between different stream ciphers for our sequential and random I/O workloads with cipher switching using the Forward strategy. After a certain number of write-read I/O operations, a cipher switch is initiated and SwitchCrypt begins using the secondary cipher to encrypt and decrypt data. For each pair

of ciphers, this is repeated three times: once at every ratio point *between* our static configuration points (*i.e.*, 7:3, 5:5, and 3:7 described above).

The point of this experiment is to determine if SwitchCrypt can effectively transition the drive between ciphers without devastating performance. For the 40MB, 5MB, and 512KB workloads (40MB is shown), we see that SwitchCrypt can achieve dynamic security/energy tradeoffs reaching points not accessible with prior work, all with minimal overhead.

Again, due to the overhead of metadata management for non-Freestyle ciphers (see Section 4.3) and the fast completion time of the 4KB workloads preventing SwitchCrypt from taking advantage of amortization, ChaCha8 and ChaCha20 take longer to complete than Freestyle Fast for 4KB reads. We also see very high latency for ratios between Freestyle Fast and Freestyle Strong cipher configurations. This is because Freestyle is not length-preserving, so extra write operations must be performed, and the algorithm itself is generally much slower than the ChaCha variants (see Fig. 4.3). Doubly invoking Freestyle in a ratio configuration means these penalties are paid more often.

Fig. 4.5 show the performance of the Mirrored and Selective strategies with the same configuration of ratios as Fig. 4.4.

For the 40MB, 5MB, and 512KB workloads (40MB is shown), we see that Mirrored and Selective *read* workloads and the Selective *write* workload achieve parity with the Forward strategy experiments. This makes sense, as most of the overhead for Selective and Mirrored reads is determining which part of the drive to commit data to. The same applies to Selective writes. For the 4KB Mirrored and Selective *read* workloads and the Selective *write* workload, we see behavior similar to that in Fig. 4.4, as expected.

Mirrored writes across all workloads are very slow. This is to be expected, since the data is being mirrored across all areas of the drive. In our experiments, the drive can be considered partitioned in half. This overhead is most egregious for the 4KB Mirrored write workload. This makes Selective preferable to Mirrored. However, it is a tradeoff; Selective

Mirrored/Selective Switching I/O Ratio Performance

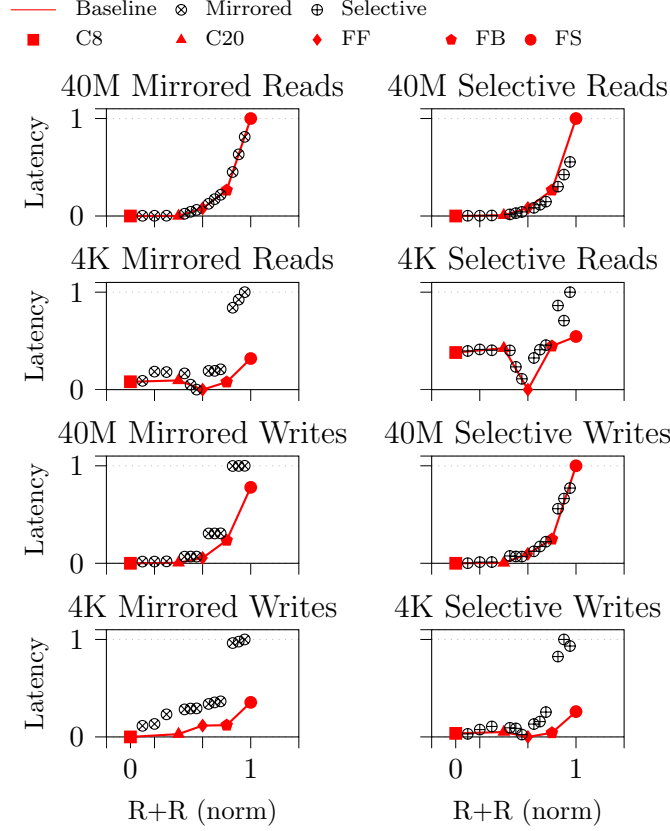


Figure 4.5: Median sequential and random write and then read back performance comparison of Mirrored and Selective switching strategies to baseline.

cannot quickly converge the drive to a single cipher configuration or survive the loss of an entire region.

4.4.3 Cipher Switching Overhead

We calculate that Forward switching has average overhead at 0.08x/0.10x for 40MB, 5MB and 512KB read/write workloads compared to baseline I/O, demonstrating SwitchCrypt’s amortization of cipher switching costs. Average overhead is 0.38x/0.44x for 4KB read/write workloads when SwitchCrypt is unable to amortize cost. There is no spatial overhead with the Forward switching strategy.

Similarly, we calculate that Selective switching has average overhead at 0x/0.3x for

40MB, 5MB and 512KB read/write workloads compared to baseline I/O. Average overhead is 0.22x/0.71x for 4KB read/write workloads. Spatial overhead in our experiment was half of all writable space on the drive.

Finally, we calculate that Mirrored switching has average overhead at 0.25x/0.61x for 40MB, 5MB and 512KB read/write workloads compared to baseline I/O, with high write latency due to mirroring. Average overhead is 0.55x/0.77x for 4KB read/write workloads. Spatial overhead in our experiment was half of all writable space on the drive.

These overhead numbers are the penalty paid for the additional flexibility of being able to reach configurations points that are unachievable without SwitchCrypt. SwitchCrypt’s design keeps these overheads acceptably low in practice, achieving the desired goal of flexibly navigating latency/security tradeoffs for FDE.

4.4.4 Revisiting Our Threat Model

The incorporation of cipher switching requires considering each attack in the context of each strategy and novel attacks on mixed-cipher nugget states. Table 4.3 lists possible attacks and their results. SwitchCrypt addresses its threat model and maintains confidentiality and integrity guarantees.

4.5 Case Studies

In this section, we provide three case studies demonstrating the practical utility of cipher switching. We cover a wide range of situations, highlighting concerns like meeting latency goals (§4.5.3), trading off security and writable space (§4.5.2), and keeping within an energy budget (§4.5.1). We also demonstrate the utility of both temporal and spatial switching strategies, exploring the range of conditions under which certain strategies are optimal.

Table 4.3: Attacks on SwitchCrypt and their results

Attack	Result	Explanation
Nugget data in drive is mutated out-of-band online	SwitchCrypt immediately fails with exception on successive IO request	Regardless of switching strategy, Merkle Tree check fails on read-in
Header/cipher metadata in drive is mutated out-of-band online	SwitchCrypt immediately fails with exception on successive IO request	Regardless of switching strategy, Merkle Tree check fails on read-in
drive is rolled back to a previously consistent state while online	SwitchCrypt immediately fails with exception on successive IO request	Regardless of switching strategy, secure monotonic counter is out of sync with the system
drive is rolled back to a previously consistent state while offline, secure counter wildly out of sync	SwitchCrypt refuses to mount; allows for force mount with root access	Regardless of switching strategy, secure monotonic counter is out of sync with the system
Merkle Tree made inconsistent by mutating drive out-of-band while offline, secure counter in sync	SwitchCrypt refuses to mount	Secure monotonic counter is in sync with the system, yet illegal data manipulation occurred
Nugget accessed out-of-band in mixed-cipher drive	Nugget’s cipher may not match active configuration	Worst case, the nugget data is available encrypted with the lowest R+R cipher in the system

4.5.1 *Balancing Security Goals with a Hard Energy Cap*

Here we revisit the motivating example from Section 4.1. It illustrates that, because latency and energy use are correlated among the ciphers we examined, we can exploit that to save battery life when necessary while maintaining confidentiality when uploading encrypted backups to our enterprise solution.

To simulate I/O activity, we begin randomly writing 10 40MB files using the Freestyle Balanced cipher configuration over the course of approximately 120-125 seconds. After 5 seconds, the device enters “battery saver” mode, also pausing backup uploads. We simulate this event by 1) underclocking the cores to their lowest frequencies and 2) using `taskset` to transition the SwitchCrypt processes to the energy-efficient LITTLE cores. After this event, we complete the remaining workload using the ChaCha8 cipher. We repeat this experiment three times.

In Fig. 4.6, we see time versus energy used. At 0 seconds, we begin writing. At 5 seconds, the “battery saver” event occurs, causing the system to be underclocked. At 120 seconds,

Battery Saver Use Case: Energy-Security Tradeoff vs Strict Energy Budget

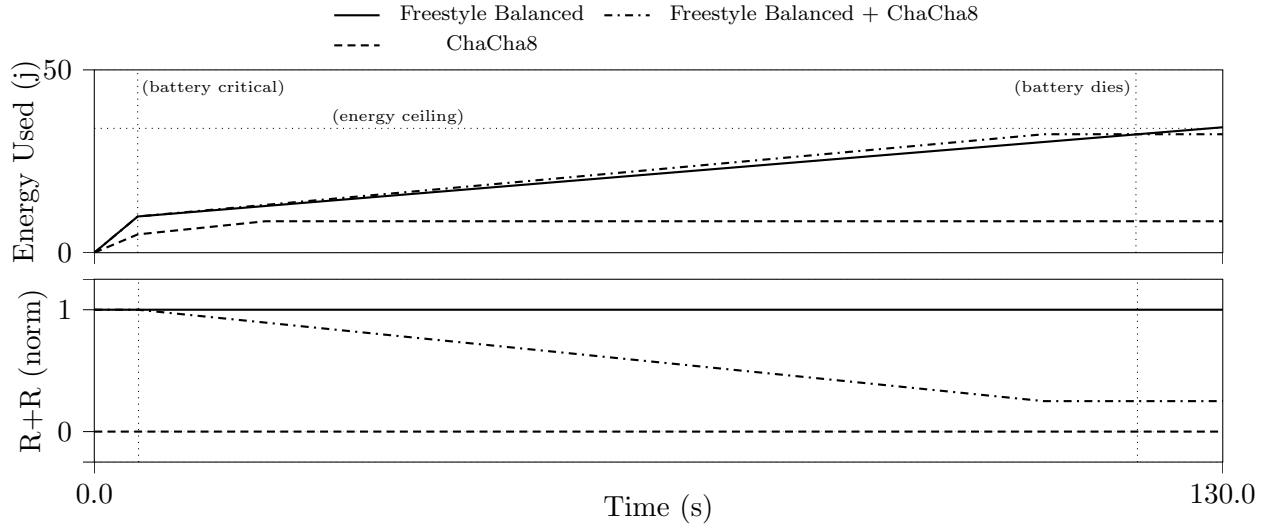


Figure 4.6: Median sequential write total energy use with respect to time with respect to time.

the system will die. If we blow past our energy ceiling, the system will die.

Our goal is to complete I/O before the device dies. We have three cipher configuration choices. 1) Favor security even when backups are paused and use Freestyle Balanced exclusively. Our results show that the device will die before I/O completes. 2) Favor low energy use even when backups are being uploaded and use ChaCha8 exclusively. Our results show that the device will finish writing early, but we cannot safely upload backups when nuggets are encrypted using ChaCha8. Finally, we have 3) favor security and use Freestyle Balanced when uploading backups, and switch to ChaCha8 when the system enters the low power state. Our results show that, while the system uses slightly more power in the short term, we stay within our energy budget and finish before the devices dies. Further, when we get our device to a charger, SwitchCrypt can converge nuggets back to Freestyle Balanced and resume uploading backups.

On average, using Forward cipher switching resulted in a 3.3x total energy use reduction compared to exclusively using Freestyle Balanced, allowing us to remain within our energy budget. We note, however, that the energy savings is not the point of this experiment.

Rather, the lesson learned is that SwitchCrypt enables the system to move to the right point in the energy/security tradeoff space so that the current task can still be accomplished before the battery is drained and without compromising backup security at any point.

4.5.2 *Variable Security Regions*

This usecase illustrates utility of spatial Selective switching to achieve a performance win over prior work where the entire drive is encrypted with a single cipher. We demonstrate *Variable Security Regions* (VSR), where we can choose to encrypt select files or portions of files with different keys and ciphers below the filesystem level.

Storing classified materials, corporate secrets, etc. require the highest level of discretion, yet sensitive information like this can appear within a (much) larger amount of data that we value less. But if only a small percentage of the data needs the strongest encryption, then only a small percentage of the data should have that associated overhead. In this scenario, a user wants to indicate one or more regions of a file are more sensitive than the others. For example, perhaps banking transaction information is littered throughout a PDF; perhaps passwords and other sensitive information exists within several much larger files. Using prior techniques, either all the data would be stored with high overhead, the critical data would be stored without the mandated cipher type, or the data would have to be split among separate files requiring potentially complex and error-prone management schemes. SwitchCrypt VSRs allows us to sidestep these issues.

We begin by with 10 5MB and 4KB write-read operations to two SwitchCrypt instances: one using ChaCha8 (C8) and the other using Freestyle Strong (FS). These results represent I/O without cipher switching where 100% of the data is stored with either high overhead (FS) or using an inappropriate cipher (C8). We then use a third SwitchCrypt instance initialized with Selective switching and write-read with a 7:3 ratio of ChaCha8 versus Freestyle Balanced I/O operations. Here, 30% of the data is considered sensitive. We repeat this experiment

three times.

VSR Use Case: ChaCha8 vs Freestyle Strong Sequential 4KB, 5MB Performance

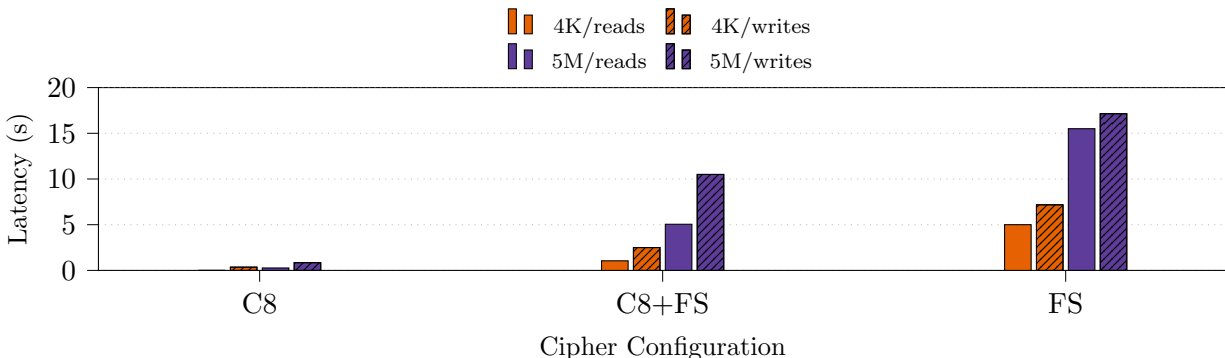


Figure 4.7: Median sequential read and write performance comparison of 4KB, 5MB I/O with 7-to-3 ratio, ChaCha8 vs Freestyle Strong (respectively).

In Fig. 4.7, we see the sequential read and write performance of 4KB and 5MB workloads when nuggets are encrypted exclusively with ChaCha8 or Freestyle Balanced. Between them, we see Selective switching 7:3 ratio I/O results.

Our goal is to use VSRs to keep our sensitive data at the mandated security level while keeping the performance and battery life benefits of using a fast cipher for the majority of I/O operations. Using SwitchCrypt Selective switching versus prior work results in a reduction of 3.1x to 4.8x for read latency and 1.6x to 2.8x for write latency, all without compromising the security needs of the most sensitive data.

4.5.3 Responding to End-of-Life Slowdown in SSDs

This usecase illustrates using temporal Forward switching to offset the debilitating decline in performance when SSDs reach end-of-life (EoL) [45]. We demonstrate the utility of such a system to dynamically stay within a strict latency budget while meeting minimum security requirements, which is not possible using prior work.

Due to garbage collection and wear-leveling requirements of SSDs, as free space becomes constrained, I/O performance drops precipitously [45]. With prior work, our strict latency

ceiling is violated. However, if SwitchCrypt is made aware when the drive is in such a state, we can offset some of the performance loss by switching the ciphers of high traffic nuggets to the fastest acceptable cipher available using Forward switching.

We begin by writing 10 40MB files to SwitchCrypt per each cipher as a baseline. We then introduce a delay into SwitchCrypt I/O of $20ms$, simulating drive slowdown, and repeat the experiment three times.

SSD EoL Use Case: Latency-Security Tradeoff vs Goals

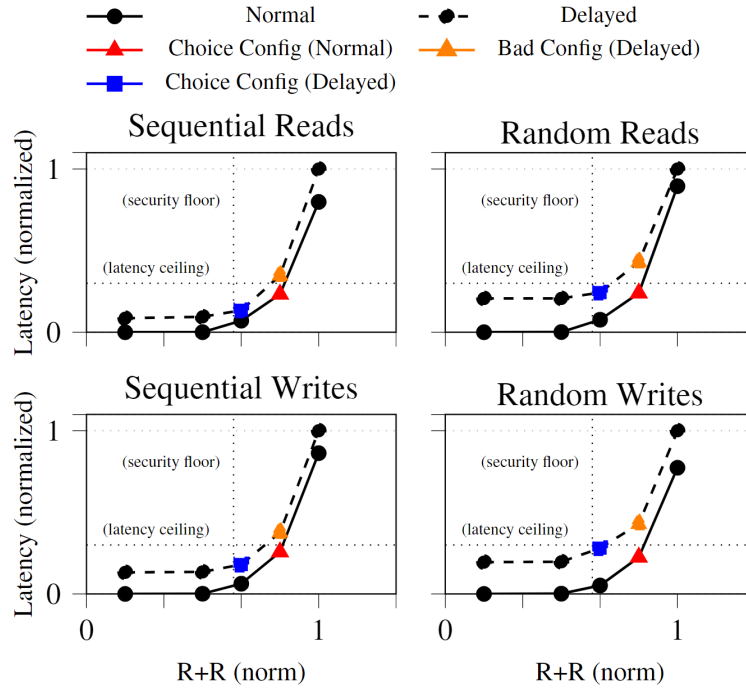


Figure 4.8: Median sequential and random 40MB read and write performance comparison: baseline versus simulated faulty block device.

In Fig. 4.8, we see the sequential and random read and write performance of a 40MB workload when nuggets are encrypted exclusively with our choice ciphers. While the latency ceiling and security floor have not changed, we see increased latency in the delayed workloads.

Our goal is to remain under the latency ceiling while remaining above the security floor. Thanks to Forward switching, accesses to highly trafficked areas of the drive can remain performant even during drive end-of-life.

CHAPTER 5

HASCHK: TRADING OFF BUILD PROCESS COMPLEXITY FOR RESOURCE SECURITY

5.1 Motivation

In 2010, through compromising legitimate applications available on trusted vendor websites, nation-state actors launched the Havex malware, targeting aviation, defense, pharmaceutical, and other companies in Europe and the United States [46, 71]. In 2012, attackers compromised an official phpMyAdmin download mirror hosted by reputable software provider SourceForge. The backdoored version of the popular database frontend was downloaded by hundreds of users, potentially allowing attackers to gain access to private customer data [76, 77]. In 2016, attackers broke into the Linux Mint distribution server and replaced a legitimate Mint ISO with one containing a backdoor, infecting hundreds of machines with the malware [5, 96]. Over a four day period in 2017, users of the popular HandBrake open source video transcoder on Mac/OSX were made aware that, along with their expected video software, they may have also downloaded a trojan that was uploading their sensitive data to a remote server [44]. HandBrake developers recommended users perform *checksum verification* to determine if their install was compromised [43].

Clearly, downloading resources over the internet (TCP/IP) comes with considerable risk. This risk can be divided into three broad concerns: response authentication, communication confidentiality, and resource integrity. Response authentication allows us to determine if a response received indeed originates from its purported source through, for instance, the adoption of a Public Key Infrastructure (PKI) scheme [19]. Communication confidentiality allows us to keep the data transacted between two or more parties private through some form of encryption, such as AES [25]. Finally, resource integrity allows us to verify that the data we are receiving is the data we are expecting to receive.

When it comes to response authentication and communication confidentiality concerns on the internet, the state-of-the-art in attack mitigation is Transport Layer Security (TLS) and its Hyper Text Transfer Protocol (HTTP)/PKI based implementation, HTTPS [14, 19, 27, 28, 84]. Assuming well behaved certificate authorities and modern browsing software, TLS and related protocols, when properly deployed, mitigate myriad attacks on authentication and confidentiality.

However, as a *communication* protocol, TLS only guarantees the integrity of each *end-to-end communication* via message authentication code (MAC) [28]. But protected encrypted communications mean nothing if the contents of those communications are corrupted before the fact. Hence, attacks against the integrity of resources at the application layer (rather than the transport layer) are outside the threat model addressed by TLS and HTTPS [28, 84].

Attacks on resource integrity can be considered a subset of *Supply Chain Attacks* (SCA). Rather than attack an entity directly, SCAs are the compromise of an entity's software source code (or any product) via cyber attack, insider threat, upstream asset compromise, trusted hardware/vendor compromise, or other attack on one or more phases of the software development life cycle [74]. These attacks are hard to detect, even harder to prevent, and have the goal of infecting and exploiting targets and victims by abusing the trust between consumer and reputable software vendor [72].

Ensuring the integrity of resources exchanged over the internet despite SCAs and other active attacks is a hard and well studied problem [1, 3, 16, 18, 19, 34, 56, 63, 70, 84]. The de facto standard for addressing this risk in the generic case is using *checksums* coupled with some secure transport medium like TLS/HTTPS. Checksums in this context are cryptographic digests generated by a cryptographic hashing function [87] run over the resource's file contents. When a user downloads a file from some source, they are expected to run the same cryptographic hashing function over their version of the resource to yield a local

checksum and then match it with a checksum given to them by some trusted authority.

However, checksums come up short as a solution to the resource integrity problem. Foremost is a well-understood but harsh reality: **user apathy**. Most users will not be inconvenienced with manually calculating checksums for the resources they download [18, 32]; moreover, most users will not take the time to understand how checksums and integrity verification work [18, 50, 95]. While detailing how they gained unauthorized access to the servers, one of the hackers behind the 2016 breach of Linux Mint’s distribution system went so far as to comment (in respect to checksums): “Who the [expletive] checks those anyway?” [107]. Hardly unique to checksums, designers of security schemes from HTTPS to PGP to Google Chrome dangerous download warnings have found user apathy a difficult problem space to navigate [4, 13, 18, 30, 51, 69, 81, 93, 103, 108].

Even if a user feels the urge to manually calculate and verify a resource’s checksum, they must search for a corresponding “authoritative checksum” to compare against. As there is no standard storage or retrieval methods for checksums, they could be stored anywhere, or even in multiple different locations that must then be kept consistent [18]; users are not guaranteed to find an authoritative checksum, even if they are published online somewhere, even if they appear on the same page as the resource they are trying to protect. If users do manage to find the authoritative checksum manually and also recognize the checksums are different, the user is then expected to “do the right thing,” whatever that happens to be in context.

A major contributor to this confusion is the tradeoff made by **co-hosting** a resource and its authoritative checksum on the same distribution system, *e.g.*, a web page hosting both a hyperlink pointing to a resource and that resource’s authoritative checksum together. While cost-effective for the provider and less confusing for the user, an attacker that compromises a system hosting both a resource and its checksum together can mutate both, rendering the checksum irrelevant [56]. This is true for automated checksum verification solutions

as well [18]. The co-hosting problem was demonstrated by the 2016 hack of Linux Mint’s distribution server [5, 96].

For these reasons, checksums as they are typically deployed are not very effective at guaranteeing resource integrity, even if automatic verification by web clients is attempted. Recognizing this, some corporations and large entities rely instead on approaches like digital signature verification, code signing, and Binary Transparency [19, 91]. These roll-your-own solutions, often proprietary, have been deployed successfully to mitigate resource integrity attacks in mature software package ecosystems like Debian/apt and Red Hat/yum and walled-garden app stores like Google Play, Apple App Store, and the Microsoft Store.

Unfortunately, not all resources available on the internet are acquired through mature software package ecosystems with built-in PKI support. In the United States for instance, most internet users download software directly from websites or other locations [18, 89]. Moreover, such schemes are not compatible with one another and cannot scale to secure arbitrary resources on the internet without significant cost and implementation/deployment effort.

This work addresses these problems by proposing HASCHK, a novel protocol for verifying the integrity of arbitrary resources downloaded over the internet that is a complete replacement for typical checksum-based schemes, significantly raises the bar for the attacker, and can be implemented in more than just browser software. To overcome the challenges posed by user apathy and co-hosting, HASCHK is implemented in two parts: a backend for resource *providers* and a frontend for resource *consumers*—*i.e.*, (end) users. Providers use a high availability backend to advertise which resources they provide for download. To defeat co-hosting, this backend exists separately from the system offering those resources. To account for user apathy, the frontend client automatically computes a (non-authoritative) checksum identifying the resource, queries the backend using that checksum, and mitigates the threat to the user in the case where the download is deemed compromised. Hence,

HASCHK consists of both the protocol by which these pieces communicate and their implementation.

We approach these problems with four key concerns in mind. (1) HASCHK frontends must provide security guarantees transparently without adding any extra user burden in the common case. Here, an optimal implementation avoids relying on the user to overcome apathy in the interest of security while accounting for the tendency of some users to click through security warnings so as to not be inconvenienced. The former is achieved through automation and the latter through careful design. (2) HASCHK must be low effort for providers to integrate and deploy in concert with the resource(s) they are meant to protect. There must be no requirement to configure a secondary system solely dedicated to hosting checksums. (3) The protocol is not tightly coupled with any particular high availability system. (4) Neither application, website source code changes, user-facing server, nor web infrastructure modifications are necessary for providers to deploy HASCHK.

To demonstrate the general applicability of our protocol, we implement a frontend Google Chrome extension and two different high availability backends: one based on the public Domain Name System (DNS) [67, 68] via Google DNS [52] and another based on the Ring OpenDHT network [37, 85] via a custom Representational State Transfer (REST) API. Of course, these HASCHK components of our implementation should be considered proof-of-concept.

We evaluate the security, performance impact, scalability, and deployment overhead of our implementation using a publicly available patched HotCRP instance. While not a panacea, we show that our implementation is capable of detecting real-world resource compromises, even when the server is under the attacker’s control. Additionally, we find no practical obstacles to efficient deployment at scale or to security outside of those imposed by the Chrome V2 Extension API.

In summary, our primary contributions are:

First, we propose a practical automated approach to ensuring the integrity of arbitrary downloads. Our protocol requires no modifications to web standards/infrastructure or source code, does not employ unreliable heuristics, does not expect checksums to be co-hosted on the same page as do other automated approaches, and can be transparently implemented. Further, our protocol can be used by more than just browsers; HASCHK can protect downloads in FTP clients, wget/curl clients, and other software.

Second, we present our proof-of-concept implementation, a Google Chrome extension, and demonstrate our protocol’s effectiveness empirically. We show that our implementation is capable of detecting resource compromises when the server is under the attacker’s control, thus significantly raising the bar for an attacker. We additionally make our frontend implementation and OpenDHT JSON API available open source (see chapter A).

Third, we evaluate our implementation and find marginal integration and deployment overhead with no practical obstacles to scalability or security outside those imposed by the Chrome API. To the best of our knowledge, this is the first approach that is not susceptible to the pitfalls of co-hosting. Hence, we conclude that HASCHK is more effective at detecting resource integrity attacks than manual checksum verification and prior automated schemes.

5.1.1 Resource Integrity SCAs

Modern software requires a complex globally distributed supply chain and development ecosystem for organizations and other providers to design, develop, deploy, and maintain products efficiently [72]. Such a globally distributed ecosystem necessitates integration with potentially many third party entities, be they specialty driver manufacturers, external content distribution network (CDN) providers, third party database management software, download mirrors, etc.

Critically, reliance on third parties, while often cost-effective and feature-rich, also increases the risk of a security compromise at some point in the supply chain [56, 72]. These

Concept	Design	Development	Integration	Deployment	Maintenance	Retirement
X	X	X	X	✓	✓	✓

Table 5.1: The generic software engineering supply chain.

types of compromises are known as Supply Chain Attacks (SCA). In the context of software development, SCAs are the compromise of an entity’s software source code via cyber attack, insider threat, upstream asset/package management compromise, trusted hardware/vendor compromise, or some other attack on one or more phases of the software development life cycle or “supply chain” to infect an unsuspecting end user [74].

Every year, major SCAs become more frequent and their fallout more widely felt [72, 74]. Whether major or minor, SCAs are hard to detect, even harder to prevent, and have the goal of infecting and exploiting victims by violating the trust between consumer and reputable software vendor.

Table 5.1 details the phases of a generic software development supply chain. For the purposes of this research, we focus exclusively on SCAs targeting the deployment, maintenance, and retirement phases.

5.1.2 Real World Motivations

Here, we select four relatively recent real-world attacks we believe most effectively articulate the threat posed by resource integrity SCAs and how HASCHK might have been used to more effectively mitigate fallout. We examine each attack, noting the critical points of failure in their checksum-based resource security models.

Case 1: PhpMyAdmin. For an unspecified amount of time circa 2012, a compromised download mirror in SourceForge’s official HTTPS-protected CDN was distributing a malicious version of the popular database administration software phpMyAdmin [24]. The administrator of the mirror in question confirmed the attack was due to a vulnerability not

shared by SourceForge’s other mirrors [76].

Attackers mutated the software image, injecting files that would allow any attacker aware of their existence to remotely execute arbitrary PHP code on the victim’s system [77]. SourceForge estimates approximately 400 unique users downloaded this corrupted version of phpMyAdmin before the mirror was disconnected from their CDN, potentially allowing attackers access to the private customer data of any number of organizations [76].

While the attackers were able to penetrate a mirror in SourceForge’s CDN, the official phpMyAdmin website was entirely unaffected; the authoritative checksums listed on the site’s download page were similarly unaffected [76]. Hence, a user who was sufficiently motivated, had sufficient technical knowledge of checksums and how to calculate them, and was also privy to the location of the correct checksum for the official phpMyAdmin image *might* have noticed the discrepancy between the two digests. Clearly, a non-trivial number of users do not meet these criteria. This attack demonstrates the problem of *user apathy*.

Case 2: Linux Mint. In 2016, the Linux Mint team discovered an intrusion into their official HTTPS-protected distribution server [96]. Attackers mutated download links originally pointing to the Linux Mint 17.3 Cinnamon edition ISO, redirecting unsuspecting users to a separate system hosting a custom Mint ISO compiled with the IRC-based Linux backdoor malware *Tsunami* [5]. The attack affected hundreds of the downloads during that day, with the attackers claiming that a “few hundred” Linux Mint installs were explicitly under their control. The primary motivation behind the intrusion was the construction of a botnet [107]. The authoritative checksum displayed on the official website was also mutated to corroborate the backdoored ISO [107], illustrating the *co-hosting* problem.

Storing the checksum elsewhere may have prevented mutations on the checksum; still, as demonstrated by the first case, such an effort is not itself a solution. Hosting a checksum on a secondary system is not very useful if users downloading the resource protected by that

checksum cannot find it or are not actually *checking* it against a manual calculation.

Case 3: Havex. As part of a widespread espionage campaign beginning in 2010, Russian Intelligence Services targeted the industrial control systems of numerous aviation, national defense, critical infrastructure, pharmaceutical, petrochemical, and other companies and organizations with the Havex remote access trojan [46, 71]. The attack was carried out in phases whereby innocuous software images hosted on disparate *legitimate* vendor websites were targeted for replacement with versions infected with the Havex malware [71]. The goal here, as is the case with all SCAs, was to infect victims indirectly by having the Havex malware bundled into opaque software dependencies, *e.g.*, a hardware driver or internal communication application.

It is estimated that Havex successfully impacted hundreds or even thousands of corporations and organizations—mostly in United States and Europe [71]. The motivation behind the Havex malware was intelligence exfiltration and espionage [46]. How many of these vendors employed checksums and other mitigations as part of their software release cycle is not well reported, though investigators note said vendors’ distribution mechanisms were insecure [71]; however, an automated resource verification method could have helped mitigate the delivery of compromised software to users.

Case 4: HandBrake. In May of 2017, users of HandBrake, a popular open source video transcoder for Mac/OSX, were made aware that they may have downloaded and installed a trojan riding atop their transcoding software. Attackers breached an HTTPS-protected HandBrake download mirror, replacing the legitimate software with a version containing a novel variant of the *Proton* malware [44]. The number of users potentially affected is unreported.

The goal of the attack was the exfiltration of victims’ sensitive data, including decrypted

keychains, private keys, browser password databases, 1Password/Lastpass vaults, decrypted files, and victims’ personal videos and other media [44]. The HandBrake developers recommended users perform manual checksum verification to determine if their installation media was compromised [43].

Despite the attackers mutating the HandBrake binary, the authoritative checksums listed on the official HandBrake download page were reportedly left untouched [43]. Further, the developers of HandBrake store their authoritative checksums both on their official website and in their official GitHub repository [43]. A sufficiently knowledgeable, sufficiently motivated user *might* have noticed the discrepancy between their calculated checksum and the authoritative checksum listed on the download page.

Suppose, however, that the attackers *had* managed to mutate the checksums on the official website. Then there would be a discrepancy between the “authoritative” checksums on the official site and the “authoritative” checksums in the GitHub repository—that is *if* users are even aware that a second set of checksums are available at all. Which are the actual authoritative checksums? On top of requiring the technical knowledge, a user in this confusing situation is then expected to “do the right thing,” whatever that happens to be in context.

5.2 Protocol Design

In this section, we describe the components of the HASCHK protocol, step through each in detail, and then introduce our proof-of-concept implementation of these components.

5.2.1 Participants

Provider. The *provider* is the entity in control of both the server and backend with the goal of ensuring the integrity of resources downloaded from their system.

HASCHK Frontend. The *frontend* is responsible for calculating the Uniform Resource Name (URN) and Backend Domain (BD) of the resource downloaded from the server. Afterwards, the frontend queries the backend using this URN and, if an integrity violation is detected, quarantines the resource and warns the user.

Server. The *server* is a distribution system (hopefully) controlled by the provider that hosts resources for download. It can be internal or external, a single server or many, first-party or third-party.

HASCHK Backend. The *backend* is responsible for advertising a queryable listing of URNs that HASCHK frontends can use to judge the legitimacy of downloads. It is a high availability system that is wholly separate from the server (not co-hosted) and controlled by the provider.

5.2.2 Protocol Overview

Fig. 5.1 gives a high level overview of the HASCHK protocol. Initially, when a user finishes downloading a resource from the provider’s server, the frontend runs the resource’s contents through the SHA-256 hashing function, yielding a 256-bit digest. Any hashing function can be used so long as it is pre-image and collision resistant [87]. This digest is used to construct a hash-based Uniform Resource Name [99] (URN) uniquely identifying the resource. Additionally, a Backend Domain (BD) is derived from the domain name of the server. The frontend uses the BD in an implementation-dependent manner to locate and query the backend, checking for the existence of the constructed URN and essentially asking: “*is this a compromised resource?*” If the URN is found, a negative response is returned indicating a verified resource. If the URN is not found, a positive response is returned indicating a compromised resource.

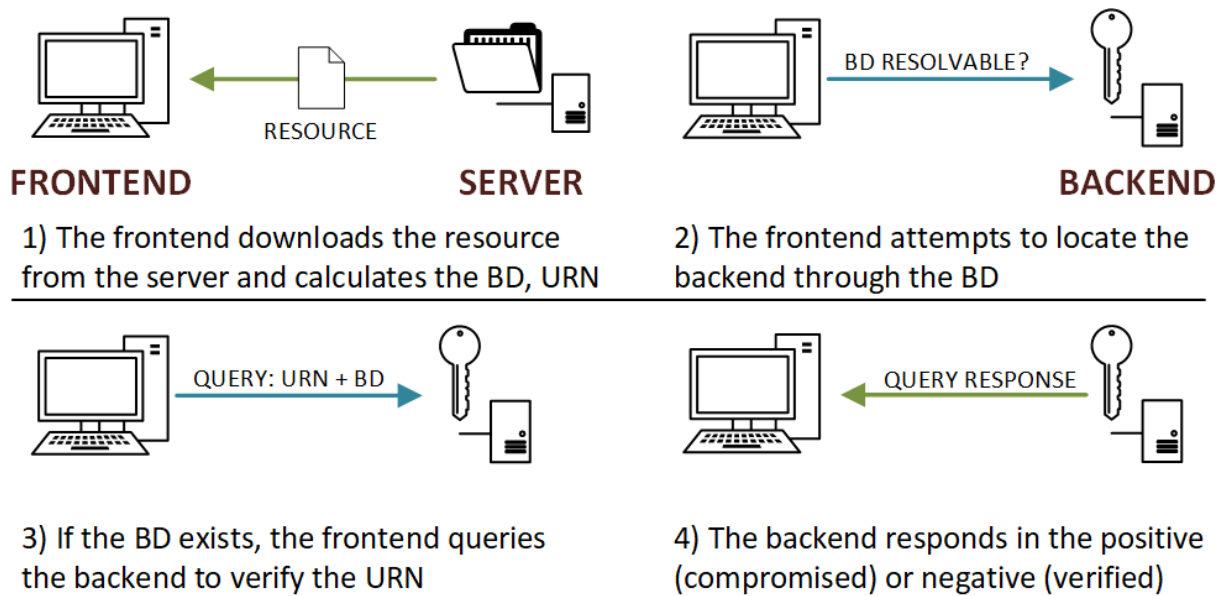


Figure 5.1: A high level overview of the (generic) automated checksum verification process beginning when a user downloads a resource.

If the query returns a positive response: (1) the user should be warned pursuant to the recommendations of Akhawe et al [4] (avoid warning fatigue, be invisible), Cherubini et al [18] (simple non-technical language, secure default action), Modic et al [69] (issue warnings from a position of authority), and others; (2) the download should be deleted, renamed, or otherwise made inaccessible/quarantined by default; and (3) the user should still be allowed to “click through” and override the warning and the default quarantine behavior, though ideally this should be less convenient than the default action [18].

If the query returns a negative response, the frontend should indicate this inconspicuously to mitigate the threat of warning/popup fatigue [4, 18] and habituation [94]. For example, our frontend implementation simply changes its icon when downloads are successfully verified and only issues popup warnings when compromised downloads are positively identified.

To prevent false positives, integrity checking is skipped if the backend’s location is unresolvable or HASCHK is not properly deployed. Determining when this is the case is implementation-dependent. To prevent false-negatives, when HASCHK is properly deployed

and a URN is not found during lookup, the backend response will always be interpreted as positive. As a result, it is not possible to only secure “some” resources on a server.

Deriving the Backend Domain (BD)

Before we can communicate with a provider’s backend, we require some scheme to locate it. We refer to this scheme as *deriving the Backend Domain* (BD). The BD is some identifier that allows the frontend to locate the backend. For our Domain Name System (DNS) based implementation (below), the BD is the Third-Level Subdomain (3LD) or Second-Level Domain (2LD) based on the server URI’s host subcomponent [9] and are queried in that order.

Example 1: an FTP frontend (*e.g.*, Filezilla, Transmit, et cetera) downloading a resource from an FTP server at `ftp://un:pw@ftp.example1.com:8080/some/resource` has a host subcomponent of `ftp.example1.com` and a BD of `ftp.example1.com` or `example1.com`.

Example 2: a browser frontend (*e.g.*, Lynx, Google Chrome, Internet Explorer, et cetera) downloading a resource at `https://s4.l.cdn.example2.com/f1` from a hyperlink on the page `https://dl.app.example3.com/index/page` has a host subcomponent of `dl.app.example3.com` (*not* `s4.l.cdn.example2.com`) and a BD of `app.example3.com` or `example3.com`.

It is important that the right BD is derived to ensure correct operation of the protocol. This concern is implementation-dependent. Specifically, in the case of the browser frontend in example 2 (above), the BD is not derived from the resource’s URI directly but from the URI of the HTML page containing the hyperlink pointing to that resource. This prevents an adversary from trivially fooling HASCHK by, for instance, replacing

`https://s4.1.cdn.example2.com` with a hyperlink pointing to `https://attacker.com` and hosting a conforming HASCHK backend that would cause the frontend to respond with a false negative.

Further, depending on the implementation, a frontend or backend may not be using URIs and DNS to transact information over the internet at all. An example of this is a purely Distributed Hash Table (DHT) based backend. In such a case, any derivation algorithm (or no derivation at all, *e.g.*, the BD is hardcoded) can be used as long as correct operation of the protocol is ensured.

Constructing Uniform Resource Names (URN)

To ensure the integrity of arbitrary resources, we require some method to uniquely and durably identify those resources. We accomplish this through the adoption of the informal IETF draft for the construction of hash-based *Uniform Resource Names* (URNs) [99], which the frontend follows when calculating URNs for each resource downloaded. Through whatever implementation-specific method, the backend must “advertise” or allow lookups against a set of expected URNs corresponding to the resources hosted on the provider’s server, even if those resources have unstable access paths or URIs; *e.g.*, , when resources are hosted externally, on download mirrors, on CDNs, et cetera. This requirement is satisfied by implementations combining URNs with the BD, thus durably associating the URNs calculated in the frontend with the URNs advertised by a provider’s backend regardless of where the corresponding resources are hosted on the provider’s server.

Since the backend advertising URNs is *never* co-hosted alongside the system that distributes the corresponding resources—like a web or FTP server—HASCHK retains the ability to protect users from dangerous downloads *even when the system distributing the resource has been completely compromised*. This is not true of prior approaches to automated checksum verification of arbitrary resources [18].

5.3 Implementation

We implement a proof-of-concept HASCHK frontend as a Google Chrome extension. To demonstrate the general applicability of our approach, our frontend currently works with two backends: (1) directly with DNS via Google’s JSON API for DNS over HTTPS (DoH) and (2) indirectly with DHT (Ring OpenDHT) via a local Representational State Transfer (REST) API we designed to mimic the response syntax of Google’s DoH JSON API. Other candidate backends include storage clusters, relational and non-relational databases, and any high availability key-value store.

Our extension operates following the high level overview in Fig. 5.1 with some key implementation-specific functionality that we explore in the remainder of this subsection. After the user initiates a download either directly (*e.g.*, typing a URI manually) or by following a hyperlink, our extension, having observed the initial web request, associates that request with the new download item. The original request may have directly triggered the download or the download may have been triggered after one or more redirections. Our extension derives the correct BD in both cases (see below). At this point, if the backend does not exist or does not conform to the protocol, the protocol terminates. Otherwise, after the download completes, a URN is calculated and combined with the BD to make a final query to the backend. In effect, this query asks: *is this resource compromised?* If the response to the query is negative (*i.e.*, a DNS TXT record or DHT data value), the extension considers the resource validated. On the other hand, if the response to the query is positive (*i.e.*, no record found or bad data value returned), the extension considers the resource compromised, deletes the resource file, and warns the user.

In keeping with UX suggestions of prior work, our extension is virtually transparent to end users in the common case that a download is successfully verified by a provider’s backend or when HASCHK has not been properly deployed by a provider. However, in the relatively uncommon case that a resource is deemed compromised, the extension will delete the file

and alert the user with the primary option to “dismiss” the alert, mimicking Chrome’s own highly effective dangerous download warning [51]. Specifically: the user has the option of clicking through the warning via a low-key secondary interface where they can force the extension to ignore the compromised nature of the resource *the next time it is downloaded*, forcing the user to trigger the download again. This inconvenience, favoring users’ security over choice, is in keeping with the recommendations of prior work regarding security warning UX (see Section 5.1).

As no JavaScript OpenDHT client implementation exists, we developed a REST API to facilitate communication between our extension and the Ring OpenDHT network via HTTP and JSON. In a production implementation, a JavaScript OpenDHT client would be baked directly into the extension.

Deploying the DNS backend is as simple as adding certain TXT records to our DNS zone. This is a straightforward operation. Similarly, deploying the DHT backend requires adding certain key-value pairs to the OpenDHT network, which is trivial. Moreover, both DNS and DHT backends are performant and highly available. The Ring OpenDHT network is also free to use. In the case of DNS, the vast majority of web-facing providers and IT teams are already using it, already pay for their own DNS zones, and are already quite familiar with configuring and managing them. Hence, no exotic secondary backend system is required for providers with web servers. Additionally, we argue updating the URNs stored by these backends automatically—by integrating a URN calculation and record insertion/update step into a modern development toolchain or resource deployment pipeline—is relatively low-effort and straightforward for providers.

No application or website source code changes, costly user-facing server or web infrastructure customizations, or modifications to web standards are needed to enable our extension to protect a provider’s resources. Given a production-ready implementation of our frontend—coupled with the near ubiquitous adoption of DNS—HASCHK (with a DNS backend) could

be deployed immediately by interested providers.

5.3.1 URNs, BDs, and Falthrough in Google Chrome

BD derivation in the browser is non-trivial. Users can initiate downloads through clicking links inside *and outside* the browser (*e.g.*, in an email application), through asynchronous JavaScript, and by entering URIs into the browser manually. To catch these and other edge cases, we implement our extension using the WebRequest API [39], which allows us to monitor all navigation events, collate redirects into an interrogable chain of requests, and associate new download items with the URI where they were originally initiated.

To query the backend, we: (1) BASE32 encode the resource’s URN. (2) Divide the 112-character result into two 56-character strings `C1` and `C2`. (3) We calculate the BD, which is either the 3LD and 2LD from `details.originUrl`. We choose by issuing up to two queries of the form `AL.BD`, where the Application Label (AL) is the constant string `_haschk`, looking for a response containing the value `OK`. We first query the 3LD as BD and, if we do not receive the proper response there, query the 2LD as BD. If the proper response is not received from either query, the extension assumes HASCHK has not been properly deployed and terminates. (4) Otherwise, concatenating `C1`, `C2`, `AL`, and `BD`, we issue a query of the form `C1.C2.AL.BD`, again looking for a response containing `OK` (negative) or that the query was not found (positive).

To handle redirection, we use Chrome’s Web Request API to associate redirected requests with one another. The originating request’s `origin` at the top of this chain is used to derive the BD using the `details.originUrl` and `details.documentUrl` properties (also avoiding iframe issues). This prevents an adversary from trivially fooling HASCHK by replacing a legitimate hyperlink with a malicious one. A naive implementation might use the `DownloadItem.referrer` property to derive the BD, since it should be populated with the originating URL. Unfortunately, this property can be manipulated with one or more

redirections causing the BD to point into the attacker’s DNS zone. If the attacker properly deploys a HASCHK backend, they could then trivially force false negatives.

Keeping a chain of associated requests also allows us to implement “fallthrough” functionality where, if the original request at the head of the chain has not deployed HASCHK, the extension can walk the chain, checking each point of redirection for a proper HASCHK deployment. This ensures URL shorteners and other redirection services do not trigger false positives.

5.4 Evaluation

5.4.1 Security Goals and Threat Model

The goal of HASCHK is to ensure the integrity of arbitrary resources downloaded over the internet, even in the case where the system hosting those resources is completely compromised. Given a HASCHK-aware client and a resource provider with a conforming backend, the user must be automatically warned whenever what they are downloading does not match a corresponding authoritative checksum. Given proper deployment, HASCHK should, to whatever extent possible, operate without issuing false negatives, *i.e.*, compromised resources that do not trigger a warning, or false positives, *i.e.*, benign resources that do trigger a warning.

We consider the following entities: (1) a HASCHK-aware client as the *frontend*, (2) a *server* (or servers) as the distribution system hosting the *resource*, and (3) a separate high availability system implementing HASCHK as the *backend*. Specifically, we consider a *generic frontend* that might be any web-facing software, such as FileZilla, and a *browser frontend* such as Google Chrome or Mozilla Firefox.

For a generic frontend, we assume the adversary can make the server respond to a resource request with any resource, including a compromised version of a resource. We also assume the adversary can tamper with any other server response, including adding, removing, or

manipulating one or more checksums if they appear.

For a browser frontend and web server, we contemplate two scenarios. From either an existing tab/window or a new one, the user (1) directly enters the resource URI into the browser, initiating a direct download or (2) navigates to an HTML file (*web page*) on the server containing a hyperlink pointing to the resource. The user clicks this hyperlink to download the resource. This resource is hosted on the same server as the web page or externally on a third party server such as a CDN. Both are valid deployments in the context of HASCHK. We assume the adversary can manipulate the resource and web page wherever they are stored. The adversary may: (1) compromise the resource, (2) modify the hyperlink to point to a compromised resource anywhere on the internet, and/or (3) add, remove, or manipulate any checksums that appear on the web page or elsewhere.

Hence, we do not trust the integrity of the server’s responses in any scenario. We do, however, trust the integrity and authenticity of the backend’s responses. Further, we expect the backend to be highly available. In Section 5.4, we go over the implications of a compromised backend.

As an aside, we consider here the standard non-HASCHK case where the resource is co-hosted alongside a web page containing both a hyperlink pointing to the resource *and an authoritative checksum corresponding to the resource*. As demonstrated throughout this work, when a server co-hosting resources and checksums is compromised, it is trivial to manipulate both checksum and resource, rendering all forms of checksum verification irrelevant. Assuming proper deployment, it is the goal of HASCHK to ensure this is never the case.

5.4.2 Security and Performance

To empirically evaluate our implementation, we launch a lightly modified version of the popular open source research submission and peer review software, HotCRP (version 2.102; see chapter A). Our modifications allow anyone visiting the site to interactively corrupt

submissions and manipulate relevant DNS entries at will.

For our evaluation, we upload 10 different PDFs to our HotCRP instance. Upon their upload, HotCRP calculates and displays the unique checksum (a SHA-256 digest) of each PDF. After each PDF is uploaded, we immediately download it and manually calculate a checksum locally, matching each to the checksum displayed by the HotCRP software. Next, we utilize the custom functionality we patched into HotCRP to populate our DNS backend with each file’s expected URN.

After installing the frontend into our Google Chrome browser, we again download each file. For each observed download, our extension indicates a “safe” judgement. We then utilize our patched functionality to add junk data onto the end of each of the uploaded PDFs, thus corrupting them. We also modified HotCRP so that it updates the displayed checksums to match their now-corrupted counterparts.

Once again, we download each file. Our extension reports an “unsafe” judgement (a true positive) for each corrupted PDF file. Calculating the local checksum and checking it against the value reported by our HotCRP instance leads to a match (a false negative; *i.e.*, the result of co-hosting), defeating prior approaches to both manual and automated checksum verification.

We run this experiment three times, each with different sets of PDFs and using both the DNS and DHT based backends. We observe consistent results.

Finally, we utilize our patched functionality to test a “redirection” attack where the hyperlink pointing to the correct PDF is replaced with a hyperlink to a dummy malware file hosted in a distinct malicious DNS zone with conforming HASCHK deployment. When an unsuspecting user clicks such a link, they expect to download the PDF document from HotCRP but are instead navigated to a PHP script that redirects the request one or more times before landing on the dummy malware file. This process corrupts Chrome’s `DownloadItem.referrer` property. Even in this case, our implementation correctly flags

this download as suspicious as the download begins, successfully warning the user.

While evaluating our implementation, we observe no additional network load or CPU usage with the extension loaded into Chrome. Measurements are taken using the Chrome developer tools. Intuitively, this makes sense given the lightweight nature of the cryptographic operations involved.

We also consider the implications of a compromised backend, such as if an attacker tampers with the provider’s DNS server or its response. Since we trust the integrity and authenticity of responses from the backend, this is ultimately outside our threat model. However, in the case of a compromised DNS zone by itself, at worst the attacker can perpetuate a denial of service attack by triggering false positives. Without compromising both the backend and the distribution server, the attacker still cannot deliver compromised resources to users. Further, we argue a provider has much bigger problems if their DNS zone or other backend is compromised.

5.4.3 Scalability and Deployment

As HASCHK assumes a high availability backend, we conclude that the scalability of HASCHK can be reduced to the scalability of its backend. We are aware of no other obstacles to scalability beyond those inherited from the underlying backend system.

Obviously, our DNS backend relies on DNS [67]. DNS was not originally designed to transport or store relatively large amounts of data, but the content of our DNS TXT records are very small (usually two bytes or less). Further, the URNs queryable via DNS request are exactly 112 characters, *i.e.*, the length of a BASE32 encoded URN, and are divided into two 53 character labels, conforming to DNS label length limits [68].

We are also unaware of any practical limitation on the number of resource records a DNS zone file can support. A DNS server can host tens of thousands of resource records in their backend file [67, 68]. Moreover, several working groups have considered using DNS as a

storage medium for checksums/hash output, so the concept is not novel. Examples include securitytxt [36] and DKIM [21].

Additionally, using DNS as a backend does not add to the danger of amplification and other reflection attacks on DNS; these are generic DNS issues addressable at other layers of the protocol.

With the HotCRP demo, our entire resource deployment scheme consists of (1) the addition of a new TXT entry to our DNS backend and (2) a new value published to our DHT backend during the paper (resource) submission process. We argue updating DNS record (or DHT value) during the resource deployment process is simple enough for developers and providers to implement and presents no significant burden to deployment. For reference, we implement the functionality that automatically adds (and updates) the DNS TXT records advertising the URNs of papers uploaded to our HotCRP instance in under 10 lines of JavaScript.

5.4.4 *Limitations*

While still effective, our extension would be even more effective if Chrome/Chromium or the more general WebExtensions API allowed for an explicit `onComplete` event hook in the downloads API. This hook would fire immediately before a file download completes and the file becomes executable, *i.e.*, has its `.crdownload` or `.download` extension removed. The hook would consume a `Promise/AsyncFunction` that kept the download in its fully-downloaded but non-complete state until said `Promise` completed. Ideally, this would allow an extension to alter a download's `DangerType` property after some computation, prompting Chrome to handle alerting the user using its Dangerous Download UX [51], which would have the advantage of communicating intent through the browser's familiar and authoritative UI and prevent the corrupted download from becoming immediately executable. Unfortunately, the closest the Chrome WebExtensions API comes to allowing `DangerType` mutations is the

`acceptDanger` method on the downloads API, but it is not suitable for our purposes because it can only be called after the download completes while leaving the file in an accessible and executable state until the method is eventually called.

Redirection services, like URI shortening apps, might still lead to false positives even with the fallthrough functionality if a domain on the request chain has deployed HASCHK. We view this as a rare scenario, and it does not violate HASCHK's security guarantees. Further, our extension does not work for PDFs and other downloads handled directly by the browser. And, given the topology of the webrequest API, iframes and similar elements may require special consideration beyond examining `details.documentUrl`.

Additionally, not all servers/backends on the internet use DNS, and our extension does not support downloads made that bypass DNS. In future work, our DHT backend would be able to handle such downloads. Further, our extension keeps 1000 requests in memory so that they can be mapped to download items later in time. This might be vulnerable to attacks involving excessive redirection and overflow.

CHAPTER 6

CONCLUSION

The conventional wisdom is that securing data at rest requires one must pay the high performance overhead of encryption with AES in XTS mode. This work shows that technological trends overturn this conventional wisdom: log-structured file systems and hardware support for secure counters make it practical to use a stream cipher to secure data at rest. We demonstrate this practicality through our implementation of StrongBox which uses the ChaCha20 stream cipher and the Poly1305 MAC to provide secure storage and can be used as a drop-in replacement for dm-crypt.

Our empirical results show that under F2FS—a modern, industrial-strength Log-structured file system—StrongBox provides upwards of $2\times$ improvement on read performance and average $1.27\times$ improvement on write performance compared to dm-crypt. Further, our results show that F2FS plus StrongBox provides a higher performance replacement for Ext4 backed with dm-crypt. We make our implementation of StrongBox available open source so that others can extend it or compare to it.¹ Our hope is that this work motivates further exploration of fast stream ciphers as replacements for AES-XTS for securing data at rest.

Further, this work advocates for a more flexible approach to FDE where the storage system can dynamically adjust the tradeoffs between security and latency/energy. To support this vision of agile encryption, we proposed an interface that allows multiple stream ciphers with different input and output characteristics to be composed in a generic manner. We have identified three strategies for using this interface to switch ciphers dynamically and with low overhead. We have also proposed a quantification framework for determining when to use one cipher over another. Our case studies show how different strategies can be used to optimize for different goals in practice. We believe that agile encryption will become increasingly important as successful systems are increasingly required to balance conflicting

1. <https://github.com/Xunnamius/strongbox-switchcrypt>

operational requirements. We hope that this work inspires further research in achieving this balance. Our work is publicly available open-source¹.

When it comes to data in motion—specifically, downloading arbitrary resources over the internet—it is indeed a risky endeavor. Resource integrity and other Supply Chain Attacks are becoming more frequent and their impact more widely felt. In this work, we showed that the de facto standard for protecting the integrity of arbitrary resources on the internet—the use of *checksums*—is insufficient and often ineffective. We presented HASCHK, a practical resource verification protocol that automates the tedious parts of checksum verification while leveraging pre-existing high availability systems to ensure resources and their checksums are not vulnerable to co-hosting. Further, we demonstrated the effectiveness and practicality of our approach versus real-world resource integrity attacks in a production application.

The results of our final evaluation show that our approach is more effective than checksums and prior work mitigating integrity attacks for arbitrary resources on the internet. Further, we show HASCHK is capable of guarding against a variety of attacks, is deployable at scale for providers that already maintain a DNS presence, and can be deployed without fear of adversely affecting the user experience of clients that are not HASCHK-aware. Though not a panacea, we believe our protocol significantly raises the bar for the attacker. We intend to continue developing our extension and we make it available to a wide audience (see chapter A).

6.1 Future Work

As it stands now, our StrongBox and SwitchCrypt implementations are single threaded. The cryptographic systems we compared to StrongBox and SwitchCrypt and all multi-threaded, perhaps making our performance wins more significant. What performance gains (i.e. more slack) might be available if we parallelize portions of StrongBox and SwitchCrypt source? Examples include: 1) given that nuggets are all independent agents, new switching strategies

might be developed that leverage any speedups in parallelizing the encryption and decryption processes and 2) garbage collection and cipher switching can happen in background worker threads and could even leverage a scheduler and 3) StrongBox and SwitchCrypt could be integrated into F2FS directly, sharing its threading/scheduling model in a production implementation; currently, StrongBox and SwitchCrypt are implemented on top of the BUSE emulation device.

CHAPTER A

CODE AVAILABILITY

This appendix provides links for the StrongBox, SwitchCrypt, and HASCHK source code. The two libraries/APIs that StrongBox and SwitchCrypt rely on are additionally provided. Note that resource locations, URLs, frameworks, interfaces, etc. will likely change overtime, while this text remains static.

We also make our HASCHK frontend and DHT backend components available open source for the benefit of the community. We also make publicly available our evaluation environment: a patched HotCRP instance.

You can find instructions on how to build, test, and modify the StrongBox source in the provided README documentation linked below. Our hope is that this work motivates further exploration of resource integrity and other SCA mitigation strategies and leads to further progress on more exotic FDE schemes.

Table A.1: Provides URLs for the products yielded and/or used by this research. The first four URIs refer to repositories on GitHub.

Project Source	Language	URI
StrongBox Source	C	Xunnamius/strongbox-switchcrypt
SwitchCrypt Source	C	Xunnamius/strongbox-switchcrypt
SBD MT Source	C	IAIK/secure-block-device
BUSE Source	C/Shell	acozzette/BUSE
HASCHK Source	JavaScript/Shell	https://haschk.dev
HotCRP Testbed	PHP/C/Shell	https://hotcrp.haschk.dev

BIBLIOGRAPHY

- [1] D. E. E. 3rd. *Domain Name System Security Extensions*. RFC 2535. <http://www.rfc-editor.org/rfc/rfc2535.txt>. RFC Editor, 1999. URL: <http://www.rfc-editor.org/rfc/rfc2535.txt>.
- [2] *A block device in userspace*. 2012. URL: <https://github.com/acozzette/BUSE> (visited on 04/26/2017).
- [3] D. Akhawe, F. Braun, J. Weinberger, and F. Marier. *Subresource Integrity*. W3C Recommendation. <http://www.w3.org/TR/2016/REC-SRI-20160623/>. W3C, 2016.
- [4] D. Akhawe and A. P. Felt. “Alice in Warningland: A Large-Scale Field Study of Browser Security Warning Effectiveness”. In: *Proceedings of the 22nd USENIX Conference on Security*. SEC13. Washington, D.C.: USENIX Association, 2013, 257272. ISBN: 9781931971034.
- [5] T. Anderson. “Linux Mint hacked: Malware-infected ISOs linked from official site”. In: *The Register* (2016). URL: https://www.theregister.co.uk/2016/02/21/linux_mint_hacked_malwareinfected_isos_linked_from_official_site.
- [6] *Android Open Source Project: Full-Disk Encryption*. URL: <https://source.android.com/security/encryption/full-disk> (visited on 04/26/2017).
- [7] P. A. Babu and J. J. Thomas. *Freestyle, a randomized version of ChaCha for resisting offline brute-force and dictionary attacks*. Cryptology ePrint Archive, Report 2018/1127. <https://eprint.iacr.org/2018/1127>. 2018.
- [8] C. Berbain, O. Billet, A. Canteaut, N. Courtois, H. Gilbert, L. Goubin, A. Gouget, L. Granboulan, C. Lauradoux, M. Minier, T. Pornin, and H. Sibert. “Sosemanuk, a Fast Software-Oriented Stream Cipher”. In: *New Stream Cipher Designs: The eSTREAM Finalists*. Ed. by M. Robshaw and O. Billet. Berlin, Heidelberg: Springer Berlin Heidelberg, 2008, pp. 98–118. ISBN: 978-3-540-68351-3. DOI: 10.1007/978-3-540-68351-3_9. URL: https://doi.org/10.1007/978-3-540-68351-3_9.
- [9] T. Berners-Lee, R. T. Fielding, and L. Masinter. *Uniform Resource Identifier (URI): Generic Syntax*. STD 66. <http://www.rfc-editor.org/rfc/rfc3986.txt>. RFC Editor, 2005. URL: <http://www.rfc-editor.org/rfc/rfc3986.txt>.
- [10] D. J. Bernstein. *The Poly1305-AES message-authentication code*. Tech. rep. University of Illinois at Chicago, 2005.
- [11] D. J. Bernstein. *ChaCha, a variant of Salsa20*. Tech. rep. University of Illinois at Chicago, 2008.
- [12] D. J. Bernstein. “The Salsa20 Family of Stream Ciphers”. In: *The eSTREAM Finalists*. 2008.
- [13] A. Bianchi, J. Corbetta, L. Invernizzi, Y. Fratantonio, C. Kruegel, and G. Vigna. “What the App is That? Deception and Countermeasures in the Android User Interface”. In: *2015 IEEE Symposium on Security and Privacy*. 2015, pp. 931–948. DOI: 10.1109/SP.2015.62.

- [14] S. Blake-Wilson, M. Nystrom, D. Hopwood, J. Mikkelsen, and T. Wright. *Transport Layer Security (TLS) Extensions*. RFC 3546. RFC Editor, 2003.
- [15] M. Boesgaard, M. Vesterager, and E. Zenner. “The Rabbit Stream Cipher”. In: *New Stream Cipher Designs: The eSTREAM Finalists*. Ed. by M. Robshaw and O. Billet. Berlin, Heidelberg: Springer Berlin Heidelberg, 2008, pp. 69–83. ISBN: 978-3-540-68351-3. DOI: 10.1007/978-3-540-68351-3_7. URL: https://doi.org/10.1007/978-3-540-68351-3_7.
- [16] J. Callas, L. Donnerhake, H. Finney, D. Shaw, and R. Thayer. *OpenPGP Message Format*. RFC 4880. <http://www.rfc-editor.org/rfc/rfc4880.txt>. RFC Editor, 2007. URL: <http://www.rfc-editor.org/rfc/rfc4880.txt>.
- [17] D. Chakraborty, C. Mancillas-Lpez, and P. Sarkar. “STES: A Stream Cipher Based Low Cost Scheme for Securing Stored Data”. In: *IEEE Transactions on Computers* 64.9 (2015), pp. 2691–2707. ISSN: 0018-9340. DOI: 10.1109/TC.2014.2366739.
- [18] M. Cherubini, A. Meylan, B. Chapuis, M. Humbert, I. Bilogrevic, and K. Huguenin. “Towards Usable Checksums: Automating the Integrity Verification of Web Downloads for the Masses”. In: *Proceedings of the 2018 ACM SIGSAC Conference on Computer and Communications Security*. CCS 18. Toronto, Canada: Association for Computing Machinery, 2018, 12561271. ISBN: 9781450356930. DOI: 10.1145/3243734.3243746. URL: <https://doi.org/10.1145/3243734.3243746>.
- [19] D. Cooper, S. Santesson, S. Farrell, S. Boeyen, R. Housley, and W. Polk. *Internet X.509 Public Key Infrastructure Certificate and Certificate Revocation List (CRL) Profile*. RFC 5280. <http://www.rfc-editor.org/rfc/rfc5280.txt>. RFC Editor, 2008. URL: <http://www.rfc-editor.org/rfc/rfc5280.txt>.
- [20] M. Cornwell. “Anatomy of a Solid-state Drive”. In: *Queue* 10.10 (Oct. 2012), 30:30–30:36. ISSN: 1542-7730. DOI: 10.1145/2381996.2385276. URL: <http://doi.acm.org/10.1145/2381996.2385276>.
- [21] D. Crocker, P. Hallam-Baker, and T. Hansen. *DomainKeys Identified Mail (DKIM) Service Overview*. RFC 5585. 2009. DOI: 10.17487/RFC5585. URL: <https://rfc-editor.org/rfc/rfc5585.txt>.
- [22] P. Crowley and E. Biggers. “Adiantum: length-preserving encryption for entry-level processors”. In: *IACR Transactions on Symmetric Cryptology* 2018(4) (2018), pp. 39–61. URL: <https://tosc.iacr.org/index.php/ToSC/article/view/7360>.
- [23] A. Cunningham and Utc. *Google quietly backs away from encrypting new Lollipop devices by default*. 2015. URL: <https://arstechnica.com/gadgets/2015/03/google-quietly-backs-away-from-encrypting-new-lollipop-devices-by-default/>.
- [24] *CVE-2012-5159*. Available from MITRE, CVE-ID CVE-2012-5159. 2012. URL: <https://cve.mitre.org/cgi-bin/cvename.cgi?name=CVE-2012-5159>.
- [25] J. Daemen and V. Rijmen. “AES proposal: Rijndael”. In: (1999).

- [26] B. Dickens III, H. S. Gunawi, A. J. Feldman, and H. Hoffmann. “StrongBox: Confidentiality, Integrity, and Performance Using Stream Ciphers for Full Drive Encryption”. In: *Proceedings of the Twenty-Third International Conference on Architectural Support for Programming Languages and Operating Systems*. ASPLOS ’18. Williamsburg, VA, USA: ACM, 2018, pp. 708–721. ISBN: 978-1-4503-4911-6. DOI: 10.1145/3173162.3173183. URL: <http://doi.acm.org/10.1145/3173162.3173183>.
- [27] T. Dierks and C. Allen. *The TLS Protocol Version 1.0*. RFC 2246. <http://www.rfc-editor.org/rfc/rfc2246.txt>. RFC Editor, 1999. URL: <http://www.rfc-editor.org/rfc/rfc2246.txt>.
- [28] T. Dierks and E. Rescorla. *The Transport Layer Security (TLS) Protocol Version 1.2*. RFC 5246. <http://www.rfc-editor.org/rfc/rfc5246.txt>. RFC Editor, 2008. URL: <http://www.rfc-editor.org/rfc/rfc5246.txt>.
- [29] M. van Dijk, J. Rhodes, L. F. G. Sarmenta, and S. Devadas. “Offline Untrusted Storage with Immediate Detection of Forking and Replay Attacks”. In: *Proceedings of the 2007 ACM Workshop on Scalable Trusted Computing*. STC ’07. Alexandria, Virginia, USA: ACM, 2007, pp. 41–48. ISBN: 978-1-59593-888-6. DOI: 10.1145/1314354.1314364. URL: <http://doi.acm.org/10.1145/1314354.1314364>.
- [30] S. Egelman, L. F. Cranor, and J. Hong. “Youve Been Warned: An Empirical Study of the Effectiveness of Web Browser Phishing Warnings”. In: *Proceedings of the SIGCHI Conference on Human Factors in Computing Systems*. CHI 08. Florence, Italy: Association for Computing Machinery, 2008, 10651074. ISBN: 9781605580111. DOI: 10.1145/1357054.1357219. URL: <https://doi.org/10.1145/1357054.1357219>.
- [31] *EMBEDDED MULTI-MEDIA CARD (eMMC), ELECTRICAL STANDARD (5.1)*. 2015. URL: <https://www.jedec.org/standards-documents/results/jesd84-b51> (visited on 04/26/2017).
- [32] M. Fagan and M. M. H. Khan. “Why Do They Do What They Do?: A Study of What Motivates Users to (Not) Follow Computer Security Advice”. In: *Twelfth Symposium on Usable Privacy and Security (SOUPS 2016)*. Denver, CO: USENIX Association, June 2016, pp. 59–75. ISBN: 978-1-931971-31-7. URL: <https://www.usenix.org/conference/soups2016/technical-sessions/presentation/fagan>.
- [33] A. Ferraiuolo, R. Xu, D. Zhang, A. C. Myers, and G. E. Suh. “Verification of a Practical Hardware Security Architecture Through Static Information Flow Analysis”. In: *Proceedings of the Twenty-Second International Conference on Architectural Support for Programming Languages and Operating Systems, ASPLOS 2017, Xi’an, China, April 8-12, 2017*. 2017, pp. 555–568. DOI: 10.1145/3037697.3037739. URL: <http://doi.acm.org/10.1145/3037697.3037739>.
- [34] R. Fielding and J. Reschke. *Hypertext Transfer Protocol (HTTP/1.1): Semantics and Content*. RFC 7231. <http://www.rfc-editor.org/rfc/rfc7231.txt>. RFC Editor, 2014. URL: <http://www.rfc-editor.org/rfc/rfc7231.txt>.
- [35] Floodyberry. *floodyberry/chacha-opt*. 2015. URL: <https://github.com/floodyberry/chacha-opt>.

- [36] E. Foudil and Y. Shafranovich. *A Method for Web Security Policies*. Internet-Draft draft-foudil-securitytxt-04. <http://www.ietf.org/internet-drafts/draft-foudil-securitytxt-04.txt>. IETF Secretariat, 2018. URL: <http://www.ietf.org/internet-drafts/draft-foudil-securitytxt-04.txt>.
- [37] *GitHub: savoirfairelinux/openssh*. URL: <https://github.com/savoirfairelinux/openssh>.
- [38] J. Goodman, A. P. Dancy, and A. P. Chandrakasan. “An energy/security scalable encryption processor using an embedded variable voltage DC/DC converter”. In: *IEEE Journal of Solid-State Circuits* 33.11 (1998), pp. 1799–1809.
- [39] Google. *Chrome Extension APIs*. URL: <https://developer.chrome.com/extensions/devguide>.
- [40] T. C. Group. *TCG: Trusted platform module summary*. 2008.
- [41] M. Haleem, C. Mathur, R. Chandramouli, and K. Subbalakshmi. “Opportunistic Encryption: A Trade-Off between Security and Throughput in Wireless Networks”. In: *IEEE Transactions on Dependable and Secure Computing* 4.4 (2007), pp. 313–324. DOI: 10.1109/TDSC.2007.70214.
- [42] S. Halevi and P. Rogaway. “A Tweakable Enciphering Mode”. In: *Advances in Cryptology - CRYPTO 2003: 23rd Annual International Cryptology Conference, Santa Barbara, California, USA, August 17-21, 2003. Proceedings*. Ed. by D. Boneh. Berlin, Heidelberg: Springer Berlin Heidelberg, 2003, pp. 482–499. ISBN: 978-3-540-45146-4. DOI: 10.1007/978-3-540-45146-4_28. URL: http://dx.doi.org/10.1007/978-3-540-45146-4_28.
- [43] HandBrake. *Mirror Download Server Compromised*. 2017. URL: <https://forum.handbrake.fr/viewtopic.php?f=33&t=36364>.
- [44] “HandBrake hacked to drop new variant of Proton malware”. In: *MalwareBytes Labs* (2017). URL: <https://blog.malwarebytes.com/threat-analysis/mac-threat-analysis/2017/05/handbrake-hacked-to-drop-new-variant-of-proton-malware/>.
- [45] M. Hao, G. Soundararajan, D. Kenchammana-Hosekote, A. A. Chien, and H. S. Gunawi. “The Tail at Store: A Revelation from Millions of Hours of Disk and SSD Deployments”. In: *14th {USENIX} Conference on File and Storage Technologies ({FAST} 16)*. 2016, pp. 263–276.
- [46] “Havex”. In: *New Jersey Cybersecurity and Communications Integration Cell Threat Profiles* (2017). URL: <https://www.cyber.nj.gov/threat-profiles/ics-malware-variants/havex>.
- [47] D. Hein, J. Winter, and A. Fitzek. “Secure Block Device – Secure, Flexible, and Efficient Data Storage for ARM TrustZone Systems”. In: *2015 IEEE Trustcom/BigDataSE/ISPA*. Vol. 1. 2015, pp. 222–229. DOI: 10.1109/Trustcom.2015.378.

- [48] M. Hicks, C. Sturton, S. T. King, and J. M. Smith. “SPECS: A Lightweight Runtime Mechanism for Protecting Software from Security-Critical Processor Bugs”. In: *Proceedings of the Twentieth International Conference on Architectural Support for Programming Languages and Operating Systems, ASPLOS '15, Istanbul, Turkey, March 14-18, 2015*. 2015, pp. 517–529. DOI: 10.1145/2694344.2694366. URL: <http://doi.acm.org/10.1145/2694344.2694366>.
- [49] J. Ho and B. Chester. *Encryption and Storage Performance in Android 5.0 Lollipop*. 2014. URL: <https://www.anandtech.com/show/8725/encryption-and-storage-performance-in-android-50-lollipop>.
- [50] H.-C. Hsiao, Y.-H. Lin, A. Studer, C. Studer, K.-H. Wang, H. Kikuchi, A. Perrig, H.-M. Sun, and B.-Y. Yang. “A Study of User-Friendly Hash Comparison Schemes”. In: *Proceedings of the 2009 Annual Computer Security Applications Conference*. ACSAC 09. USA: IEEE Computer Society, 2009, 105114. ISBN: 9780769539195. DOI: 10.1109/ACSAC.2009.20. URL: <https://doi.org/10.1109/ACSAC.2009.20>.
- [51] *Improving Chrome’s Security Warnings [public]*. URL: https://docs.google.com/presentation/d/16ygiQS0_5b9A4NwHxpcd6sW3b_Up81_qXU-XY86JHc4/htmlpresent.
- [52] *JSON API for DNS over HTTPS (DoH)*. URL: <https://developers.google.com/speed/public-dns/docs/doh/json>.
- [53] D. Kirovski, M. Drinić, and M. Potkonjak. “Enabling Trusted Software Integrity”. In: *Proceedings of the 10th International Conference on Architectural Support for Programming Languages and Operating Systems*. ASPLOS X. San Jose, California: ACM, 2002, pp. 108–120. ISBN: 1-58113-574-2. DOI: 10.1145/605397.605409. URL: <http://doi.acm.org/10.1145/605397.605409>.
- [54] R. Konishi, Y. Amagai, K. Sato, H. Hifumi, S. Kihara, and S. Moriai. “The Linux Implementation of a Log-structured File System”. In: *SIGOPS Oper. Syst. Rev.* 40.3 (July 2006), pp. 102–107. ISSN: 0163-5980. DOI: 10.1145/1151374.1151375. URL: <http://doi.acm.org/10.1145/1151374.1151375>.
- [55] C. Lee, D. Sim, J. Hwang, and S. Cho. “F2FS: A New File System for Flash Storage”. In: *13th USENIX Conference on File and Storage Technologies (FAST 15)*. Santa Clara, CA: USENIX Association, 2015, pp. 273–286. ISBN: 978-1-931971-201. URL: <https://www.usenix.org/conference/fast15/technical-sessions/presentation/lee>.
- [56] A. Levy, H. Corrigan-Gibbs, and D. Boneh. “Stickler: Defending against Malicious Content Distribution Networks in an Unmodified Browser”. In: *IEEE Security Privacy* 14.2 (2016), pp. 22–28. ISSN: 1558-4046. DOI: 10.1109/MSP.2016.32.
- [57] J. Li and E. R. Omiecinski. “Efficiency and Security Trade-Off in Supporting Range Queries on Encrypted Databases”. In: *Data and Applications Security XIX*. Ed. by S. Jajodia and D. Wijesekera. Berlin, Heidelberg: Springer Berlin Heidelberg, 2005, pp. 69–83. ISBN: 978-3-540-31937-5.

- [58] X. Li, V. Kashyap, J. K. Oberg, M. Tiwari, V. R. Rajarathinam, R. Kastner, T. Sherwood, B. Hardekopf, and F. T. Chong. “Sapper: a language for hardware-level security policy enforcement”. In: *Architectural Support for Programming Languages and Operating Systems, ASPLOS '14, Salt Lake City, UT, USA, March 1-5, 2014*. 2014, pp. 97–112. DOI: 10.1145/2541940.2541947. URL: <http://doi.acm.org/10.1145/2541940.2541947>.
- [59] A. Limited. *ARM security technology: Building a secure system using TrustZone technology*. PRD29-GENC-009492C. 2009.
- [60] *Linux kernel device-mapper crypto target*. 2013. URL: <https://gitlab.com/cryptsetup/cryptsetup> (visited on 04/26/2017).
- [61] Lvella. *lvella/libestream*. URL: <https://github.com/lvella/libestream>.
- [62] S. Maitra. *Chosen IV Cryptanalysis on Reduced Round ChaCha and Salsa*. Tech. rep. Applied Statistics Unit, Indian Statistical Institute, 2015.
- [63] G. Markham. *Link Fingerprints*. 2008. URL: <http://www.gerv.net/security/link-fingerprints/>.
- [64] A. Merkel and F. Bellosa. “Balancing Power Consumption in Multiprocessor Systems”. In: *Proceedings of the 1st ACM SIGOPS/EuroSys European Conference on Computer Systems 2006*. EuroSys '06. Leuven, Belgium: ACM, 2006, pp. 403–414. ISBN: 1-59593-322-0. DOI: 10.1145/1217935.1217974. URL: <http://doi.acm.org/10.1145/1217935.1217974>.
- [65] R. C. Merkle. “A Digital Signature Based on a Conventional Encryption Function”. In: *A Conference on the Theory and Applications of Cryptographic Techniques on Advances in Cryptology*. CRYPTO 87. Berlin, Heidelberg: Springer-Verlag, 1987, 369378. ISBN: 3540187960.
- [66] *Message Authentication Code Standard ISO/IEC 9797-1:2011*. 2011. URL: <https://www.iso.org/standard/50375.html> (visited on 04/26/2017).
- [67] P. Mockapetris. *Domain names - concepts and facilities*. STD 13. <http://www.rfc-editor.org/rfc/rfc1034.txt>. RFC Editor, 1987. URL: <http://www.rfc-editor.org/rfc/rfc1034.txt>.
- [68] P. Mockapetris. *Domain names - implementation and specification*. STD 13. <http://www.rfc-editor.org/rfc/rfc1035.txt>. RFC Editor, 1987. URL: <http://www.rfc-editor.org/rfc/rfc1035.txt>.
- [69] D. Modic and R. Anderson. “Reading this may harm your computer: The psychology of malware warnings”. In: *Computers in Human Behavior* 41 (2014), 7179. DOI: 10.1016/j.chb.2014.09.014.
- [70] J. Myers and M. Rose. *The Content-MD5 Header Field*. RFC 1864. RFC Editor, 1995.
- [71] N. Nelson. “The impact of dragonfly malware on industrial control systems”. In: *SANS Institute* (2016).

- [72] NIST. *Cyber Supply Chain Risk Management*. URL: <https://csrc.nist.gov/Projects/Supply-Chain-Risk-Management>.
- [73] NIST. *Public Comments on the XTS-AES Mode*. 2008.
- [74] NIST. *Software Supply Chain Attacks*. 2017. URL: https://csrc.nist.gov/csrc/media/projects/supply-chain-risk-management/documents/ssca/2017-winter/ncsc_placemat.pdf.
- [75] Oracle blog: *ZFS End-to-End Data Integrity*. 2005. URL: <https://blogs.oracle.com/bonwick/zfs-end-to-end-data-integrity> (visited on 04/26/2017).
- [76] “phpMyAdmin corrupted copy on Korean mirror server”. In: *SourceForge Official Blog* (2012). URL: <https://sourceforge.net/blog/phpmyadmin-back-door/>.
- [77] “PMASA-2012-5”. In: *PMASA-2012-5* (2012). URL: <https://www.phpmyadmin.net/security/PMASA-2012-5/>.
- [78] *Recommendation for Block Cipher Modes of Operation: The XTS-AES Mode for Confidentiality on Storage Devices*. NIST Special Publication 800-38E. 2010. URL: <http://nvlpubs.nist.gov/>.
- [79] A. K. Reddy, P. Paramasivam, and P. B. Vemula. “Mobile secure data protection using eMMC RPMB partition”. In: *2015 International Conference on Computing and Network Communications (CoCoNet)*. 2015, pp. 946–950. DOI: 10.1109/CoCoNet.2015.7411305.
- [80] *RedHat: Device-mapper Resource Page*. URL: <https://www.sourceware.org/dm> (visited on 04/26/2017).
- [81] R. W. Reeder, A. P. Felt, S. Consolvo, N. Malkin, C. Thompson, and S. Egelman. “An Experience Sampling Study of User Reactions to Browser Warnings in the Field”. In: *Proceedings of the 2018 CHI Conference on Human Factors in Computing Systems*. CHI 18. Montreal QC, Canada: Association for Computing Machinery, 2018. ISBN: 9781450356206. DOI: 10.1145/3173574.3174086.
- [82] *Reproducible Builds: A Set Of Software Development Practices That Create An Independently Verifiable Path From Source To Binary Code*. URL: <https://reproducible-builds.org/>.
- [83] *Reproducible Builds (Debian Wiki)*. URL: <https://wiki.debian.org/ReproducibleBuilds>.
- [84] E. Rescorla. *HTTP Over TLS*. RFC 2818. <http://www.rfc-editor.org/rfc/rfc2818.txt>. RFC Editor, 2000. URL: <http://www.rfc-editor.org/rfc/rfc2818.txt>.
- [85] S. Rhea, B. Godfrey, B. Karp, J. Kubiatowicz, S. Ratnasamy, S. Shenker, I. Stoica, and H. Yu. “OpenDHT: A public DHT service and its uses”. English (US). In: *Computer Communication Review* 35.4 (Oct. 2005), pp. 73–84. ISSN: 0146-4833. DOI: 10.1145/1090191.1080102.
- [86] P. Rogaway. *Efficient Instantiations of Tweakable Blockciphers and Refinements to Modes OCB and PMAC*. Tech. rep. University of California at Davis, 2004.

- [87] P. Rogaway and T. Shrimpton. “Cryptographic Hash-Function Basics: Definitions, Implications, and Separations for Preimage Resistance, Second-Preimage Resistance, and Collision Resistance”. In: *Fast Software Encryption*. Ed. by B. Roy and W. Meier. Berlin, Heidelberg: Springer Berlin Heidelberg, 2004, pp. 371–388. ISBN: 978-3-540-25937-4.
- [88] M. Rosenblum and J. K. Ousterhout. “The Design and Implementation of a Log-structured File System”. In: *ACM Trans. Comput. Syst.* 10.1 (Feb. 1992), pp. 26–52. ISSN: 0734-2071. DOI: 10.1145/146941.146943. URL: <http://doi.acm.org/10.1145/146941.146943>.
- [89] C. Ryan. *Computer and Internet Use in the United States: 2016*. Technical Report ACS-39.
- [90] P. Sarkar. *Tweakable Enciphering Schemes From Stream Ciphers With IV*. Tech. rep. Indian Statistical Institute, 2009.
- [91] *Security/Binary Transparency*. URL: https://wiki.mozilla.org/Security/Binary_Transparency.
- [92] T. J. Seppala. *Google won’t force Android encryption by default*. 2019. URL: <https://www.engadget.com/2015/03/02/android-lollipop-automatic-encryption/>.
- [93] M. Silic and A. Back. “Deterrent Effects of Warnings on User’s Behavior in Preventing Malicious Software Use”. In: *HICSS*. 2017.
- [94] J. Sunshine, S. Egelman, H. Almuhiemedi, N. Atri, and L. F. Cranor. “Crying Wolf: An Empirical Study of SSL Warning Effectiveness”. In: *Proceedings of the 18th Conference on USENIX Security Symposium*. SSYM09. Montreal, Canada: USENIX Association, 2009, 399416.
- [95] J. Tan, L. Bauer, J. Bonneau, L. F. Cranor, J. Thomas, and B. Ur. “Can Unicorns Help Users Compare Crypto Key Fingerprints?” In: *Proceedings of the 2017 CHI Conference on Human Factors in Computing Systems*. CHI 17. Denver, Colorado, USA: Association for Computing Machinery, 2017, 37873798. ISBN: 9781450346559. DOI: 10.1145/3025453.3025733. URL: <https://doi.org/10.1145/3025453.3025733>.
- [96] L. M. Team. *Beware of hacked ISOs if you downloaded Linux Mint on February 20th!* 2016. URL: <https://blog.linuxmint.com/?p=2994>.
- [97] G. P. D. Technology. *TEE client API specification version 1.0*. GPD_SPE.007. 2010.
- [98] *The XTS-AES Tweakable Block Cipher*. IEEE Std 1619-2007. 2008.
- [99] P. Thiemann. *A URN Namespace For Identifiers Based on Cryptographic Hashes*. Internet-Draft draft-thiemann-hash-urn-01. Archived. Internet Engineering Task Force, 2003. 10 pp. URL: <https://datatracker.ietf.org/doc/html/draft-thiemann-hash-urn-01>.

- [100] M. Tiwari, J. Oberg, X. Li, J. Valamehr, T. E. Levin, B. Hardekopf, R. Kastner, F. T. Chong, and T. Sherwood. “Crafting a usable microkernel, processor, and I/O system with strict and provable information flow security”. In: *38th International Symposium on Computer Architecture (ISCA 2011), June 4-8, 2011, San Jose, CA, USA*. 2011, pp. 189–200. DOI: 10.1145/2000064.2000087. URL: <http://doi.acm.org/10.1145/2000064.2000087>.
- [101] *TLS Symmetric Crypto*. 2014. URL: <https://www.imperialviolet.org/2014/02/27/tlssymmetriccrypto.html> (visited on 04/26/2017).
- [102] *Using Advanced Encryption Standard Counter Mode (AES-CTR) with the Internet Key Exchange version 02 (IKEv2) Protocol*. URL: <https://tools.ietf.org/html/rfc5930>.
- [103] J. Vahrenhold. “On the Importance of Being Earnest: Challenges in Computer Science Education”. In: *Proceedings of the 7th Workshop in Primary and Secondary Computing Education*. WiPSCE 12. Hamburg, Germany: Association for Computing Machinery, 2012, 34. ISBN: 9781450317870. DOI: 10.1145/2481449.2481452. URL: <https://doi.org/10.1145/2481449.2481452>.
- [104] J. Valamehr, M. Chase, S. Kamara, A. Putnam, D. Shumow, V. Vaikuntanathan, and T. Sherwood. “Inspection resistant memory: Architectural support for security from physical examination”. In: *39th International Symposium on Computer Architecture (ISCA 2012), June 9-13, 2012, Portland, OR, USA*. 2012, pp. 130–141. DOI: 10.1109/ISCA.2012.6237012. URL: <https://doi.org/10.1109/ISCA.2012.6237012>.
- [105] P. Wang, D. Feng, and W. Wu. “HCTR: A Variable-Input-Length Enciphering Mode”. In: *Information Security and Cryptology: First SKLOIS Conference, CISC 2005, Beijing, China, December 15-17, 2005. Proceedings*. Ed. by D. Feng, D. Lin, and M. Yung. Berlin, Heidelberg: Springer Berlin Heidelberg, 2005, pp. 175–188. ISBN: 978-3-540-32424-9. DOI: 10.1007/11599548_15. URL: http://dx.doi.org/10.1007/11599548_15.
- [106] *What makes LastPass secure?* URL: <https://support.logmeininc.com/lastpass/help/what-makes-lastpass-secure-lp070015>.
- [107] Z. Whittaker. “Hacker explains how he put ”backdoor” in hundreds of Linux Mint downloads”. In: *ZDNet* (2016). URL: <https://www.zdnet.com/article/hacker-hundreds-were-tricked-into-installing-linux-mint-backdoor/>.
- [108] A. Whitten and J. D. Tygar. “Why Johnny Can’t Encrypt: A Usability Evaluation of PGP 5.0”. In: *Proceedings of the 8th Conference on USENIX Security Symposium - Volume 8*. SSYM’99. Washington, D.C.: USENIX Association, 1999, pp. 14–14. URL: <http://dl.acm.org/citation.cfm?id=1251421.1251435>.
- [109] K. Wolter and P. Reinecke. “Performance and security tradeoff”. In: *International School on Formal Methods for the Design of Computer, Communication and Software Systems*. Springer. 2010, pp. 135–167.

- [110] W. Zeng and M. Chow. “Optimal Tradeoff Between Performance and Security in Networked Control Systems Based on Coevolutionary Algorithms”. In: *IEEE Transactions on Industrial Electronics* 59.7 (2012), pp. 3016–3025. DOI: 10.1109/TIE.2011.2178216.
- [111] W. Zeng and M. Chow. “Modeling and Optimizing the Performance-Security Tradeoff on D-NCS Using the Coevolutionary Paradigm”. In: *IEEE Transactions on Industrial Informatics* 9.1 (2013), pp. 394–402. DOI: 10.1109/TII.2012.2209662.
- [112] R. Zhang, N. Stanley, C. Griggs, A. Chi, and C. Sturton. “Identifying Security Critical Properties for the Dynamic Verification of a Processor”. In: *Proceedings of the Twenty-Second International Conference on Architectural Support for Programming Languages and Operating Systems, ASPLOS 2017, Xi'an, China, April 8-12, 2017*. 2017, pp. 541–554. DOI: 10.1145/3037697.3037734. URL: <http://doi.acm.org/10.1145/3037697.3037734>.